Metabolic Sensing in the Hypothalamus

A thesis submitted to the University of Manchester for the degree of Doctor of Philosophy in the Faculty of Life Sciences

2014

Hanna Terese Sjoberg

Faculty of Life Sciences

Table of Contents

Abbreviations 5
Abstract 8
Declaration 9
Intellectual Property Statement 9
Acknowledgements 10

Chapter 1. Introduction and background 11

1.1 Energy balance regulation 11
1.2 Polygenic disease 12
1.3 The role of the hypothalamus in metabolic regulation 14
1.3.1 The arcuate nucleus 14
1.3.2 Hormonal signalling in the arcuate nucleus 17
1.4 Nutrient sensing in the hypothalamus 19
1.4.1 Glucose signalling 19
1.4.2 Central lipid sensing 21
1.4.3 Integration of signals 22
1.5 The importance of the VMN 23
1.6 PhD aims and objectives 29

Chapter 2. General Methods 30

2.1 Animals 30
2.1.1 Generation of transgenic mouse lines 30
2.2 *In Vivo* Techniques 34
2.2.1 Implantation of Guide Cannulae and intracerebroventricular injections 34
2.2.2 Feeding experiments 34
2.2.3 Oral Glucose Tolerance Test 35
2.2.4 Tissue collection and fixation 35
2.3 Molecular Techniques 36
2.3.1 DNA Extraction and genotyping 36
2.3.2 Laser-Capture Microdissection and Tissue Preparation 40
2.3.3 RNA Extraction and reverse transcription 40
2.3.4 Primer Design and validation 41
2.3.5 Relative Quantitative Real-Time PCR 42
2.4 Immunohistochemistry 42
2.4.1 Standard single-label immunohistochemical protocol 43
2.4.2 Standard single-label fluorescent immunohistochemical protocol 43
2.5 Imaging 44
2.5.1 Cell dissociation 44
2.5.2 Ca^{2+} Imaging 45
2.5.3 Patch Clamping 46
2.6 Statistical analysis 47

2.6.1 Quantitative Trait Loci (QTL) and Correlational analysis of the BXD lines 47

Chapter 3. Gene expression in outbred mice following metabolic manipulation 49

3.1 Introduction 49

3.2 Methods 52

3.2.1 Animals and diets 52

3.2.2 OGTT 52

3.2.3 Serum insulin ELISA 52

3.2.4 LCM and tissue preparation 52

3.2.5 RNA extraction, reverse transcription and qPCR 53

3.3 Results 53

3.3.1 Changes in mRNA expression after 48h fasting 53

3.3.2 Weight Gain after HED 54

3.3.3 Change in Glucose and Insulin after HED 56

3.3.4 Changes in mRNA Expression after 8 Weeks of HED 58

3.4 Discussion 59

3.5 Summary 66

Chapter 4. Metabolic sensitivity of PACAP neurons in the hypothalamus 67

4.1 Introduction 67

4.2 Methods 70

4.1.1 Animals and in vivo work 70

4.1.2 Immunohistochemistry 70

4.1.3 Imaging 71

4.3 Results 71

4.1.4 Testing a PACAP antibody for immunohistochemical staining 71

4.1.5 Expression of eGFP in two transgenic strains. 72

4.1.6 Generation of Pacap-i-cre X Lepr flox mice: growth curve, OGTT and leptin ip 75

4.1.7 Response of PACAP neurones to systemic hypoglycaemia 78

4.1.8 Acute response of PACAP neurones to changes in glucose. 81

4.4 Discussion 86

4.5 Summary 92

Chapter 5. The anorectic effects of PACAP and downstream targets 94

5.1 Introduction 94

5.2 Methods 95

5.2.1 Animals 95

5.2.2 i.c.v. PACAP or VIP in CD1 mice 95

5.2.3 i.c.v. PACAP and antagonist 96

5.3 Results 96

5.3.1 Effect of PACAP and VIP on food intake 96

5.3.2 Co-administration of an oxytocin receptor antagonist with PACAP 97

5.4 Discussion 97

Chapter 6. Diet-induced obesity in recombinant inbred mouse strains..... 101
6.1 Introduction.....101
6.2 Methods 103
6.2.1 BXD experiment 103
6.2.2 C57 experiments 104
6.2.3 QTL and Correlational analyses 104
6.2.4 RNA extraction, reverse transcription and qPCR 105
6.3 Results 105
6.3.1 Biometric traits of the BXD lines 105
6.3.2 QTL analysis of the biometric traits for the BXD mice 108
6.3.3 Correlational analyses 108
6.3.4 BXD pacap and bdnf hypothalamic expression.....109
6.3.5 C57 mice on HED and the expression of gprc5c.....112
6.3.6 Expression of gprc5c in the BXD hypothalamus, liver and BAT.....114
6.3.7 Final correlational analyses and mapping.....116
6.4 Discussion 117
6.5 Summary.....123

Chapter 7. Summary of conclusions and future work 124
7.1 *Pacap* and *bdnf* transcripts are differentially regulated in the VMN in response to metabolic manipulation.....124
7.2 PACAP neurons in the VMN are glucose inhibited 125
7.3 The anorectic effects of PACAP and downstream targets.....126
7.4 Identification of a new target, GPRc5c, and confirmation of old in hypothalamic signaling in obesity 127
7.5 Future work 127
7.6 Final remarks 128

References 129

Final word count: 49 136

Abbreviations

2DG – 2-deoxy-glucose
ACOX1 – acyl-coenzyme A oxidase 1
acyl-CoA – acyl-coenzyme A
ACC - acyl-coenzyme A carboxylase
ACS – acyl-coenzyme A synthetase
aCSF – artificial cerebrospinal fluid
ADCYAP1 – PACAP gene name
AgRP – agouti-related peptide
AMPK – 5'-AMP-activated protein kinase
α-MSH - α-melanocyte-stimulating hormone
ANOVA – analysis of variance
Arc – arcuate nucleus of the hypothalamus
a.u. – arbitrary units
AUC – area under the curve
BAT – brown adipose tissue
BDNF – brain-derived neurotropic factor
BMI – body mass index
BSA – bovine serum albumin
CCK – cholecystokinin
cDNA – complementary DNA
CRR – counter-regulatory response
C_t – threshold cycle
DIO – diet-induced obesity
DIO-R – diet-induced obesity-resistant
DMN – dorsomedial nucleus of the hypothalamus
DMSO – dimethyl sulphoxide
DNA - deoxyribonucleic acid
dNTPs – deoxynucleotide triphosphates
EDTA – ethylenediaminetetraacetic acid
eGFP – endogenous green fluorescent protein
ELISA – enzyme-linked immunosorbent assay
epiWAT – epididymal WAT
F1 generation – first filial generation
F2 generation – second filial generation
FAS – fatty acid synthase
FADS6 – fatty acid desaturase 6
FOXO1 – forkhead box protein O1
FTO – fat mass and obesity associated
GABA – gamma-Aminobutyric acid
GALR2 – galanin receptor 2
GE – glucose excited
GHRH – growth-hormone-releasing hormone
GHSR – growth hormone secretagogue receptor
GI – glucose inhibited
GLP-1 – glucagon-like peptide 1

GPCRs – G-protein coupled receptors
GWAS – genome-wide association studies
HAAF – hypoglycaemia associated autonomic failure
HED – high-energy diet
i-Cre – IRES-Cre-recombinase
i.c.v. – intracerebroventricular
ingWAT – inguinal WAT
i.p. - Intraperitoneously
LacZ – beta-galactosidase gene
LCM – laser capture microdissection
LEPR – leptin receptor
LH – lateral hypothalamus
LRS – likelihood ratio statistic
MCD – malonyl-CoA decarboxylase
MCH – melanin-concentrating hormone
MC_3R – melanocortin 3 receptor
MC_4R – melanocortin 4 receptor
MEM – minimum essential media
mRNA – messenger RNA
mTOR – mammalian target of rapamycin
NCBI – national centre for biotechnology information
NPY – neuropeptide Y
NTS – nucleus of solitary tract
OGTT – oral glucose tolerance test
PACAP – pituitary adenylate cyclase-activating peptide
PB – phosphate buffer
PBT– phosphate buffer containing triton x-100
PCR – polymerase chain reaction
PDL – poly-D-lysine
PFA - paraformaldehyde
POMC – pro-opiomelanocortin
PVN – paraventricular nucleus of the hypothalamus
PYY – peptide YY
qPCR – relative quantitative real-time PCR
QTL – quantitative trait
RAIGs – retinoic acid-inducible genes
RNA – ribonucleic acid
RT – room temperature
SDS – sodium dodecyl sulphate
SEM – standard error of the mean
SF-1 – steroidogenic factor 1
SIRT1 – silent information regulator 1
SK muscle – skeletal muscle
SNPs – single nucleotide polymorphisms
TrkB – tyrosine-kinase receptor
UTR – untranslated region
VIP – vasoactive intestinal peptide
VMH – ventromedial hypothalamus
VMN – ventromedial nucleus of the hypothalamus
WAGR syndrome –Wilms tumour, Aniridia, Genitourinary abnormalities and mental retardation

WAT – white adipose tissue

Abstract

University of Manchester, Hanna Terese Sjoberg for the degree of Doctor of Philosophy, 2014.

Metabolic Sensing in the Hypothalamus

The hypothalamus is an established regulatory hub with regards to energy homeostasis. While the arcuate nucleus has been researched extensively and substantial emphasis has been put on its role in energy balance, the ventromedial nucleus of the hypothalamus (VMN) is still poorly understood. However, the anorexia-inducing pituitary adenylate-cyclase activating peptide (PACAP) and brain-derived neurotrophic factor (BDNF) have both been proposed as potential candidates as VMN-produced regulators. The mRNAs of both neuropeptides is up regulated in diet-induced obesity (DIO)-resistant mice, but not in DIO-prone mice, indicating that they could be responsible for signalling in the VMN, especially in terms of countering the effects of an obesogenic diet.

The initial objective of this PhD project was to evaluate the effect of metabolic manipulation, in the form of fasting or feeding with high-energy diet (HED), on the gene expression of these two possible neuronal markers in the VMN. This was done using quantitative PCR and, while our findings did not fully support the hypothesis that PACAP and BDNF have protective roles against obesity, we determined that metabolic manipulation differentially regulates *pacap* and *bdnf* transcripts in the VMN of outbred mice. The presence of several *bdnf* transcripts in the VMN, and their differential regulation, indicates that the transcripts play distinct roles in the response to metabolic manipulation. The findings also added further support for the role of PACAP and BDNF as important signalling molecules in the VMN. Their identification as important cellular phenotypes, allows future manipulation of specific neurons in the VMN, which should help us to rapidly increase our knowledge of the nucleus and its functions.

We utilised a transgenic mouse model where leptin receptor deletion is driven by *pacap* expression in PACAP—IRES-Cre recombinase mice, to study whether leptin is having a physiological role through PACAP neurons. However, since we may not have achieved full expression of cre recombinase in all PACAP neurons, it was difficult to interpret our results, leaving open the question of what is the role of PACAP neurons in leptin signalling. Further, attempts have been made here to characterise this subtype of VMN neuron by using two GFP-reporter lines: Adcyap1-eGFP and PACAP-i-cre X Z/EG transgenic mouse lines. These were used to study the responsiveness of PACAP neurons to fluctuations in glucose availability, and our very promising early results indicate that PACAP VMN neurons are glucose inhibited.

We studied the anorectic effects of PACAP and the peptide's downstream targets, including the corticotrophin-releasing hormone (CRH), melanocortin and oxytocin pathways. The anorexic effect of central PACAP were maintained in $VPAC_1$ and $VPAC_2$ receptor (which also binds the related VIP) knockout animals, implicating the PAC_1 receptor as the mediator of the hypophagic response. We also showed that the feeding effects of PACAP are mediated by CRH, rather than by melanocortin or oxytocin pathways.

Finally, we utilised a systems-genetics approach in the BXD set of recombinant inbred mouse strains, in an attempt to tease apart underlying networks of genes contributing to metabolic phenotypes. Quantitative trait analysis identified several loci, which contained genes of potential interest (for example: a QTL related to adiposity contained the orphan G-protein-coupled receptor, GPRC5C). Joint mapping revealed that the phenotypic traits we measured correlated with each other and with trait data from BXD mice recorded in other laboratories. For example, this supported the role of PACAP and BDNF in body-weight management. The candidate gene, *gprc5c*, was further investigated. Its mRNA was found in the hypothalamus, but was also widely distributed in peripheral tissues. *Gprc5c* mRNA was regulated by HED in normal C57 mice in the hypothalamus, liver and brown adipose tissue, indicating a possible role for this orphan receptor in metabolism. In fact, similar to PACAP and BDNF, in BXD mice, expression of *gprc5c* in the hypothalamus was inversely correlated with body-weight gain.

Declaration

No portion of the work referred to in this thesis has been submitted in support of an application for another degree or qualification of this or any other university or other institute of learning.

Intellectual Property Statement

i. The author of this thesis (including any appendices and/or schedules to this thesis) owns certain copyright or related rights in it (the "Copyright") and s/he has given The University of Manchester certain rights to use such Copyright, including for administrative purposes.

ii. Copies of this thesis, either in full or in extracts and whether in hard or electronic copy, may be made only in accordance with the Copyright, Designs and Patents Act 1988 (as amended) and regulations issued under it or, where appropriate, in accordance with licensing agreements which the University has from time to time. This page must form part of any such copies made.

iii. The ownership of certain Copyright, patents, designs, trade marks and other intellectual property (the "Intellectual Property") and any reproductions of copyright works in the thesis, for example graphs and tables ("Reproductions"), which may be described in this thesis, may not be owned by the author and may be owned by third parties. Such Intellectual Property and Reproductions cannot and must not be made available for use without the prior written permission of the owner(s) of the relevant Intellectual Property and/or Reproductions.

iv. Further information on the conditions under which disclosure, publication and commercialisation of this thesis, the Copyright and any Intellectual Property and/or Reproductions described in it may take place is available in the University IP Policy (see http://www.campus.manchester.ac.uk/medialibrary/policies/intellectual- property.pdf), in any relevant Thesis restriction declarations deposited in the University Library, The University Library's regulations (see http://www.manchester.ac.uk/library/aboutus/regulations) and in The University's policy on presentation of Theses

Acknowledgements

The author would like to thank Professor Simon Luckman for his supervision, guidance and advice, as well as Professor Hugh Piggins and Dr Maria Canal for support and advice. And thanks go to Dr Garron Dodd, Dr Mino Belle, Dr Nicolas Nunn and Dr Ian Millar for their expertise, along with Ms Amy Worth for her invaluable assistance, and Ms Holly Hopkins and Ms Kate Merritt for their hard work. Finally, the author sends her appreciation to the staff in the university animal unit for their continued support.

Chapter 1. Introduction and background

1.1 Energy balance regulation

Although there are large differences in body weights recorded within populations, an individual maintains his or her body weight with remarkable stability over long periods of time. This is achieved by controlling the balance between energy expenditure and intake through coordinated adjustments that cancel out any temporary discrepancy. The brain and peripheral tissues are required to be in constant communication; those in the periphery relaying urgent metabolic requirement information to the brain (McMinn et al 2000), which then responds by activating the neuronal circuitry involved in metabolic homeostasis. Downstream, this circuitry affects behaviour, food intake, physical activity, sympathetic nervous system activation and basal metabolism (Schwartz et al 2000, Spiegelman & Flier 2001, Woods & D'Alessio 2008).

In the last 25 years, major advances have been made in the understanding of the neuroanatomical and physiological bases underlying the control mechanisms in energy homeostasis. The metabolic sensing neurons responsible for the integration of both hormonal and neuronal inputs, originating in the periphery, have been identified and their cellular phenotypes have largely also been described. Glucose and other metabolic indicators are utilized by these neurons as signaling molecules to, unlike other neurons, regulate cell firing rate and membrane potential. These neurons also express the crucial neuropeptides, receptors and transmitters that underpin the behavioural and endocrine responses to metabolic stimuli (Levin 2006, Schwartz et al 2000). There are potential pharmaceutical targets to be discovered in the central circuitry underlying energy metabolism, and this is a very important field for further research, considering the pandemic problem obesity has become today.

Peptide hormones originating in peripheral tissues relay the metabolic status of the animal to central targets, mainly in the hypothalamus and brainstem (Luckman & Lawrence 2003). One of the major peripheral sources is the gastrointestinal tract, which provides a majority of the acute feedback signals received centrally that relate to energy consumption. These signals include hormones such as ghrelin, an orexigenic peptide, and the satiety factors cholecystokinin (CCK),

peptide YY (PYY) and glucagon-like peptide 1 (GLP-1), which are released post-prandially from the stomach and intestines (Dhillon & Bloom 2004, Mendieta-Zeron et al 2008, Murphy et al 2006). Circulating metabolites acquired from the diet also signal energy status to the brain, including glucose and free-fatty acids (Schwartz et al 2000). Another major source of hormonal signaling is the white adipose tissue (WAT), which relays information back to the brain, signaling lipogenesis, fat storage and lipolysis. In the last two decades, the understanding of WAT as nothing more than a passive storage repository has been revised, and it is now viewed as an important and dynamic secretory organ (Wozniak et al 2009). This shift followed the discovery of leptin in 1994 (Zhang et al 1994) and subsequently, factors such as adiponectin, resistin and adipsin, have all been found to be secreted by adipocytes in the WAT, which are thought to signal long-term changes to energy balance by matching energy intake to fat stores. In conclusion, in concert with everyday bodily processes, such as feeding, digestion, energy metabolism and storage, a plethora of signals are released throughout the body that converge centrally to regulate the neural circuitry that maintains energy homeostasis.

1.2 Polygenic disease

According to a report by Diabetes UK (2005), one in five adults in Britain is now defined as clinically obese, and evidence suggests that Britain has one of the fastest growing rates of obesity in the developing world (see Type 2 Diabetes and Obesity: A Heavy Burden, 2005). The report also states that obese people are up to 80% more likely to develop type 2 diabetes. The burden on health services and the economic consequences of the growing number of people with obesity and type 2 diabetes make research into their etiologies essential. There are a well-known monogenic causes for the tendency to become obese (e.g. mutation in the *leptin* gene or its receptor (Farooqi et al 1999, Farooqi et al 2001) or the more common mutation in the melanocortin 4 receptor (Farooqi et al 2003). However, occurrences of individuals with these major genetic defects in the leptin and melanocortin signalling system are relatively rare (Farooqi et al 2003, Maffei et al 1996), and it has become clear that there are a substantial number of genes, gene interactions and gene x environment interactions involved in the complex mechanism of body weight regulation and in the more common forms of obesity. This polygenic background results from the integrated activity of numerous genes, each of which carries only a small risk factor on its own. These polygenes, which have small influence on body weight, are common in the general population and obesity results via the interaction of several of such polygenic variants and their combined interaction with environmental factors (such as diet or lack of exercise).

From studies looking at the similarity in body weight between monozygotic and dizygotic twins, it is thought that 65% of variation in obesity is genetic (Segal & Allison 2002), with the rest due to the environment. The precise percentages are probably of less importance, with the point being rather that both genes and the environment interact in the development of metabolic disease. Indeed, it is impossible for a genotype to work outside the framework of the environment, and the environmental effects are determined by genotype (Speakman et al 2011). Hence, the understanding of the gene-by-environment interaction in the development of obesity and diabetes is paramount (Speakman 2004).

One of the major approaches to investigate the large genetic component of metabolic disease has been the genome-wide association studies, or GWAS. These studies have been important in complex diseases, finding associations between a given disease phenotype and a representation of all common variations in the genome. Many single nucleotide polymorphisms (SNPs) revealed by GWAS studies as associated with metabolic diseases are linked to genes previously unidentified as candidates. For example, in 2007, a genome-wide search for type 2 diabetes-susceptibility genes identified a common variant in the *fto* (fat mass and obesity associated) gene that predisposes to diabetes through an effect on body mass index (BMI) (Frayling et al 2007). In addition, GWAS studies have further confirmed the importance of established candidates, such as the mutations in the melanocortin 4 receptor (*mc_4r)* gene, in the development of obesity (Chambers et al 2008, Loos et al 2008, Willer et al 2009). However, relatively little variation in phenotype is described by the genetic variation described in these studies. For example, in a very large study involving 249,796 individuals (Speliotes et al 2010a), 18 new genes were identified in which all their variation together explains less than 4% of the variation in BMI.

Environmental drivers of obesity include changes in lifestyle, including the increased availability of palatable and energy-dense foods, a reduced need for physical activity and a reduction in sleep (Mavanji et al 2012, McAllister et al 2009). In particular, a diet containing long-chain saturated fats is known to result in metabolic dysfunction with increased adiposity and weight gain that is defended so that any subsequent weight loss through calorie restriction is difficult to maintain (Velloso & Schwartz 2011). So, the increase in the occurrence of obesity is believed to be related to gene-by-environment interactions, where the genetic background of an individual who is living in an obesogenic environment and lifestyle, together promote the development of metabolic syndrome. This is comprised by a heterogeneous group of metabolic disorders and is defined by impaired insulin sensitivity, glucose intolerance or diabetes mellitus type II in combination with at

least two other metabolic derangements, including abdominal obesity, dyslipidaemia and urinary microalbuminuria (Wozniak et al 2009). In addition, there is a proposed epigenetic component in addition to the classic genetic and the environmental contributors, which has been most extensively studied in terms of foetal programming and the effects of early-life nutrition and long-term metabolism. Epigenetics is the study of changes in gene expression or cellular phenotype, which are heritable or occur during a lifetime (Wolffe & Guschin 2000). These changes are caused by mechanisms other than changes in genomic sequence, and include DNA methylation and histone modification, which both regulate gene expression. For example, foetal over-nutrition and obesity in mothers have been linked to an increased risk in development of obesity later in life (Rooney & Ozanne 2011, Symonds et al 2011, Symonds et al 2009).

Even though we have seen large advances in the field of metabolic research, the precise mechanism driving the gene-by-environment interactions remains elusive. In addition, little is still known of the brain circuitry controlling metabolic homeostasis.

1.3 The role of the hypothalamus in metabolic regulation

In the 1940s and 1950s, crude rodent lesion studies of the hypothalamus revealed several areas with critical roles in the regulation of energy balance. Destruction the arcuate nucleus (Arc), paraventriclar nucleus (PVN), dorsomedial nucleus (DMN) or the ventromedial nucleus (VMN) of the hypothalamus, all caused immediate hyperphagia and the development of obesity; while the destruction of the lateral hypothalamus (LH) had the opposite effect, leading to hypophagia and weight loss (Anand & Brobeck 1951). The conclusions drawn from these results were that different areas of the hypothalamus played opposing roles in the maintenance of energy balance (although the lesions were not specifically selective and connections to other brain areas were destroyed as well). Later studies have identified many of the molecular correlates of these effects, and specific neuropeptidergic neuronal populations have been discovered.

1.3.1 The arcuate nucleus

The Arc has been the focus of metabolic research, especially since the discovery of leptin in the mid 1990s (Zhang et al 1994). The leptin receptor isoform B is widely expressed in the Arc and the nucleus was found to be integral in mediating the anorectic properties of leptin (Takeda et al 2002). The position of the Arc, next to the third ventricle and median eminence (distinctive for its discontinuous blood-brain-barrier), is ideal as a centre for metabolic sensing (Cone et al 2001).

Indeed, the Arc neurons are sensitive to a numerous hormones and nutrients, which include glucose, insulin, ghrelin and peptide YY (PYY) (reviewed in Dhillon and Bloom (2004). The phenotypic characterization of Arc cells revealed the distribution of neuronal populations that were spatially distinct and that were oppositely regulated by metabolic signals, such as leptin (Cheung et al 1997, Elias et al 1999, Mercer et al 1996).

Specifically, a dense population of the powerfully orexigenic neuropeptide Y (NPY) expressing neurones characterizes the ventromedial part of the Arc. When administered centrally, NPY induces extreme hyperphagia, leading chronically to an increase in fat mass (Zarjevski et al 1993). Conversely, when endogenous NPY action is blocked by antisense oligodeoxynucleotides, a reduction in food intake and body weight is observed (Kalra & Kalra 2000). In addition, a negative energy balance leads to an increase in hypothalamic NPY levels (Dube et al 1992, Kalra et al 1991), indicating that NPY release from the Arc is nutritionally regulated. NPY has also been linked to the control of energy expenditure (Egawa et al 1991) and fat storage (Billington et al 1991). The effects on energy balance exerted by NPY are mediated through two of the peptide's receptors Y_1R and Y_5R, and these receptors are expressed in the Arc, PVN, LH and DMN (Herzog 2003, Inui 1999). However, when NPY or either of its two receptors is knocked out, the result is not the expected lean phenotype, indicating that the role of NPY and its receptors in the regulation of feeding and energy expenditure is more complex than previously thought (as reviewed in Thiele et al (1997). Indeed, GABA receptors are abundant on NPY neurons in the Arc, and it is known that GABA plays crucial stimulatory role in feeding (as reviewed in Meister (2007)), hence the NPY knockout does not necessarily mean that the neuron is eliminated from the signalling circuitry. It has been proposed that the neuropeptide agouti-related peptide (AgRP), which is another orexigenic peptide that is co-expressed with NPY, can compensate for the lack of NPY signalling in the knockout animals.

The discovery of AgRP and its role in metabolic regulation came following the observation that when AgRP or Agouti is ubiquitously over-expressed in the mouse, it leads to the development of severe hyperphagia and obesity (Ollmann et al 1997). AgRP is a protein that is expressed in Arc NPY neurones, shares high sequence homology with the pigment protein Agouti, and has a powerful orexigenic effect when administered centrally in rodents (Ollmann et al 1997, Shutter et al 1997). Similar to NPY, it is also up-regulated by fasting (Wilson et al 1999). When AgRP is given centrally, mice still exhibit an increase in adiposity when compared with pair-fed animals, which has been attributed to an effect of AgRP on energy expenditure (Small et al 2001). In addition,

when AgRP RNA expression is disrupted in the Arc, it leads to an increase in metabolic rate without effecting food intake (Makimura et al 2002). AgRP acts as an inverse agonist on melanocortin receptors, actively supressing receptor tone (Ollmann et al 1997).

Another neuronal population has been identified in the ventral part of the Arc, which expresses pro-opiomelanocortin (POMC). POMC is a precursor to a number of peptides, including α-melanocyte-stimulating hormone (α-MSH), which binds to the centrally expressed melanocortin receptors MC_3R and MC_4R (Mountjoy et al 1994, Roselli-Rehfuss et al 1993). While NPY is up regulated by negative energy balance, POMC expression is down regulated, but its expression is rapidly rescued by re-feeding or leptin administration (Mizuno et al 1998a, Swart et al 2002). When POMC or MC_4R is knocked out, the animal exhibits a morbidly obese phenotype, while the MC_3R knockout results in a obese phenotype that is much less severe (as reviewed in Butler and Cone (2002)). As can be expected by its function, the MC_4R is expressed in several hypothalamic nuclei including the Arc, VMN and PVN (all involved in energy homeostasis) (Mountjoy et al 1994), and in the sympathetic pathways to both white and brown adipose tissues (Song et al 2005, Song et al 2008).

A schematic showing the major established intra-hypothalamic connections involved in the control of energy homeostasis are shown in Figure 1.1.

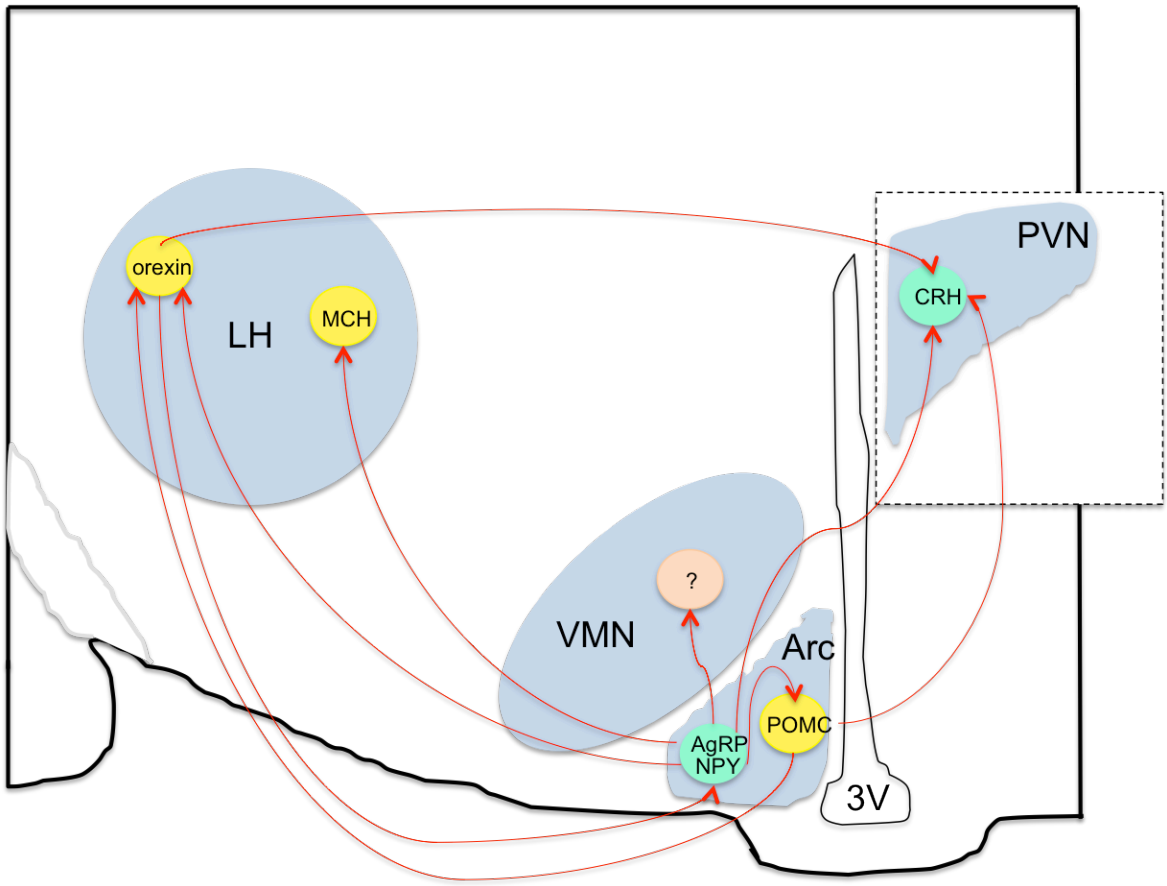

Figure 1.1 **Hypothalamic energy balance circuits.** Schematic showing the major established intra-hypothalamic connections involved in the control of energy homeostasis (red lines). The signaling molecules of the VMN have not yet been fully characterised. Yellow spheres denotes orexigenic peptides, turquoise spheres anorexigenic peptides. LH Lateral Hypothalamus, VMN Ventromedial Nucleus, Arc Arcuate Nucleus, PVN Paraventricular Nucleus. MCH Melanin-concentrating Hormone, AgRP Agouti-related Peptide, NPY Neuropeptide-Y, POMC Pro-opiomelanocortin, CRH Corticotrophin-releasing hormone.

1.3.2 Hormonal signalling in the arcuate nucleus

The Arc neurons express insulin and leptin receptors (Bruning et al 2000, Schwartz et al 1996), and insulin's anorexigenic effect is mainly mediated through the inhibition of NPY/AgRP neurons and the stimulation of POMC neurons (Morton et al 2006, Plum et al 2006). When insulin is infused into the brain, it leads to a reduction in food intake and body weight, and insulin has been proposed to serve as an adiposity signal in the brain (Porte & Woods 1981, Woods et al 1979). As such, it provides a signal that is related to the amount of body fat and leads to long-term effect on net catabolic response. Insulin reaches the brain from the periphery under non-experimental conditions through the availability of a transporter across the blood-brain-barrier (Banks 2006). Insulin is secreted by pancreatic β-cells in response to an increase in blood glucose, for example following a meal, and plasma insulin levels correlate with adiposity (Bagdade et al 1967, Polonsky et al 1988a, Polonsky et al 1988b). Throughout the body, insulin binds to one receptor, which is

part of the tyrosine kinase receptor family (Kahn 1994), but a brain-specific knockout of the receptor leads to obesity, further implicating insulin as a signalling molecule in fuel metabolism (Bruning et al 2000) Among others, the biological actions of insulin includes the stimulation of glucose transport into skeletal muscle and adipose tissue, and the suppression of hepatic glucose production (Kahn 1994). In addition, insulin signalling affects regulation of neuropeptide transcription and release, through which the hormone also mediates its role in central control of energy homeostasis and peripheral glucose metabolism (Plum et al 2006).

The other adiposity signal identified to date is leptin, which was discovered in 1994 as the product of the *ob* (obese) gene (Zhang et al 1994). Leptin is released into the bloodstream by white adipose cells, in direct proportion to body fat content (Frederich et al 1995, Maffei et al 1996). When the leptin gene (*ob/ob*) or its receptor (db/db) is mutated, the animal exhibits an extreme obese phenotype and the development of diabetes (Chen et al 1996, Zhang et al 1994). The loss-of-function mutation in the leptin gene occurs spontaneously in humans (but is very rare), and leads to the development of early-onset obesity, which can be successfully rescued by leptin replacement therapy (Farooqi et al 1999, Montague et al 1997). When the leptin receptor is selectively knocked out only in the brain, a phenotype that resembles that of the *db/db* mouse is produced (Cohen et al 2001), indicating that leptin's role in energy homeostasis is mediated entirely through its actions in the central nervous system. In support of this, when leptin is given centrally it reduces food intake and body weight in several species, further underlining the hormone's pivotal role in the regulation of energy homeostasis (Schwartz et al 2000).

Ghrelin is another hormone that has been linked to a neuronal population in the Arc, namely the NPY neurones. Ghrelin is a potent orexigenic peptide that is mainly secreted from the stomach (Kojima et al 1999). The peptide was first discovered as a natural ligand for the growth hormone secretagogue receptor (GHSR) (Kojima et al 1999), and the receptor is expressed in almost all NPY neurons of the Arc (Willesen et al 1999, Zigman et al 2006). A role for ghrelin in entero-hypothalamic signaling has been established (Nakazato et al 2001), and central and peripheral administration has been seen to increase food intake and adiposity in both rodents (Asakawa et al 2001, Tschop et al 2000) and in humans (Rodriguez et al 2009, Wren et al 2001a). The plasma concentration of ghrelin rises shortly before and falls shortly after every meal in humans, suggesting a possible role in meal initiation (Cummings et al 2001). In addition, chronic central administration of ghrelin leads to an increase in cumulative food intake and a decrease in energy expenditure, and finally body weight gain (Nakazato et al 2001, Tschop et al 2000, Wren et al

2001a, Wren et al 2001b). Ghrelin does not stimulate feeding in the NPY/AgRP double knockout mice, indicating the importance of the activation of these neurons in ghrelin's orexigenic effect (Chen et al 2004). In this way, the lack of ghrelin or its receptor acts as protection against the development of early-onset obesity (Wortley et al 2005, Zigman et al 2005) and the deletion of both hormone and receptor leads to an increase in energy expenditure (Pfluger et al 2008). Since both ghrelin and NPY have strong orexigenic properties, the axis between ghrelin-releasing cells in the stomach and Arc NPY neurons, with subsequent NPY release, may be an essential pathway in feeding.

A second gut hormone that has been implicated in signalling in the Arc is PYY, which is released from specialised enteroendocrine cells called L-cells in the intestine following a meal, mainly in the shortened form of PYY_{3-36} (Adrian et al 1985). PYY_{3-36} is a selective agonist for the NPY receptor NPY-Y2R, its binding leading to an inhibition of food intake both when the hormone is of endogenous and exogenous origin (Abbott et al 2005, Batterham et al 2002). Y_2R is expressed on NPY/AgRP Arc neurones and acts as an autoreceptor inhibiting their activity, and thereby inhibiting food intake (Abbott et al 2005). In support of this, when the activity of the Y_2R is blocked by a selective antagonist (BIIE0246), it leads to an increase in food intake, implicating a role for the receptor in meal cessation (Abbott et al 2005, Scott et al 2005).

1.4 Nutrient sensing in the hypothalamus

The hypothalamus is thought to be the primary site for convergence and integration of nutrient signals; including central and peripheral neuronal signals, as well as hormonal inputs (Sanchez-Lasheras et al 2010). In addition to adiposity signals from leptin and insulin, publications indicate that glucose and lipids are detected by specialist nutrient-sensing neurons in the hypothalamus, and that circulating nutrients work together with hormones like leptin, insulin and ghrelin to regulate the hypothalamic neural circuits involved in energy homeostasis.

1.4.1 Glucose signalling

Glucose-sensitive hypothalamic neurons were identified in the 1960s, and were shown to regulate their firing rate in response to fluctuations in extracellular glucose (Anand et al 1964, Oomura et al 1969). Glucose-sensing neurons can either increase their firing rate in response to glucose, being glucose excited or GE, or they can decrease their firing rate, being glucose inhibited or GI (Oomura & Yoshimatsu 1984). GE and/or GI neurons have been identified in several hypothalamic

nuclei involved in the control of energy homeostasis, including the Arc, the VMN (where they are especially abundant), the PVN and the LH (Silver & Erecinska 1998), as well as in the brain stem, especially in the nucleus of solitary tract (NTS) (Marty et al 2007). The NTS is sensitive to small fluctuations in blood glucose concentrations, and is thought to regulate the activity of hypothalamic neurons, integrating signals from the periphery and the hypothalamus, as the NTS neurons project widely into nuclei implicated in glucose regulation (Norgren 1978). The Arc NPY/AgRP and POMC populations have both been identified as glucose-sensing neurons. Specifically, electrophysiological recordings have shown that NPY/AgRP neurons are inhibited by increasing glucose concentrations, while the same activates POMC neurons (Fioramonti et al 2007, Ibrahim et al 2003, Mountjoy et al 2007, Muroya et al 1999). Both Arc populations have wide projections to the LH, which also contains two glucose-sensing populations, namely the orexin-expressing and the melanin-concentrating hormone (MCH) neurons. MCH neurons are GE and orexin neurons are GI, while both receives inputs from NPY/AgRP and POMC neurons (Broberger et al 1998, Burdakov et al 2005b, Elias et al 1998).

Circulating levels of glucose drop before food intake initiation (Louis-Sylvestre & Le Magnen 1980), and when the drop is counteracted by glucose infusion, meal initiation is suppressed (Campfield et al 1985). When infused in the hypothalamus, glucose has an anorectic effect and leads to a decrease in body weight (Davis et al 1981, Kurata et al 1986, Panksepp & Rossi 1981). On the other hand, when glucose metabolism is inhibited by central administration of 2-deoxy-glucose (2DG), an analogue to glucose, food intake is induced (Berthoud & Mogenson 1977, Miselis & Epstein 1975). As mentioned above, glucose-sensing populations have been identified in the PVN and Arc. When these populations are destroyed by immunotoxin, the feeding response to peripheral 2DG is ameliorated (Ritter et al 2001), and 2DG injection also has a suppressing effect of the regulation of NPY and AgRP (Fraley & Ritter 2003). However, it is unclear how important NPY/AgRP neuronal populations are in the glucose-induced reduction in feeding. A study by Luquet et al (2007) found that when these neurons were destroyed in neonatal mice, the feeding response to glucoprivation was unaffected (Luquet et al 2007). In fact, earlier findings by this group showed that the ablation of NPY/AgRP neuronal populations in neonatal mice had little effect on feeding behaviour, which is in contrast to their findings in adults with the same populations destroyed, highlighting the plasticity in this circuitry (Luquet et al 2005).

Glucose is also involved in energy expenditure, and it's thermogenic effects are most likely mediated through the hypothalamic glucose-sensing neurons. Injections either into the carotid

artery, or directly into the ventromedial hypothalamus and the PVN increase the activity of sympathetic efferents to brown adipose tissue (Sakaguchi & Bray 1987, Sakaguchi & Bray 1988). It is also thought that the hypothalamus regulates hepatic glucose production, which needs to be suppressed when glucose availability is high (Rother et al 2008); that is, when hypothalamic glucose concentrations are high, gluconeogenesis and glycogenolysis are reduced (Lam et al 2005).

One of the most important roles of glucose sensing in the brain is the initiation of the counter-regulatory response (CRR) to hypoglycaemia, which specifically involves the activation of glucagon release from the pancreas and catecholamines from the adrenal glands (Cryer 2004, Mitrakou et al 1991, Taborsky et al 1998). Hypoglycaemia can be experimentally induced by either insulin infusion or injection of 2DG; glucoprivation is detected by peripheral receptors, and the information then forwarded to the brainstem and the hypothalamus. However, these brain areas can also be directly activated by hypoglycaemia. Lesion studies have identified hypothalamic nuclei involved in CRR, in particular the VMN (Frizzell et al 1993). Glucagon secretion can be induced by 2DG injection directly into the VMN (Borg et al 1995), while glucose infusion in the VMN can abolish the hypoglycaemia-induced glucagon release (Borg et al 1997). More recently, human hyperinsulinemic clamp studies have shown that the hypothalamus is sensitive to small changes in circulating glucose, and that hypothalamic neuronal activation precedes the CRR to hypoglycaemia, as imaged by an increase in blood flow (Page et al 2009).

1.4.2 Central lipid sensing

Evidence for a role for fatty acids as cellular messengers in the central nervous system is mounting, suggesting that fatty acids act much like glucose to relay the body's energy status to the brain and specifically to the hypothalamus, which contains lipid-sensing neurons. Initially it was thought that fatty acids could not cross the blood-brain-barrier, but in recent years it has become clear that cerebral lipids arise from both local synthesis and plasma origin. Fatty acids cross the blood-brain-barrier mainly through diffusion and levels in the brain are therefore a reflection of plasma concentrations (Miller et al 1987, Rapoport 1996), but uptake also occurs through lipoprotein receptors (Qi et al 2002, Rapoport 2001). In the cell, fatty acids are rapidly synthesised into fatty acyl-coenzyme A (acyl-CoA) via a process that is catalysed by the enzyme acyl-CoA synthetase (ACS).

A study using c-Fos immunreactivity as a neuronal marker for activation showed that lipid infusion activated neurons in LH, while neurons in the Arc, DMN, VMN and PVN were inhibited by fatty acids (Cruciani-Guglielmacci et al 2004). Specifically, neurons in the Arc modify their neuronal firing rate in response to fatty acids and these effects are dependent on extracellular glucose levels (Wang et al 2006). The physiological relevance of lipid sensing is supported by the fact that intravenous infusion of lipids reduces food intake in baboons (Woods et al 1984), an effect that is independent of changes in plasma insulin and gastrointestinal absorption (Matzinger et al 2000, Monnikes et al 1997, Schwartz et al 1999a, Woods et al 1984). In addition, central administration of the long-chain fatty acid oleic acid inhibits food intake and leads to a decrease in hepatic glucose production (Morgan et al 2004, Obici et al 2002). It is thought that the anorectic effect of oleic acid is due to its action on orexigenic Arc neuropeptide expression, leading to a suppression of *agrp* and *npy* mRNAs.

The metabolism of fatty acids is thought to be crucial in relaying the central action of fatty acids on energy homeostasis, and the process involves three key enzymes: acetyl-CoA carboxylase (ACC), fatty acid synthase (FAS) and malonyl-CoA decarboxylase (MCD) (Kahn et al 2005, Lopez et al 2006), and these enzymes are all expressed in Arc, VMN and DMN neurons (Sorensen et al 2002). Evidence from pharmacological and genetic studies show that when altered the activity and expression levels of these enzymes have a modulating effect on food intake (Chakravarthy et al 2007, Loftus et al 2000, Lopez et al 2006, Minokoshi et al 2004, Obici et al 2003, Wolfgang & Lane 2006).

1.4.3 Integration of signals

One of the main intracellular proteins involved in the integration of nutritional and hormonal signals in the brain is 5'-AMP-activated protein kinase or AMPK (Cota et al 2006, Kahn et al 2005, Lage et al 2008, Minokoshi et al 2004, Ropelle et al 2008b, Xue & Kahn 2006), and hypothalamic modulation of AMPK has regulatory effects on the expression of both orexigenic NPY and AgRP, and anorexigenic POMC peptides in the Arc. First described in 1980s (Carling & Hardie 1989), AMPK is a heterotrimeric enzyme complex made up with one catalytic (α1 or α2), and two regulatory (β1 or β2 and γ1 or γ2 or γ3) subunits (Woods et al 1996). The signals from leptin, ghrelin, glucose and fatty acids are mediated through the modulation of AMPK (Kola et al 2005, Lopez et al 2008, Minokoshi et al 2004, Minokoshi et al 2002). Further, fasting induces hypothalamic AMPK activity, while food intake inhibits its activity (Hayes et al 2009, Minokoshi et al 2004) and leptin exerts its hypothalamic effects by suppressing AMPK-α2 activity, leading to a

reduction in food intake (Andersson et al 2004, Minokoshi et al 2004). The anorexigenic effect of hypothalamic suppression of AMPK activity is mediated by at least two mechanisms: first, through the activation of ACC, leading to the conversion of acyl-CoA into malonyl-CoA (high levels of malonyl-CoA leads to the translocation of fatty acids across the mitochondrial membrane) (Loftus et al 2000, Obici et al 2003), and secondly, through the activation of mammalian target of rapamycin (mTOR) and phosphorylation of p70S6 kinase and 4E-binding protein 1 (Ropelle et al 2008a, Ropelle et al 2008b). It is through these pathways that AMPK inhibits NPY/AgRP neurons and activates POMC neurons in the Arc (Minokoshi et al 2004).

Central administration of glucose decreases the ratio of ATP to AMP (Cha et al 2008), which is used by the cell to sense energy availability, and leads to a reduction in hypothalamic AMPK phosphorylation and, therefore AMPK activity in fasted rats (Kim et al 2004). In addition, an increase in hypothalamic glucose from the diet leads to decreased AMPK phosphorylation followed by an increase in ACC activity, malonyl-CoA and fatty acid synthesis (Wolfgang et al 2007). There is also evidence that supports a role for fatty acids in the modulation of hypothalamic AMPK. In animals fed a high-fat diet containing high levels of polyunsaturated fats, the weight gain was significantly lower than in animals fed high-fat diet containing a mix of poly- and monounsaturated fats as well as saturated fats, and there was also a decrease seen in hypothalamic *npy* and *ampk- α2* mRNA levels (Jia et al (2009), only abstract available in English). In addition, a study found that a docosahexaenoic acid-enriched (an Omega-3 fatty acid) diet in rats lead to a reduction in hypothalamic levels of AMPK phosphorylation when compared with rats on a normal chow diet (Gomez-Pinilla & Ying 2010).

1.5 The importance of the VMN

The link between VMN, situated in the ventromedial hypothalamus close to the Arc, and the regulation of energy homeostasis has been known for over 50 years. But, in contrast with the Arc, the way in which the VMN mediates its regulatory role is still largely unknown (McClellan et al 2006, Schwartz et al 1999b). Early lesion studies, ablating the VMN bilaterally, were shown to induce immediate hyperphagia and lead to the development of obesity to a larger extent than seen following similar PVN lesion (Anand & Brobeck 1951). However, later criticism pointed out that the lesions would have included the neighbouring Arc or fibres *en passage* and that, thus, the results were not conclusive (Gold 1973). Also, the discovery of NPY/AgRP and POMC neuronal circuits in the Arc lead to a focus on this nuclei over the VMN, with models of energy balance

regulation being developed without taking the VMN into consideration (Berthoud & Morrison 2008, Broberger 2005). Nonetheless, later studies involving chemical lesions, gene therapy and pharmacological approaches have confirmed the importance of the VMN and the nucleus's negative effect on food intake and positive effect on energy expenditure (Bagnasco et al 2002, Satoh et al 1999, Tejwani & Richard 1986). Finally, more recent studies have clarified the role of the VMN through the development of knockout mice lacking the steroidogenic factor 1 (SF-1) (Majdic et al 2002, Zhao et al 2004). This transcription factor is only expressed in the VMN in he brain (as well as the gonads and adrenal glands), and it is crucial for normal development of the nucleus. The knockout mouse displays late-onset obesity, thus confirming the importance of the VMN in normal body-weight regulation. However, the precise role of the VMN is still largely unknown.

The VMN has relatively few afferent projections from the Arc in comparison to the PVN and LH. Nonetheless, NPY and MC_4 receptors are widely expressed in the VMN, and NPY injection into the VMN has a potent orexigenic effect, while NPY suppression attenuates VMN-lesion induced hyperphagia (Dube et al 1995, Jolicoeur et al 1995). More recent publications have, however, indicted that the VMN- and Arc-mediated effects on energy balance are likely to be independent (Balthasar et al 2004, Dhillon et al 2006). These studies showed that the SF-1-driven knock out of the leptin receptor elicited a similar obese phenotype as the POMC-drive knock out, and that a double knock out leads to an additive severity of the ensuing obesity. Taking this into consideration, it appears that the convergence of Arc and VMN energy balance pathways is minimal. It also suggests that the VMN is another target for leptin anorexic effects.

The neuronal populations of the VMN have yet to be characterised. However, sub-populations have been shown to respond to circulating peripheral signals, including leptin, ghrelin, insulin and glucose, signalling the energy status of the body to the brain. Leptin and insulin has a positive effect on VMN neuronal activation, presumably by targeting of catabolic cell types, although leptin has the opposite effect in overfed mice (Davidowa & Plagemann 2000). A subset of VMN neurons have also been shown to respond to fluctuations in extracellular glucose concentrations by altering their firing rate and exhibiting a primary sensitivity range between 0.5-3.5mM (Oomura 1983, Silver & Erecinska 1998), tightly correlating to plasma glucose concentrations and fluctuating around one tenth of the circulating level (Silver & Erecinska 1994). Approximately 30% of VMN neurons are glucose sensing, of which the majority are considered GE (Silver & Erecinska 1998, Song et al 2001). However, an important smaller GI population of the VMN is inferred from

the fact that local 2DG-induced hypoglycaemia produced by infusion directly into the VMN triggers the CRR to glucoprivation, characteristic of systemic hypoglycaemia (Borg et al 1995).

Although these advances have been made in the understanding of the role the VMN plays in energy homeostasis, the underlying mechanisms are still poorly understood. One of the major obstacles in furthering the understanding is the lack of appropriate specific markers for VMN neurons, the availability of which in the Arc, PVN and LH have lead to rapid appreciation of their functions. However, recent molecular biology studies have led to some discoveries of VMN-enriched genes (Kurrasch et al 2007, Segal et al 2005). From these studies, the robustly VMN-expressed neuropeptides pituitary adenylate cyclase-activating polypeptide (PACAP) and brain-derived neurotrophic factor (BDNF) have emerged as promising candidates that have both been implicated in energy balance.

PACAP is a member of a superfamily of bioactive peptides that also includes vasoactive intestinal peptide (VIP), glucose-dependent insulinotropic polypeptide, growth hormone-releasing hormone, peptide histidine-methionine and secretin (Sherwood et al 2000). PACAP was discovered in 1989, when it was found to stimulate cyclic adenosine monophosphate formation in rat pituitary cells (Miyata et al 1989). Since then, PACAP has been found to have multiple functions in the brain, which is extensively reviewed in the literature (Vaudry et al 2009). Notably, there is convincing evidence indicating an important role for PACAP in the regulation of energy homeostasis. When administered into the brain, PACAP reduces food intake in rodents (Hawke et al 2009, Mizuno et al 1998b, Morley et al 1992, Mounien et al 2008, Resch et al 2011), while fasting lowers levels of *pacap* mRNA in the ventromedial hypothalamus (VMH) (Hawke et al 2009). In addition, genetic impairment of PACAP signalling disrupts carbohydrate and lipid metabolism, glucose handling and brown adipose tissue thermogenesis (Adams et al 2008, Gray et al 2001, Gray et al 2002, Hashimoto et al 2000). It is unclear whether the closely related neuropeptide, VIP, is involved in the regulation of metabolism also. Central administration of VIP has previously been shown not to have an effect on food intake in mice (Mounien et al 2008), though it may reduce food intake in other species, including in rat (Ghourab et al 2011), goldfish (Matsuda et al 2005) and chick (Tachibana et al 2003).

BDNF is a growth factor that, together with its tyrosine-kinase receptor (TrkB), also is expressed widely in the brain, but particularly in the hippocampus and hypothalamus. It is indicated to play a crucial role in neuronal development and synaptic plasticity (Huang & Reichardt 2001), as well as being involved in food intake regulation (Binder & Scharfman 2004). Central BDNF administration

causes a reduction in feeding (Wang et al 2007), increases energy expenditure and alleviates hyperinsulinaemia in genetic and acquired models of obesity and leptin resistance (Nakagawa et al 2003). The BDNF null mutant is not viable (Ernfors et al 1994). However, further evidence supporting the importance of BDNF in energy homeostasis comes from the obese phenotype seen in the $BDNF^{+/-}$ heterozygote (Kernie et al 2000), in animals where BDNF has been conditionally deleted postnatally (Rios et al 2001), or deleted selectively in the ventromedial hypothalamic region (Unger et al 2007). In humans, it has been reported that a *de novo* missense mutation in the TrkB receptor gene, that disrupts downstream activation of signaling targets, leads to hyperphagia and severe obesity in the individual (Yeo et al 2004). In WAGR syndrome (involving Wilms tumour, Aniridia, Genitourinary abnormalities and mental Retardation) patients, where large parts of chromosome 11 have been deleted, 100% of individuals develop obesity by the age of ten, if the chromosomal truncation includes loss of the *bdnf* gene; if not, the incidence of obesity falls to 20% (Han et al 2008). There are also numerous publications linking a common single-nucleotide polymorphism in the human *bdnf* gene, such as the Val66Met polymorphism with higher body-mass index (Beckers et al 2008, Chen et al 2006, Skledar et al 2011, Speliotes et al 2010b, Thorleifsson et al 2009), including an association study of almost 250,000 individuals that identified *bdnf* as a genetic locus linked to obesity susceptibility in humans (Speliotes et al 2010b). Taken together, these publications confirm that BDNF has a role in metabolic regulation.

The proposed connections and positions of PACAP and BDNF in the established signaling network in the hypothalamus is illustrated in Figure 1.2, and the expression of PACAP receptors $VPAC_2$ and PAC_1, along with the BDNF receptor TrkB, are shown in Figure 1.3.

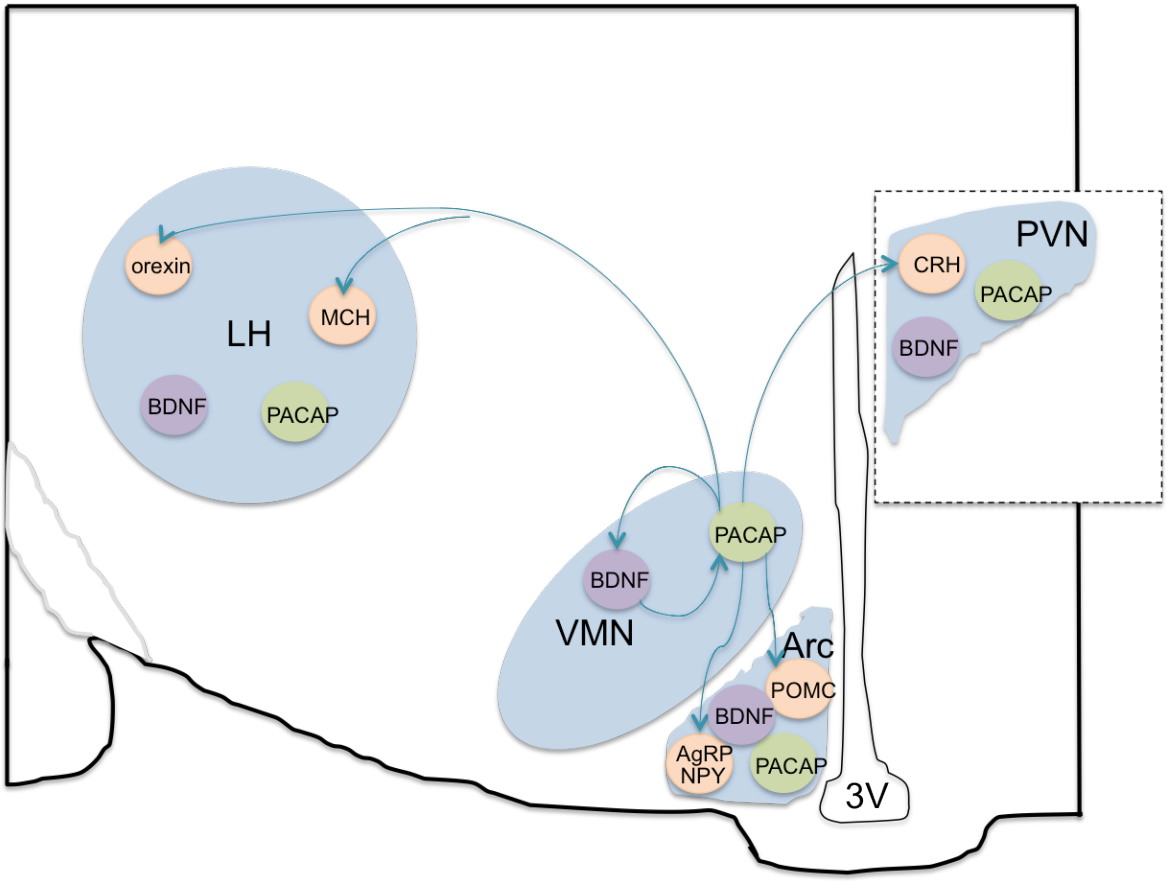

Figure 1.2 **PACAP and BDNF in the hypothalamic energy balance circuits.** Proposed positioning of PACAP and BDNF within the established signaling circuitry regulating energy homeostasis, blue lines indicate possible connections. LH Lateral Hypothalamus, VMN Ventromedial Nucleus, Arc Arcuate Nucleus, PVN Paraventricular Nucleus. MCH Melanin-concentrating Hormone, AgRP Agouti-related Peptide, NPY Neuropeptide-Y, POMC Pro-opiomelanocortin, CRH Corticotrophin-releasing hormone, PACAP Pituitary Adenylate Cyclase-activating Peptide, BDNF Brain-derived Neurotropic Factor.

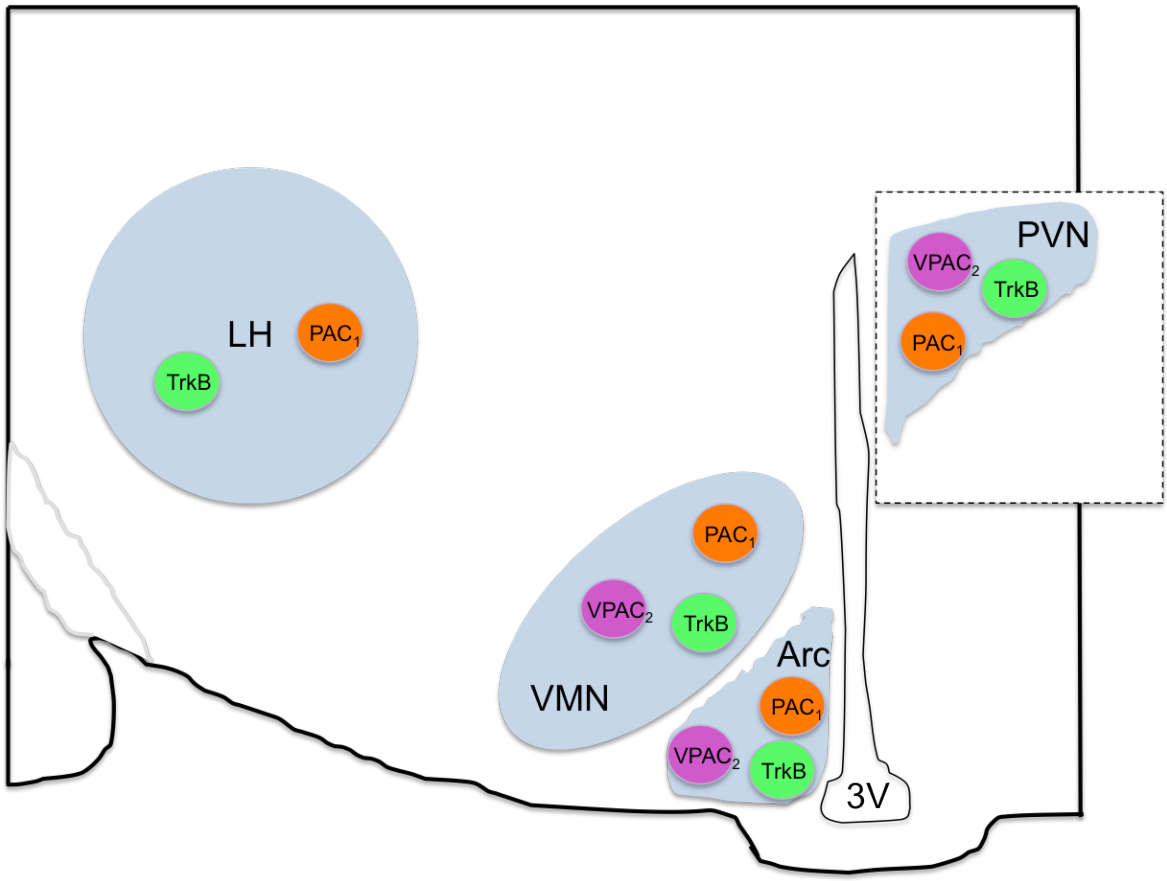

Figure 1.3 **Hypothalamic receptor placement.** The expression of PACAP and BDNF receptors in the hypothalamus. LH Lateral Hypothalamus, VMN Ventromedial Nucleus, Arc Arcuate Nucleus, PVN Paraventricular Nucleus. $VPAC_2$ and PAC_1 are PACAP receptors, TrkB binds BDNF.

1.6 PhD aims and objectives

- Evaluate the effect of metabolic manipulation in the form of fasting and high-energy diet on the gene expression of PACAP and BDNF and the effect on glucose tolerance.

- Examine the sensitivity of PACAP neurons to metabolic signals, concentrating on glucose and leptin, through the use of transgenic mouse models, immunohistochemistry, electrophysiology and Ca^{2+} imaging.

- Look closer at the anorectic effects of PACAP and the peptide's downstream targets, including the corticotrophin-releasing hormone, melanocortin and oxytocin pathways, as well as identifying the involved PACAP receptors.

- Utilise a systems-genetics approach, looking at diet-induced obesity in recombinant inbred mouse strains, in an attempt to tease apart underlying networks of genes contributing to the development of obesity and identify new gene targets.

Chapter 2. General Methods

2.1 Animals

Unless otherwise stated, experiments were performed using adult male CD-1 mice (35-40g, Harlan, UK). Animals were maintained on a 12:12 light:dark cycle at 22 ± 1 ^{o}C with 45 ± 10% humidity, and access to food (standard rodent chow; Beekay, UK)and tap water *ad libitum*. All experiments were performed in accordance with the Animals (Scientific Procedures) Act (1986) and local ethical review.

The high-energy diet (HED) used in certain experiments contains 5.12 kcal/g, of which 60% comes from fat (58Y1; TestDiet, USA). Detailed information on ingredients and nutritional profile can be found at the TestDiet website http://www.testdiet.com/Diets/High-Fat-DIO/VanHeek-Series/index.htm where the 58Y1 diet fact sheet PDF is linked.

2.1.1 Generation of transgenic mouse lines

All genotyping, identification and breeding schedules were performed/designed by me, while the animal house staff supplied the day-to-day husbandry of the animals.

$VPAC_1$ knockout mouse

Receptor $VPAC_1^{-/-}$ (*Vipr1*$^{-/-}$) null mutant mice were generated by Deltagen Inc. through the insertion of a LacZ cassette into the *vipr1* gene in embryonic stem cells by homologous recombination, thus repressing the gene. $VPAC_1$ (*Vipr1*; stock T673) were supplied via the Frozen Embryo & Sperm Archive, MRC Harwell. The mice were maintained on a mixed C57BL/6/129 background. For genotyping protocol see section 2.3.1.

$VPAC_2$ knockout mouse

$VPAC_2^{-/-}$ (*Vipr2*$^{-/-}$) mice were obtained from Professor Hugh Piggins (University of Manchester), and were maintained on a C57BL/6 background. The methods followed for generating these mice have been described previously (Cutler et al 2003). For genotyping protocol see section 2.3.1.

Adcyap1-eGFP mouse

Adcyap1-eGFP mice were developed by the Mutant Mouse Regional Resource Centre (http://www.mmrrc.org/strains/12011/012011.html). They were generated through the injection of a modified BAC, containing inserted EGFP upstream of targeted gene (*adcyap1*), into pronuclei of FVB/N fertilized oocytes. The hemizygous progeny were mated to Swiss Webster mice each generation, thereafter, and a colony maintained in house. Insertion of the eGFP gene upstream of the targeted gene allows cells containing transcribed PACAP to fluoresce. For genotyping protocol see section 2.3.1.

Pacap-i-Cre mouse

The laboratory of Professor Brad Lowell generated the Pacap-i-Cre line by using homologous recombination to insert IRES-Cre-recombinase (i-Cre) into the mouse genome downstream of the PACAP gene (Adcyap1), on a C57BL/6 background. The colony was maintained in house as a hemizygous colony, with the $cre^{-/+}$ male mouse crossed with $cre^{-/-}$ female. For genotyping protocol see section 2.3.1.

Z/EG mouse

The Z/EG reporter mice [Tg(CAG-Bgeo/GFP); JAX #003920; (Novak et al 2000)] were obtained from the Jackson Lab, USA. They were maintained as a hemizygous colony by mating a $Z/EG^{-/+}$ with a non-carrier wild-type sibling (either gender was used). For genotyping protocol see section 2.3.1.

Pacap-i-Cre X Z/EG mouse

The male Pacap-i-Cre$^{-/+}$ mouse was mated with the female Z/EG$^{-/+}$ to produce compound heterozygotes for Pacap-i-Cre and loxGFP, so that we never produce mice that are homozygous for either transgenic allele:

Pacap-i-Cre$^{+/-}$ X loxGFP$^{+/-}$

This crossing gave offspring of 4 genotypes:

Pacap-Cre$^{+/-}$ loxGFP$^{+/-}$ (will express GFP in PACAP-containing cells)

Pacap-Cre$^{+/-}$ loxGFP$^{-/-}$ (used for breeding, if male)

Pacap-Cre$^{-/-}$ loxGFP$^{+/-}$ (used for breeding, if female)

Pacap-Cre$^{-/-}$ loxGFP$^{-/-}$ (discarded)

Cre excision removes the LacZ gene, which activates expression of the second reporter, eGFP. Resulting offspring from the cross of Pacap-i-Cre and Z/EG mice that possess both transgenes express eGFP only in PACAP cells (personal communication with Prof Lowell). For genotyping protocol see section 2.3.1.

Pacap-i-Cre X lepr flox mouse

In addition, the Pacap-i-Cre mouse can be crossed with mice with floxed alleles in order to look at cell-specific gene knockout. Prof Streamson Chua (Albert Einstein College, New York) supplied us with breeding pairs of Lepr$^{flox/flox}$ mice, which were maintained as an independent homozygous colony. In order to produce Pacap-i-Cre Lepr$^{flox/flox}$ mice, we carried out the following crosses:

Pacap-Cre$^{+/-}$ X Lepr$^{flox/flox}$

This crossing will give offspring of two possible genotypes:

Pacap-Cre$^{+/-}$ Lepr$^{flox/wt}$

Pacap-Cre$^{-/-}$ Lepr$^{flox/wt}$

The double hemizygous offspring were mated, thus: mated

Pacap-Cre$^{+/-}$ Lepr$^{flox/wt}$ X Pacap-Cre$^{-/-}$ Lepr$^{flox/wt}$

This crossing will give offspring of six possible genotypes:

Pacap-Cre$^{-/-}$ Lepr$^{wt/wt}$ (used as control)

Pacap-Cre$^{-/-}$ Lepr$^{flox/wt}$ (discarded)

Pacap-Cre$^{-/-}$ Lepr$^{flox/flox}$ (used as control)

Pacap-Cre$^{+/-}$ Lepr$^{wt/wt}$ (used as control)

Pacap-Cre$^{+/-}$ Lepr$^{flox/wt}$ (discarded)

Pacap-Cre$^{+/-}$ Lepr$^{flox/flox}$ (leptin receptor knocked out of PACAP cells)

The last genotype was used to look at the effect of the loss of the leptin receptor in PACAP-expressing cells.

For genotyping protocol see section 2.3.1.

2.2 *In Vivo* Techniques

2.2.1 Implantation of Guide Cannulae and intracerebroventricular injections

The mice were anaesthetised using 3-5% isoflurane (Baxter International Incorporated, USA) in oxygen (2000 ml/min) and nitrous oxide (1000 ml/min); during the initial anaesthesia, fur was removed from the surgical area. The animal's head was immobilised using a stereotaxic frame, with ear bars and incisor bar, while anaesthesia was maintained with 2.5% isoflurane in oxygen (1500 ml/min) and depth of anaesthesia was monitored by loss of foot-pinch reflex and by breathing rhythmicity. To achieve post-operative analgesia, at this point, the mice were administered an intramuscular injection of buprenorphine (0.03 mg/kg Vetergesic, Reckitt Benckster Healthcare, UK). A 2 cm incision was made along the midline of the cranium, and a sterile guide cannula was inserted to a depth of 1 mm through a 1.5 mm diameter hole, which was drilled through the skull 0.3 mm posterior and 1 mm lateral to bregma. To fix the cannula into the right position, acrylic dental cement (Simplex Rapide, UK) was adhered to two jewellers' screws, one positioned posterior and one anterior to the cannula. The wound was then sutured (Mersilk, Ethicon, USA) closed. Following one week of recovery housed in single cages, the animals were injected intracerebroventricularly with the drug of interest, using a 5 or 10 µl Hamilton syringe attached via tubing to an injection cannula.

2.2.2 Feeding experiments

Daytime fast-induced re-feeding study

Animals were food deprived at 17:00 on the day prior to injection, but with free access to tap water. Between 11:00 and 12:00 the next day, the animals were injected intracerebroventricularly with the drug of interest. Food was returned to the mice immediately and their food intake was measured at the time points 1, 2 and 4 hours after injection.

Daytime free-feeding study

Mice had food removed 2 hours prior to injection, after which food was returned to the cage and monitored at specific time points. Water was available *ad libitum* throughout.

Nocturnal feeding study

Mice had food removed 6 hours prior to lights off. Injection was performed immediately before lights off (19:00), after which food was returned to the cage and monitored at specific time points. Water was available *ad libitum* throughout.

2.2.3 Oral Glucose Tolerance Test

For a standard oral glucose tolerance test (OGTT), the mice were subjected to a daytime fast of 6 hours. After which, the mice were tail-clipped and their fasting glucose level was established using a glucose meter (OneTouch Ultra2 and matching glucose strips; LifeScan Inc., UK). They then received an oral gavage of glucose (2g/kg body weight in 0.6g/ml) dissolved in sterile water. The rise in blood glucose was then measured with the glucose meter at 15, 30, 60, 90 and 120 min. After the last measurement, the food was returned to the cages.

2.2.4 Tissue collection and fixation

- **Whole brain**: Following decapitation, the brain was removed immediately from the scull and frozen in isopentane kept on dry ice to preserve structure. The brains were then sealed in tin foil packages on dry ice and stored at -80 ^{o}C until use.
- **Tissue**: After culling by decapitation, relevant tissue was dissected out and immediately frozen on dry ice in plastic tubes. The tissues were stored at -80 ^{o}C until use.
- **Blood**: For serum collection, the animals were culled by decapitation and blood was collected immediately from the trunk. The whole blood was left to clot at room temperature for 30 min and then spun at 4^{o}C for 15 min at 3000*g*. The separated serum was then aliquoted and stored at -80 ^{o}C until analysed.
- **Transcardial perfusion:** Mice were deeply anaesthetised in an anaesthesia box with 5% isoflurane (Concord Pharmaceuticals Ltd., UK) in O_2 (1L/min), and then this was maintained using an anaesthetic nose cone. Following incision of the thoracic cavity, diaphragm and ribcage, a 23G butterfly needle was clamped into the apex of the left ventricle, the right auricle cut and the whole body perfused transcardially with heparinised saline (10,000units/L heparin in 0.9% NaCl), using a peristaltic pump at 10-15ml/min. When blood was fully removed, 4% paraformaldehyde (PFA; Sigma, UK) in 0.1M PB (phosphate buffer) was perfused until 5 min after contraction of limbs occurred. The entire brain was collected and post-fixed overnight in 4% PFA in 0.1M PB,

then equilibrated in 30% sucrose in 0.1M PB (BDH Laboratories, UK) for 2 days to cryoprotect the tissue. Brains were frozen on dry ice and stored at -80^{o}C.

2.3 Molecular Techniques

2.3.1 DNA Extraction and genotyping

Ear punches taken at weaning for identification of mice were used as tissue to determine the genotype of each transgenic mouse.

DNA extraction

Ear punches were stored in Eppendorf tubes at -20 ˚C until extraction. 400µl lysis buffer (50 mM Trizma pH 7.4, 100 mM EDTA, and 0.5% SDS in autoclaved water; all Sigma, UK) was added to the ear punches, together with 5µl proteinase K solution (~20 KUnits/ml; Fluka, UK). After incubation over night at 56 ˚C on a slow shaker, the samples were centrifuged at 13000 rpm for 5 min at room temperature. The cleared lysate was removed into clean, autoclaved tubes and 400µl isopropanol was added. After mixing, the samples were put on ice for ~ 60 min, and later spun at 13000 rpm for 10 min at 4 ˚C. While kept on ice, the supernatant was removed from the tubes and the pellet washed with 400 µl 70% ethanol, after which the tubes were spun again at 13000 rpm for 10 min at 4 ˚C. Following removal of the ethanol, the pellets were air dried for ~ 10 min (or until all of the alcohol had evaporated) and then resuspended in 150 µl of autoclaved water. The DNA templates were stored at -20 ˚C.

Polymerase chain reaction

The PCR master mix was prepared on ice with GoTaq Hot Start Polymerase (Promega) to a final volume of 25 µl per PCR tube. Amplification of each gene requires tailored wild-type and target primers (Table 2.1), PCR master mix (standard components Promega, UK; betaine and dimethyl sulphoxide (DMSO) Sigma, UK; Table 2.2) and PCR programs (0-Table 2.6) performed on an AB Veriti 96 well thermal cycler (Applied Biosystems, UK).

Gene	Forward	Reverse
Adcyap1	5'-GGGTGCTGGGCACACACAA-3'	N/A
eGFP	5'-GGTCGGGGTAGCGGCTGAA-3'	N/A
PACAP-i-Cre	5'-GGTCAGCCTAATTAGCTCTGT-3'	5'-GATCTCCAGCTCCTCCTCTGTC-3'
PACAP-i-Cre	5'-GCCCTGGAAGGGATTTTTGAAGCA-	5'-ATGGCTAATCGCCATCTTCCAGCA-3'
Z/EG Wild-type	5'-CTAGGCCACAGAATTGAAAGA-3'	5'-GTAGGTGGAAATTCTAGCATCATCC-3'
Z/EG Reporter	5'-AAGTTCATCTGCACCACCG-3'	5'-TCCTTGAAGAAGATGGTGCG-3'
Lepr flox	5'-AATGAAAAAGTTGTTTTGGGACGA -	5'-

Table 2.1 **Genotyping PCR primers list.** Adcyap1 and eGFP primers provided by the Mutant Mouse Regional Resource Centre, all others obtained from Sigma, UK.

Component	Adcyap1-eGFP	PACAP-i-Cre	Z/EG	Lepr flox
Buffer	5µl	5µl	5µl	5µl
$MgCl_2$	1.5µl	2µl	2µl	1.5µl
Primer 1	1µl (ADCYAP1)	1µl (Control)	1.25µl (Wild type)	1.5µl (Reporter)
Primer 2	1µl (eGFP)	1.5µl	2.5µl (Reporter)	-
dNTPs	0.5µl	0.5µl	0.5µl	1.25µl
DMSO	0.325µl	-	0.325µl	-
Betaine	6.2µl	-	6.5µl	-
GoTaq	0.2µl	0.125µl	0.2µl	0.5µl
H_2O	7.975µl	13.875µl	5.725µl	13.25 µl
DNA template	1µl	1µl	1µl	0.5µl

Table 2.2 **Genotyping PCR master mix recipes.**

Step	Temperature °C	Time	Cycles
1. Initiation/Melting	94	5:00	1
2. Denaturation	94	0:15	\
3. Annealing (Steps 2-4 will cycle in sequence)	65 to 55 (↓ 1°C/cycle)	0:30	X 40
4. Extension	72	0:40	/
5. Final extension	72	5:00	1
6. Finish	4	Hold	-

Table 2.3 **Adcyap1-eGFP genotyping PCR parameters.** A touch-Down cycling protocol is used where the first 10 cycles start with an annealing temperature at 65°C and then decreasing in temperature by 1°C every cycle until 55°C is reached. For the next 30 cycles the annealing temperature stays at 55°C.

Step	Temperature °C	Time	Cycles
1. Initiation/Melting	95	2:00	1
2. Denaturation	95	0:30	\
3. Annealing	62	1:00	X 30
4. Extension	72	1.00	/
5. Final extension	72	5:00	1
6. Finish	4	Hold	

Table 2.4 **PACAP-i-Cre genotyping PCR parameters.**

Step	Temperature °C	Time	Cycles
1. Initiation/Melting	94	1:30	1
2. Denaturation	94	0:30	\
3. Annealing	60	1:00	X 40
4. Extension	72	1.00	/
5. Final extension	72	2:00	1
6. Finish	10	Hold	

Table 2.5 **Z/EG genotyping PCR parameters.**

Step	Temperature °C	Time	Cycles
1. Initiation/Melting	94	5:00	1
2. Denaturation	94	0:30	\
3. Annealing	57	1:00	X 35
4. Extension	68	1.00	/
5. Final extension	68	10:00	1
6. Finish	4	Hold	

Table 2.6 **Lepr flox genotyping PCR parameters**

Agarose gel electrophoresis

The gel was made with 1.5 % agarose (Sigma, UK) in 1X TBE (5X TBE = Tris base, boric acid and EDTA 0.5M in autoclaved water, pH 7-8), with 2.5 µl ethidium bromide (Promega, UK) added after the agarose solution was microwaved and cooled slightly. The PCR reaction was run with a 1000 bp marker Hyperladder IV (2.5 µl to confirm product size; Bioline, UK). A 10 µl aliquot of PCR product was loaded directly in each lane, and the gel was run at 100 volts for ~ 1 hour. An image of the gel was taken using the ImageQuant™ 350 system with the ImageQuant™ Capture program (both from GE Healthcare, UK).

2.3.2 Laser-Capture Microdissection and Tissue Preparation

The laser capture microdissection (LCM) procedure was performed under RNase-free conditions using RNase inhibitor-treated (0.1M NaOH, 5% SDS) or autoclaved/sterile equipment and solutions. 20µm sections were cut from the whole brains, collected using a cryostat set at -20 ^{o}C, and mounted on PALM membrane slides (P.A.L.M. Microlaser Technologies AG, Germany) by briefly warming the back of the slide with a thumb. The slides were transferred in pairs into pre-chilled 50ml Falcon tubes and stored at -80 ^{o}C, never thawing below -20 ^{o}C until day of next step. 30 min before needed, the slides were allowed to reach room temperature and to dry out completely inside their tubes, preventing condensation forming and limiting RNase activity by avoiding a wet phase. Using the mouse brain atlas (Franklin & Paxinos 2008) for appropriate coordination, the areas of interest were cut out separately from each section using a PALM Laser Capture Microdissection microscope (P.A.L.M. Microlaser Technologies AG, Germany), collected into Eppendorf tubes and stored at -80 ^{o}C.

2.3.3 RNA Extraction and reverse transcription

Microdissected and small amounts of tissue was extracted using the RNeasy Micro Kit (Qiagen, UK), which is a spin-column based system designed to extract high quality RNA from ≤5mg tissue. The extraction was performed according to manufacturer's instructions, with the initial homogenization step performed using a vortex and the buffer provided. To verify its quality, the RNA was analyzed using a NanoDrop 3300 (Thermo Scientific, USA) and any samples with 260/280 values below 1.7 were discarded. The RNA was diluted with nuclease-free water to the volume required for the number of reverse transcription reactions needed, and then stored at -80 ^{o}C.

Larger tissue samples (i.e. >5mg tissue) were extracted using the Tri-reagent method. The cube of tissue was added to a Lysing Matrix D tube (MP Biomedicals, UK) with 1 ml Tri-reagent (Sigma, UK) and kept on ice. The sample was then homogenised in a FastPrep homogeniser (Thermo Scientific, UK) for 40 seconds at a speed of 6 m/s, and then incubated at room temperature for five minutes. 200µl chloroform was added to the tube followed by vigorous shaking for 15 seconds and incubation for three minutes at room temperature. The sample was then centrifuged at 12000 rpm for 15 minutes at 4 ˚C and 500 µl of the upper aqueous layer was pipetted out into an RNase-free tube. 500 µl of isopropanol was added to the extracted RNA, and the sample was incubated for ten minutes at room temperature, after which it was centrifuged at 12000 rpm for ten minutes at 4 ˚C. After the supernatant was removed, the pellet was washed with 1 ml ethanol (70%), and after vortexing briefly, the sample was centrifuged at 12000 rpm for five minutes at 4

˚C. All of the ethanol was removed and the pellet left to air-dry briefly for three minutes, before re-suspension in nuclease-free water (Promega, UK). The amount of RNA extracted was investigated using a NanoDrop 3300 (Thermo Scientific, USA) and any samples with 260/280 values below 1.7 were discarded. The RNA stock was stored at -80 ˚C until use.

Prior to reverse transcription, all the extracted RNA was initially DNase-treated using RQ1 RNase-Free DNase (Promega, UK) according to manufacturer's instructions, to make sure there was no contamination by genomic DNA. The reverse transcription PCRs (RT-PCR) were performed using the High Capacity RNA-to-cDNA Kit (Applied Biosystems, UK) also following manufacturer's instructions. A maximum of 2 µg RNA was used in each reaction. All cDNA was stored at -80 ^{o}C until use.

2.3.4 Primer Design and validation

The mRNA sequence for the gene transcript in question was obtained from the National Centre for Biotechnology Information (NCBI) gene database (www.ncbi.nlm.nih.gov/sites/entrez?db=gene) and was put into the web-based primer design tool *Primer3* (http://primer3.wi.mit.edu/). The size of the amplification product was limited to 80-200 base pairs, the primer size ranging between 18-30 base pairs and with melting temperature set to minimum 58 ^{o}C, optimum 59 ^{o}C and maximum 60 ^{o}C. The primers were determined to cover an exon-exon boundary, where the reverse primer was designed in the coding exon. All other parameters were kept as standard in the *Primer3* software.

To determine their specificity, the primers were run through a basic local alignment tool (BLAST, http://blast.ncbi.nlm.nih.gov/) and any primers that potentially could bind to any other sequences other than the target, with a high affinity, were discarded.

When designed, the primers were ordered from Sigma Aldrich using their web ordering system for oligonucleotides (http://www.sigmaaldrich.com/configurator/servlet/DesignTool?prod_type=STANDARD). Upon arrival the primers were re-suspended in nuclease-free water to a concentration of 100 µM, and aliquots were prepared at a working concentration of 10 µM. All were stored at -20 ^{o}C until use.

To validate the primers and estimate the PCR amplification efficiency, the slope of their standard curve was examined using the ABI PRISM 7300 Sequence Detection System (Applied Biosystems, UK). The concentrations tested were: 80, 40, 4, 0.4, 0.04 and 0.004 ng/µl. An acceptable primer

pair will have a standard curve slope varying little around -3.32, which will indicate a PCR reaction with 100% efficiency.

2.3.5 Relative Quantitative Real-Time PCR

The cDNA was processed for relative quantitative real-time PCR (qPCR) using the QuantiFast SYBR Green PCR Kit (Qiagen, UK) according to manufacturer's instructions. The primer concentration used was 0.5 µM and there was approximately 50 ng cDNA template per reaction. All reactions were performed in quadruplicates. The cycle parameters were adopted from the Qiagen kit instructions and were as follows: initial denaturation step 95 ^{o}C for 5 minutes, first cycle step 95 ^{o}C for 10 seconds, second cycle step 60 ^{o}C for 30 seconds (40-50 cycles), followed by the standard steps for dissociation curve as determined by the cycler. Any reaction with multiple peaks showing in the resulting dissociation curve, i.e. which had multiple amplification products, was discarded. The reactions were performed in the ABI PRISM 7300 Sequence Detection System (Applied Biosystems, UK).

The stable cytoskeletal protein, β-actin, was used for normalization, i.e. all samples were run using the target primers and the β -*actin* primers on the same plate. The sequences for the primer pair were as follows: (F) 5'- AGA GGG AAA TCG TGC GTG AC-3´, (R) 5'- CAA TAG TGA TGA CCT GGC CGT-3´. Relative quantification was achieved using the $\Delta\Delta^{Ct}$ method: 1) all the threshold cycle (C_t) values for the target were normalized against the C_t values for β -*actin*, 2) the normalized values for the control group were averaged, before subtraction from the normalized values (including the controls), 3) these values were then taken to the power of -2, forcing the control group values to vary around 1 and the target group values to be expressed as relative to the control group values.

2.4 Immunohistochemistry

Frozen 30µm sections from perfusion-fixed brains, containing the area of interest, were cut in the coronal plane using a freezing sledge microtome (Series 8000, Bright Instruments Ltd., UK), collected into cryopreservant (5.7mM $NaH_2PO_4H_2O$ (Fisher Scientific, UK), 44mM $NaHPO_42H_2O$, 30% ethylene glycol, 20% glycerol (all Sigma, UK) in H_2O) and stored at -20^{o}C until immunohistochemical processing.

Primary and secondary antibodies used are listed in Table 2.7 and Table 2.8 respectively.

2.4.1 Standard single-label immunohistochemical protocol

Briefly, free-floating sections were incubated with gentle agitation in 1.5% hydrogen peroxide/20% methanol in 0.1 M PB for 20 min at room temperature (RT) to deactivate endogenous peroxidases. Sections were then washed briefly in 0.1M PB and non-specific staining blocked by incubation in 5% normal serum in 0.1 M PB/ 0.3% Triton X-100 (PBT) for 1h at RT. Sections were then incubated overnight at 4°C in primary antibody diluted in 1% normal blocking serum. The following day, excess antibody was removed by washing sections in 0.1 M PBT. Sections were incubated for 2h at RT in secondary antibody diluted in 5% normal blocking serum. This was followed by 0.1 M PB washes and a further incubation for 1 h in streptavidin-biotin-horseradish peroxidase complex (Amersham Biosciences, Little Chalfont UK) diluted 1:500 in 0.1 M PB. The bound antibody-peroxidase complex was visualised using nickel-intensified diaminobenzidine (Vector Laboratories, Peterborough UK) following kit instructions. The colour reaction was followed using a microscope and terminated by repeatedly rinsing in tap water. Sections were mounted from distilled water onto glass microscope slides coated with 1% gelatine, and coverslipped using xylene-based mountant (Ralmont; WWR, Lutterworth UK), left to dry and observed using an Axiovision widefield microscope.

2.4.2 Standard single-label fluorescent immunohistochemical protocol

Brain sections were removed from cryopreservant and washed three times in 0.1M PB for 15 min. Sections were permeabilised by washing three times with PBT (1L PB, 2mL Triton-X (BDH Laboratories, UK) and 1g BSA (Sigma, UK)) for 15 min. Non-specific binding was blocked using normal serum diluted to 5% in PBT at RT for 1h. Sections were incubated in primary polyclonal antibody, diluted in 1% normal serum, overnight at 4°C. Sections were washed three times in PBT for 15 min each before a further incubation in secondary antibody, diluted in 5% normal serum, for 2h at RT. Sections were washed twice in PB and once in dH_20 for 15 min before mounting onto slides and cover slipped with Vectashield Hardset mounting medium (Vectashield, CA, USA) and set overnight. At all wash and incubation stages, the assay plate was concealed from light by aluminium foil to prevent excessive photo bleaching. Fluorescence was observed using an Olympus BX51 microscope (Olympus, UK).

Primary Antibodies	PACAP (C-19)	eGFP	c-Fos
Raised in	goat anti-PACAP	chicken anti-eGFP	rabbit anti-c-Fos
Manufacturer	Santa Cruz Biotechnologies	Millipore	Calbiochem
Dilution used	1:100	1:1000	1:8000
Normal Serum	Donkey 1%	Donkey 1%	Goat 1%

Table 2.7 **Primary Antibodies.**

Secondary Antibodies	Cy3	Cy3	Cy3
Raised in	donkey anti-sheep	donkey anti-chicken	goat anti-rabbit
Manufacturer	Millipore	Millipore	Jackson ImmunoResearch Laboratories Inc.
Dilution used	1:500	1:500	1:500
Normal Serum	Donkey 5%	Donkey 5%	Goat 5%

Table 2.8 **Secondary Antibodies**

2.5 Imaging

2.5.1 Cell dissociation

Mice were decapitated, and the brain quickly dissected and collected into a small petri dish of ice-cold artificial cerebrospinal fluid (aCSF) containing (mM): KCl 3, $CaCl_2$ 1000, glucose 15, NaCl 126

(all Sigma, UK), NaH_2PO_4 1, $NaHCO_3$ 25 (both Alfa Aesar, MA, USA), $MgSO_4$ 2 (BDH Laboratories, USA); oxygenated with O_2. The ventromedial hypothalamus was coarsely dissected, collecting a 1mm slice of the hypothalamus directly behind the optic chiasm, cut into small pieces and transferred to an Eppendorf tube containing aCSF. Under aseptic conditions, aCSF was removed and replaced with 3ml/brain area of filter-sterilised 20-25U/ml papain (Sigma, UK) in aCSF and incubated at 37^{o}C for 90 minutes. The papain solution was removed and the brain tissue transferred to a 15ml Falcon tube with 2ml of a weak inhibitor (1mg/ml BSA (Fisher Scientific, UK), 1mg/ml trypsin inhibitor (Sigma, UK) in aCSF) and gently titrated 8-10 times. 2ml strong inhibitor (10mg/ml BSA + 10mg/ml trypsin inhibitor in aCSF) was added and titration repeated before the lysate was passed through a 70µm cell strainer to clear debris. The trypsin inhibitor works to counteract the breakdown of the cells during the titration steps. The cell suspension was centrifuged for 5 min at 2500 rpm, supernatant removed and cells resuspended in 1.5ml neuronal media (450ml MEM (Gibco UK), 5% foetal bovine serum, 1% L-glutamate, 2% penicillin/streptomycin, 15mM glucose, 2% B-27 supplement; all Invitrogen, UK). Cells were then centrifuged and resuspended in 80µl neuronal media. The final cell suspension was gently pipetted onto sterile coverslips (coated in house with 200µg/ml poly-D-lysine (PDL; Millipore, UK) cut to ~7 x 16mm rectangles and contained in 12-well plates), and the cells allowed to adhere by incubating at 37^{o}C for 1 hour . Each well was then flooded with neuronal media up to a volume of 1ml and maintained at 37^{o}C before use.

2.5.2 Ca^{2+} Imaging

One aliquot of Fura-2 LeakRes (AM) (Teflabs, TX, USA) containing 50µg was dissolved in 50µl pluronic F-127, 20% solution in DMSO (Biotium, CA, USA) and added to 7mL of neuronal media (to give a final concentration of 5.5mM fura). The neuronal media was removed from the well containing dissociated cells, replaced with the 5.5mM Fura and incubated for 10 min at 37^{o}C to allow uptake of the dye into the cells. The solution was removed and replaced with fresh neuronal media for at least 30 min. The cover slip was transferred to the recording chamber of the microscope rig (Olympus BX51WI with a dedicated fluorescence water immersion objective), containing artificial cerebrospinal fluid (aCSF) with 10mM glucose, and allowed to equilibrate for 1 hour (Mendieta-Zeron et al 2008). Recording using FIRSTD – OptoFluor metaimaging system software (Cairn Research, UK) was started and aCSF washed over cells at 2.5ml/min, with glucose concentration changed during the recording period (5mM, 1mM and 0.1mM) to assess the response of cells to glucose via calcium uptake and exit from the cells. Unbound fura dye can be

detected at 365nm and bound at 385nm with the Cairn Optoled LED system (Cairn Research UK), and the ratio of these readings calculated by OptoFluor to show the movement of calcium and a representation of cell activation across the time course of the experiment. Pictures were captured using an Evolve 128 EMCCD camera (Photometrics, AZ, USA) and ratio calculated automatically every 5 sec throughout the recording.

2.5.3 Patch Clamping

Slice preparation

Following deep anaesthesia with isolfluorane, the mice were decapitated. Brains were rapidly removed and the hypothalamus was sliced using a Vibroslicer (Campden Instruments, UK) into 250µm thick coronal sections whilst submerged in ice-cold incubation aCSF containing (mM): NaCl 95, KCl 1.8, KH_2PO_4 1.2, $CaCl_2$ 0.5, $MgSO_4$ 7, $NaHCO_3$ 26, glucose 15, sucrose 50, phenol red 0.5mg/l, oxygenated with 95% O_2, 5% CO_2, pH 7.4 (measured osmolality 300-310 mOsmol/kg). Brain sections were transferred into recording aCSF, and the slice to be recorded from was placed in the recording chamber to rest for 1 hour, continuously perfused with oxygenated aCSF at room temperature. Recording aCSF was identical to incubation aCSF except for the following components (mM): NaCl 127, $CaCl_2$ 2.4, $MgSO_4$ 1.3, sucrose 0, glucose 1.

Equipment and solutions

eGFP-expressing cells were viewed through a FITC filter under a 40x water immersion lens using a Leica epi-fluorescence microscope (Leica Microsystems Ltd, UK) that was linked to a fast integrating charge-coupled device camera system (also Leica Microsystems Ltd, UK) with capturing software Leica Application Suite 2.5. Thick-walled borosilicate glass capillaries (Harward Apparatus, UK) were pulled using a two-staged vertical micropipette puller (Narishige, Japan) to form patch pipette electrodes with tip resistance of 7-10 MΩ when filled with intracellular solution containing (mM): K-gluconate 130, KCl 10, $MgCl_2$ 2, K_2-ATP 2, Na-GTP 0.5, Hepes 20, ethylene glycol tetraacetic acid 0.5, pH 7.28 balanced with KOH (measured osmolality 300-310 mOsmol/kg).

Recording

Infrared-differential interference contrast was used to guide the patch pipette towards individual eGFP cells under positive pressure, and after making contact, negative pressure was applied to rupture the membrane and form the seal. Protocols designed to determine electrical

characteristics of patched cells were generated using a Micro 1401 mk II interface and Spike2 (both Cambridge Electronic Design, UK), where sequential depolarising (10 to 30 pA, 1 second duration) and hyperpolarisation (-10 to – 50 pA, 500 millisecond duration) current pulses were administered. Whole-cell current-clamp recordings were obtained using an Axoclamp 2A amplifier in bridge mode (Molecular Devices, CA, USA). Data were sampled (30kHz) and recorded with Spike2 software (version 6.00, Cambridge Electronic Design, UK). After the cell had established a consistent resting potential, 5mM or 10mM glucose dissolved in oxygenated recording aCSF was added to the recording bath medium for 2-10 minutes, and was washed off with recording aCSF containing 1mM glucose until the cell returned to its original resting potential.

2.6 Statistical analysis

Data sets were analysed using Graphpad Prism software (version 5; CA USA) using an unpaired Student's *t*-test where two groups only were compared, a one-way analysis of variance (ANOVA) followed by Bonferroni's *post hoc* tests where three or more groups were compared, or a repeated measures two-way ANOVA followed by Bonferroni's *post hoc* tests where three or more groups were compared at more than one time point. $P<0.05$ was considered statistically significant.

2.6.1 Quantitative Trait Loci (QTL) and Correlational analysis of the BXD lines

The BXD set is a recombinant inbred mouse system that is characterized by a number of related lines of defined genetic architecture and variation that approaches natural populations in complexity. The development of this system and the sophisticated analytical tools required have allowed for the analysis of phenotype, gene sequence and expression data to be explored in-depth (Gini & Hager 2012). The BXD set contains over one hundred genetically defined lines that initially was produced by crossing two well characterized progenitor strains, C57BL/6J (B) and DBA/2J (D) (hence BXD), by the Jackson Laboratory in the mid-1970s. The breeding of these mice is further explored in Chapter 5.

QTL mapping

WebQTL (http://www.genenetwork.org/webqtl) is a freely accessible system that exploits sophisticated gene-mapping methods and which includes integrated databases with both genotype and quantitative trait (phenotype) data for the BXD lines (Chesler et al 2003, Wang et al 2003). Complex trait data can be submitted by the user or retrieved from one of these integrated

databases. The first step in the analysis of new trait data is to enter it into GeneNetwork, which correlated the trait values to variation in the genotype between BXD lines, generating a QTL map for the whole genome. Where a strong association between phenotype variation and genotype could be found, a QTL is likely to be detected containing functional polymorphisms. The genomic regions with the highest correlations with trait variation are identified visually as peaks in the likelihood ratio statistic (LRS) score on the QTL map. LRS, which is a chi-square statistic, is a measurement of the association between differences in traits and differences in particular genetic markers, and estimates the significance of QTLs. LRS scores exceeding an arbitrary threshold of 13 are deemed suggestive, and significant when exceeding 25. The LRS peaks on the QTL maps are linked to the UCSC Genome Browser (Kent et al 2002) that allows easy exploration of genes or predicted genes under the peak of the QTL with the highest LRS score. The sequences of both the suggestive and significant QTLs can be mapped and analyzed using the NCBI Entrez Gene website (http://www.ncbi.nlm.nih.gov/gene) to identify potential, physiologically relevant candidate genes. These analyses were performed by Beatrice Gini in the Hager lab at the University of Manchester.

Correlational analyses

Phenotypic correlational analyses were performed following QTL mapping to determine links between multiple-related phenotypic and genotypic traits. This was done by comparing measured traits to one another and/or with archived BXD traits in the GeneNetwork database (http://www.genenetwork.org), with correlation coefficients and p values calculated using Spearman's rank tests. The results were illustrated graphically as a network map, from which it can be ascertained a) whether correlated traits have a common genetic basis, b) which traits are most highly correlated, and c) whether differences at the DNAseq level that underlie the QTL are functional.

Chapter 3. Gene expression in outbred mice following metabolic manipulation

3.1 Introduction

This chapter builds on previous findings by this lab and others (Hawke 2009b, Koza et al 2006). By looking closer at the phenomenon of heterogeneity in the response of outbred mice to high-energy diet (HED), where some animals are more susceptible to obesity than others, our laboratory found that weight gain correlated with the expression levels of specific genes in the ventromedial nucleus of the hypothalamus (VMN). In the mice resistant to diet-induced obesity (DIO), at culling there were higher levels of mRNA expression for *bdnf* and *pacap* than in mice maintained on normal chow, as measured using semi-quantitative *in situ* hybridization. By comparison, the obesity-prone mice had mRNA levels equivalent to control animals maintained on normal diet. Thus, the final body weight of mice on HED was inversely correlated with the expression of either *pacap* or *bdnf* (Figure 3.1). These data indicate that *pacap* and/or *bdnf* in the VMN may be involved in the response of mice to HED, and might act to protect against the development of DIO.

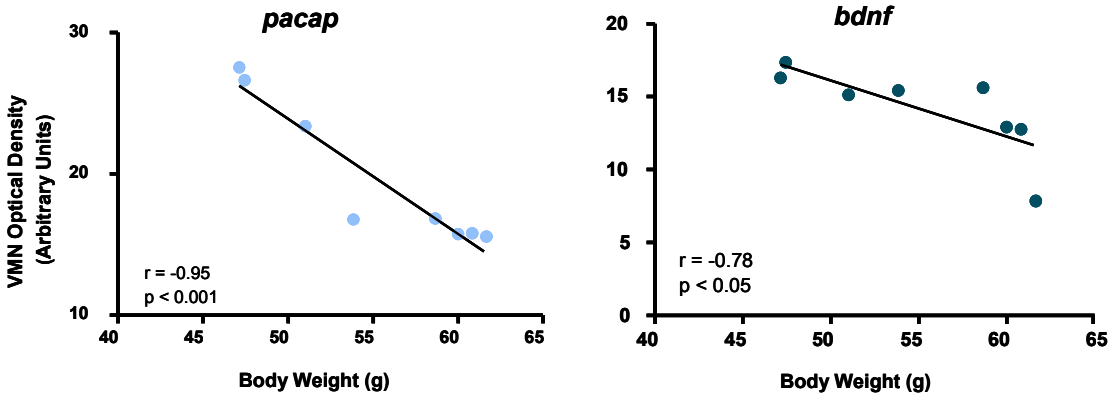

Figure 3.1 **Regulation of *pacap* and *bdnf* in the VMN.** Regression analysis relating mRNA levels, as expressed by optical density from film autoradiographs, to the final body weight of animals that had been on HED for eight weeks. n = 8.

As reviewed in chapter 1, both the arcuate nucleus (Arc) and the VMN have long been established as important in metabolic regulation. But they differ in that, for the Arc, certain neuropeptides have been identified as contributing to the phenotype of the neurons involved. The Arc sends projections from neuropeptide Y (NPY) and pro-opiomelanocortin (POMC) neurons, which carry anabolic and catabolic signals to other nuclei in the hypothalamus, respectively (Kalra et al 1999). For the VMN, however, few signaling molecules have been determined, although PACAP and BDNF are possible candidates.

The neuropeptide PACAP has multiple functions in the brain, for which there are extensive reviews in the literature (Vaudry et al 2009). There is also convincing evidence indicating an important role for PACAP in the regulation of energy balance. When centrally administered, PACAP reduces food intake in rodents (Mizuno et al 1998b, Morley et al 1992). Also, genetic impairment of PACAP signaling disrupts carbohydrate and lipid metabolism, glucose handling and brown adipose tissue thermogenesis (Adams et al 2008, Gray et al 2001, Gray et al 2002, Hashimoto et al 2000). Though PACAP is expressed in many parts of the brain, and in the sympathetic nervous system, a role for the population in the VMN is suggested since fasting lowers and leptin increases the expression of *pacap* mRNA in this nucleus (Hawke et al 2009).

BDNF is also expressed widely in the brain, but particularly in the hippocampus and hypothalamus, and is indicated to play a crucial role in neuronal development and synaptic plasticity (Huang & Reichardt 2001), and food intake regulation (Binder & Scharfman 2004). Central administration of the growth factor causes a reduction in feeding (Wang et al 2007), increases energy expenditure and alleviates hyperinsulinaemia in genetic and acquired models of obesity and leptin resistance (Nakagawa et al 2003). Further evidence supporting the importance of BDNF in energy homeostasis comes from the obese phenotype seen in the $BDNF^{+/-}$ heterozygote (Kernie et al 2000, Rios et al 2001, Unger et al 2007). Taken together, these publications confirm that BDNF has a role in metabolic regulation.

The factors that regulate *bdnf* and *pacap* at a genetic level are unknown. The difference seen in mRNA levels in the obese-resistant mice compared with the obese mice, shown in Figure 3.1, could have several explanations. We can hypothesize that mice prone to DIO have some difference or defect in their ability to regulate the expression of *bdnf* and *pacap*, such that the genes are not switched on and that the neuropeptide products, BDNF and PACAP, are unable to counteract the effects of the diet. Alternatively, it is possible that there is a higher-level controller: a specific input to those cell types; a cell-specific transcription factor, that turns on a whole set of

counter-regulatory genes (i.e. a 'master gene') only in those cells; or an epigenetic regulator. Any of these may not be functioning correctly in the obesity-prone animal. The latter alternative, that there is epigenetic modification of these genes (and presumably others), suggests a mechanism that differs in the spectrum of diet responders. This is an interesting possibility, as there is evidence that the *bdnf* gene is modified in adult animals due to epigenesis in other brain systems. For example, in the hippocampus during long-term adult adaptation, such as fear conditioning (Lubin et al 2008) and depression (Tsankova et al 2006).

There are several different transcripts of both *bdnf* and *pacap* present in the brain, and these may be differentially regulated. The genetic organisation of the two genes is described in Figure 3.2. Up to six different splice variants of the *pacap* gene have been reported (Cummings et al 2002), and according to new definitions, up to nine transcripts of BDNF (Aid et al 2007). It is, however, unknown which transcripts are regulated, either at all or in association with energy status, specifically. The *bdnf* gene has been known to produce different transcripts for some time, by splicing different non-coding exons onto a common coding exon. From the paper by Tran et al, transcripts containing the exons I, II, IV, or VI with the common exon IX were expected to be present in the ventromedial hypothalamus (Tran et al 2006), which we have since confirmed. Since that publication, the paper by Aid et al (2007) introduced a new nomenclature for the *bdnf* gene structure, as they had discovered an additional four possible transcripts expressed in the brain. This study did not include the hypothalamus, and it is unknown which of these 'new' transcripts, containing exons III, V, VII and VIII are present in the hypothalamus. From our preliminary results (not shown) using the primers and methods reported by Aid et al (2007), none of the 'new' transcripts appear to be expressed in the VMN.

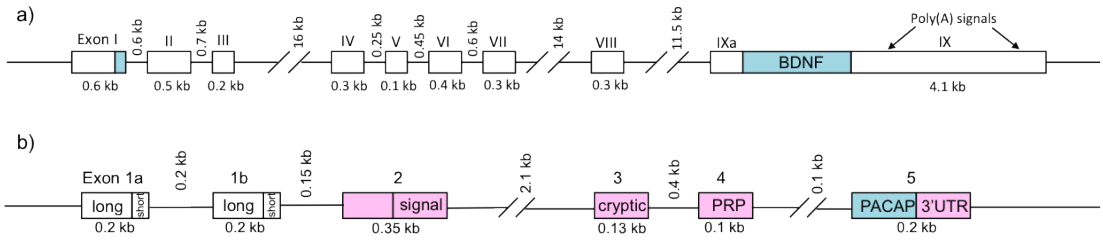

Figure 3.2 **Graphical representation of the *bdnf* and *pacap* gene.** The top a) represents *bdnf* and b) *pacap*. The boxes represent exons and the lines introns. The boxes in blue represents the coding region of each gene and the pink boxes represent related peptides encoded on the same transcript.

In this chapter, we looked at the effect of metabolic manipulation in the form of fasting and HED, on the transcription of *pacap* and *bdnf* mRNA in the VMN and Arc in outbred mice. This included

the regulation of different *bdnf* transcripts in the VMN and the addition of NPY and POMC in the Arc.

3.2 Methods

3.2.1 Animals and diets

Experiments were performed using male CD1 mice that, at beginning of experiments, were 8 weeks of age.

- **48h fasting:** A cohort of 14 mice were group housed and either fed or fasted over a 48-hour period (tap water *ad libitum)*, with their body weights monitored before and then again at culling. (n=7 per group)

- **High-energy diet:** Two cohorts of mice were group housed and either maintained on normal, control diet or HED for 8 weeks. Their body weight was measured weekly. (First cohort: n=10 control and n=20 HED; second cohort: n=9 control and n=19 HED)

3.2.2 OGTT

The first cohort of mice in the HED experiments was given OGTTs on days 0, 3, 9, 28, and 49; the second cohort only on days 0 and 49. The OGTT was performed as described in Chapter 2.

3.2.3 Serum insulin ELISA

Both cohorts of mice in the HED experiments were culled by decapitation and serum was prepared as mentioned in Chapter 2. The following ELISA was performed by Dr Garron Dodd, a post doc in the Luckman lab, to the manufacturer's instructions (Rat/Mouse Insulin ELISA; Millipore, UK) and the absorbance was read at 450 nm and 590 nm using a plate reader (Synergy™HT, BioTek) and the difference in absorbance units was recorded.

3.2.4 LCM and tissue preparation

The procedure was performed as described in Chapter 2. The brains were cut into sections starting from 1.22mm through to 2.30mm caudal of bregma (Franklin & Paxinos 2008) to cover the areas of interest i.e. the Arc and the VMN. The sections were cut onto two sets of slides, of which one set was then sampled using LCM; i.e. half the Arc and half the VMN were collected.

3.2.5 RNA extraction, reverse transcription and qPCR

The microdissected tissue was extracted using the RNeasy Micro Kit and reverse transcribed as described in Chapter 2. Primer validation method was also performed as previously described, as was the relative qPCR procedure.

To make certain that the primers would amplify all potential transcripts of *pacap, npy* and *pomc,* the forward and reverse pairs were designed to mirror sequences within the coding region and a neighbouring translating exon. For the different *bdnf* transcript primers, the forward primer was limited to fall within the desired exon (different for each transcript) and the reverse primer was limited to the coding exon IX (the same reverse primer was used for all transcripts). For the pan-*bdnf* transcript IX, the forward primer was confined within the same region (exon IX) as the reverse.

The primers used were are described in Table 3.1:

Target	Sequence Forward	Sequence Reverse
Pan-pacap	5′-CTCCAGTGCTGTTCATGCTT-3′	5′-GAGGGTCTCCAGAAAATCCA-3′
bdnf I	5′-TACCTTCCTGCATCTGTTGG-3′	5′-TTGTCCGTGGACGTTTACTT-3′
bdnf II	5′-AGCTCCGGGTTGGTATACTG-3′	5′-TTGTCCGTGGACGTTTACTT-3′
bdnf IV	5′-TCCACCAGGTGAGAAGAGTG-3′	5′-ATTCACGCTCTCCAGAGTCC-3′
bdnf VI	5′-GAAGCGTGACAACAATGTGA-3′	5′-TTGTCCGTGGACGTTTACTT-3′
bdnf IX	5′-AGAGCAGGCTCTGGAATGAT-3′	5′-TTGCTGTGCCATATTTGGAT-3′
pomc	5′-GTTCAAGAGGGAGCTGGAAG-3′	5′-GTTCTTGAAGAGCGTCACCA-3′
npy	5′-ATGCTAGGTAACAAGCGAATGG-	5′-TGTCGCAGAGCGGAGTAGTAT-3′

Table 3.1 **List of primer pairs.** The table lists the primer pairs used in qPCR experiments in this chapter. A description of the primer designing technique used is included in Chapter 2.

3.3 Results

3.3.1 Changes in mRNA expression after 48h fasting

48-hour fasting caused a significant reduction in body weights in mice, with a mean loss of more than 6 g compared with control mice that showed a slight gain (Figure 3.3.a). The fasted mice lost approximately 20% of their original body weight (data not shown).

After culling, the brains were collected and cut using the LCM method. The qPCR results showed that, in the Arc, there was a four-fold increase in *npy* mRNA levels compared with fed control mice. There was no change in expression levels for *pacap* or *pomc* (Figure 3.3.b).

In the VMN, there was a downregulation in mRNA expression for *pacap*, *bdnf* I and *bdnf* II, but an upregulation for *bdnf* VI. There was no change seen in *bdnf* IV or *bdnf* IX. The latter transcript codes for the common exon and reflects the level of total *bdnf* mRNA. This did not reach statistical significance, but there was downwards trend (Figure 3.3.c).

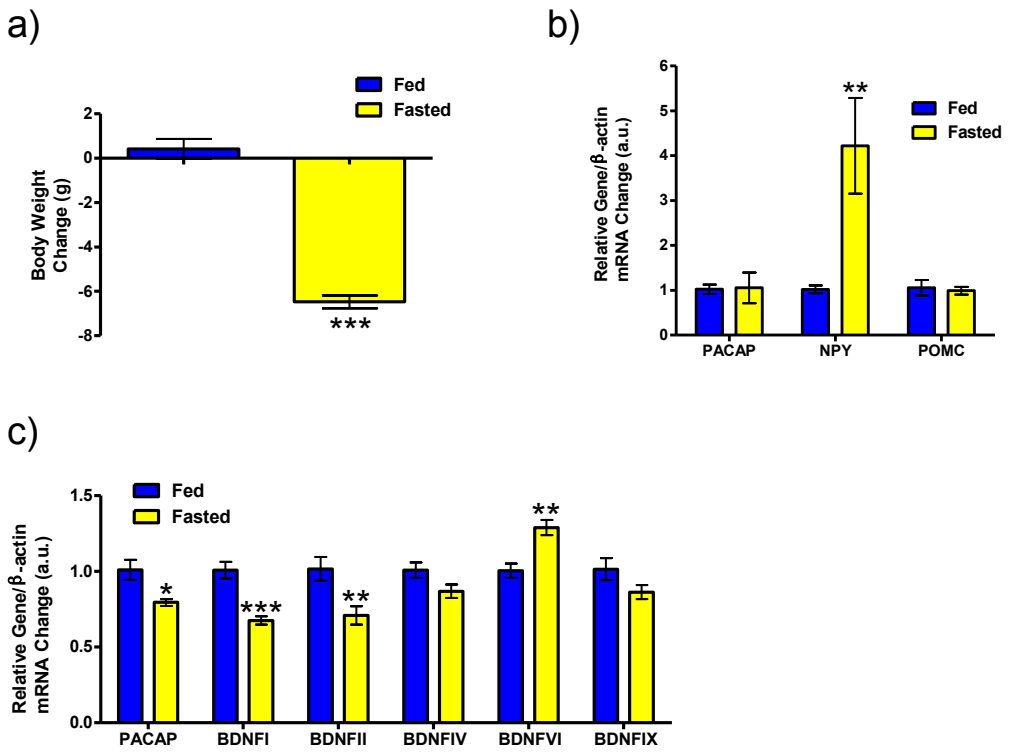

Figure 3.3 **48h Fasting Weight Loss and mRNA Expression.** The effect of 48-hour food deprivation on body-weight change (a) and mRNA expression, as measured by qPCR. In the Arc: *pacap*, *npy* and *pomc* (b) and the VMN: *pacap*, *bdnf* I, *bdnf* II, *bdnf* IV, *bdnf* VI and *bdnf* IX (c). Data are expressed as mean ± SEM. *P<o.o5, **P<0.01, *** P<0.001; Student's unpaired *t*-test. Fed n=7, fasted n=7.

3.3.2 Weight Gain after HED

Animals maintained on HED for 8 weeks were, on average, significantly heavier than chow-fed controls. However, as expected the extent of obesity varied, as has been reported previously in cohorts of outbred mice. The body-weight distribution in the HED group in both the first and second cohorts was bimodal in appearance (Figure 3.4.b and .d). Using the criteria detailed by Enriori and colleagues (2007), we further categorized the HED-fed mice by classing any mice with

a final body weight within 3 standard deviations of the mean of the control fed animals, as diet-induced obesity-resistant (DIO-R) (Enriori et al 2007). This included 50% of the mice, the rest was classified as having developed diet-induced obesity (DIO). In the first cohort, the body weights of the DIO group started to diverge from the normal-chow and DIO-R animals at day 16, and continued to do so until they were culled at day 56 (Figure 3.4.a). A similar pattern was seen in the second cohort. However, the HED groups gained less weight in the second cohort compared with the first cohort, but the data showed less in-group variance and the DIO group was seen to start diverging as early as day 7 (Figure 3.4.c).

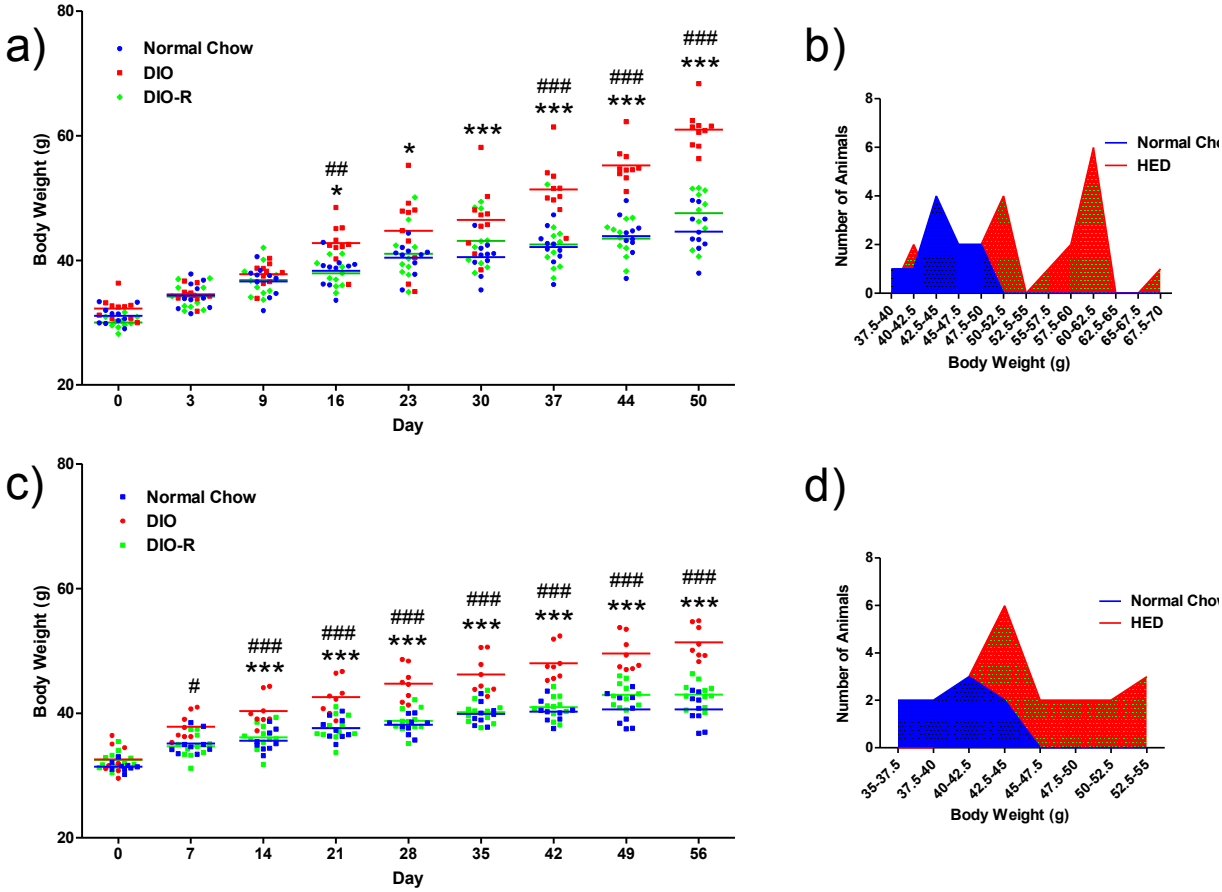

Figure 3.4 **Cumulative Body-Weight Gain and Body-Weight Group Distribution in HED Mice.** The effect of 8 weeks of normal chow or HED on body-weight gain in outbred mice. The weight gain for cohort one is shown in (a) (normal chow n=10, DIO n=10, DIO-R n=10) and the second cohort in (c) (normal chow n=9, DIO n=8, DIO-R n=11) of HED-fed animals classed DIO-R and DIO compared with normal-chow controls. Graphs on the right show final body-weight distribution, first cohort (b) (normal chow n=10, HED n=20) and second cohort (d) (normal chow n=9, HED n=19), following 8 weeks of either normal chow or HED, expressed as mean ± SEM. *P<0.05, **P<0.01, *** P<0.001; Two-way ANOVA with Bonferroni's *post hoc* test to compare all groups.*compared with normal chow, #compared with DIO-R.

3.3.3 Change in Glucose and Insulin after HED

Animals maintained on HED for 7 weeks had a reduced counter-regulatory response to an oral glucose challenge after a 6-hour fast. In the first cohort of HED-fed mice: at day 0 all the groups responded equally to the OGTT (Figure 3.5.a), but at day 3 there was significant difference between the two HED groups and the normal chow control mice at the 60 minutes time point (Figure 3.5.b). The effect was seen again for the DIO group at day 9 (Figure 3.5.c), where there was a significant difference at 30 minutes compared to the chow-controls, but was not seen for the DIO-R group although there was a trend similar to the DIO. On day 28 both the HED groups' glucose tolerance responses were significantly reduced compared with chow controls on almost all of the time points (Figure 3.5.d). At the final measuring day 49 (Figure 3.5.e), the two HED groups started to diverge with the DIO-R somewhere in between the normal chow and the DIO groups' responses, being significantly different from both at 15 minutes and from DIO at 30 minutes. Overall, the HED caused a slight shift in the OGTT response curve to the right, meaning that the mice on HED responded slower to an increase in blood glucose concentration and that the glucose level stayed higher for a prolonged period of time. At the end of the experiment, there seems to be an effect of body weight on the OGTT response in the HED groups, but no statistical significance was found (area under the curve against body weight, linear regression, r^2=0.11).

In the second cohort of HED fed mice, the reduction in the counter-regulatory response to hyperglycaemia was observed again in both HED groups (Figure 3.6.a and .c). However, the divergence in responses between the DIO and the DIO-R was not replicated. This might be due to the difference in body-weight gain between the two rounds, as seen in Figure 3.4.a and .c, where the mice on HED in the second cohort put on less weight than the mice in round one.

When the blood insulin levels where examined after culling after 8 weeks the results showed a marked difference between DIO and the other two groups, where the blood concentrations were significantly elevated compared with both normal chow and DIO-R animals (Figure 3.6.c). This increase was highly correlated with body weight in the two HED groups (Figure 3.6.d)

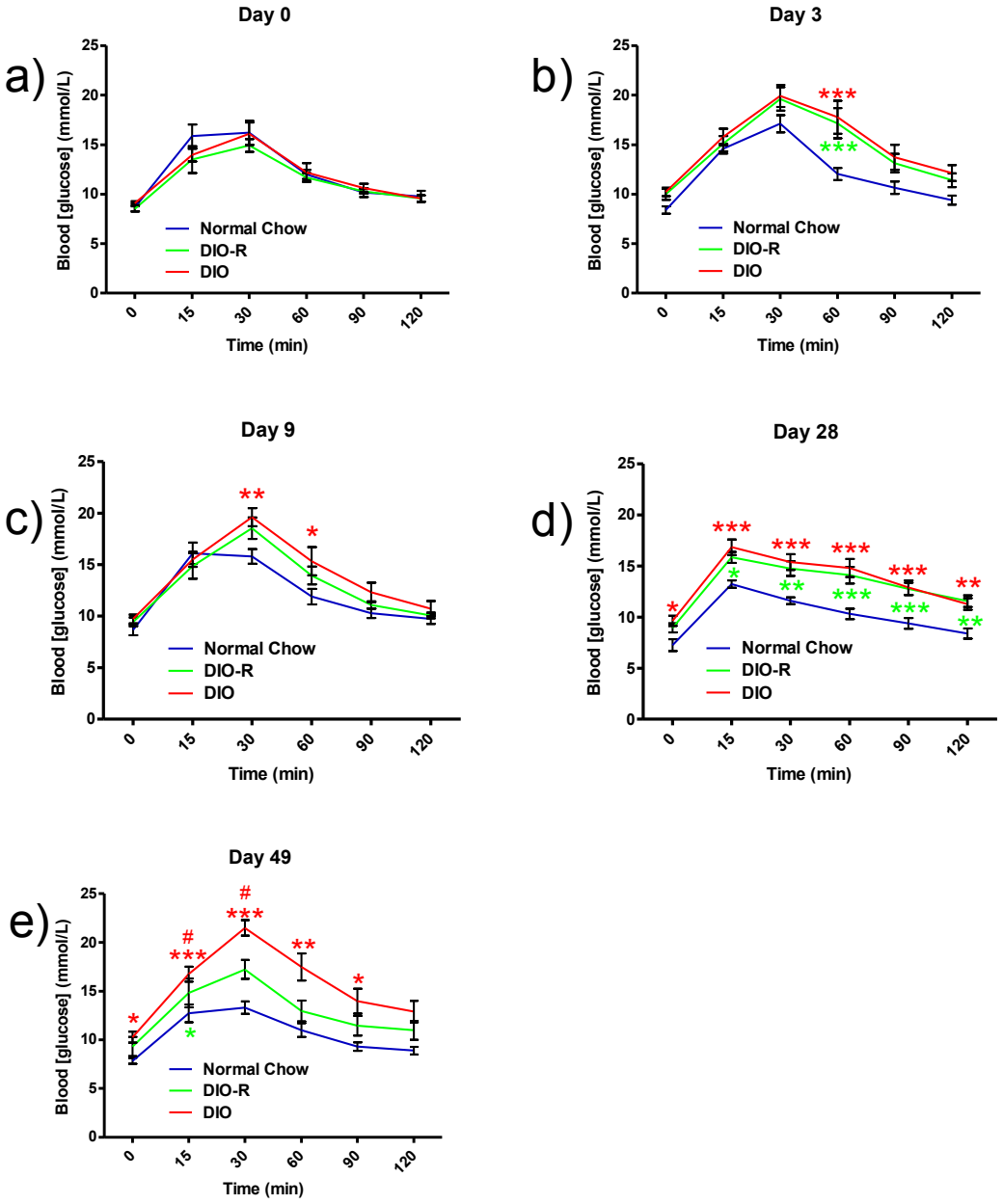

Figure 3.5 **Changing Glucose Tolerance in Mice over 7 Weeks on HED (First cohort).** The effect of HED compared with normal chow on OGTT results in mice on day 0 (a), day 3 (b), day 9 (c), day 28 (d) and day 49 (e). The data is expressed as mean ± SEM. *P<o.o5, **P<0.01, *** P<0.001; Two-way ANOVA with Bonferroni's *post hoc* test to compare all groups at every time point. *compared with normal chow, #compared with DIO-R. (normal chow n=10, DIO n=10, DIO-R n=10)

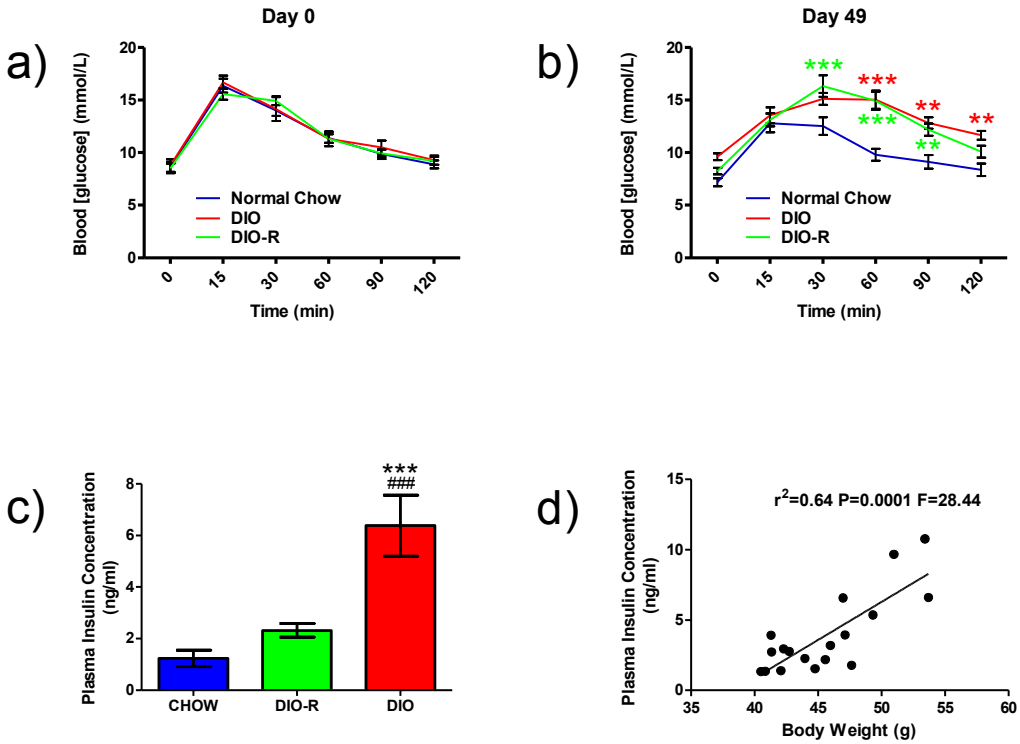

Figure 3.6 **Glucose Tolerance and Plasma Insulin Levels in Mice after 8 weeks on HED (Second cohort).** The effect of HED compared with normal chow on OGTT results on day 0 (a) and day 49 (b), and on plasma insulin concentration in mice (c) and how it correlates with body weight in the HED group only (d). The data is expressed as mean ± SEM. *P<0.05, **P<0.01, *** P<0.001; Two-way ANOVA with Bonferroni's *post hoc* test to compare all groups at every time point (a) and (b); One-way ANOVA with Bonferroni's *post hoc* test to compare all groups at every time point (c); linear regression (d). *compared with normal chow, #compared with DIO-R. (normal chow n=9, DIO n=8, DIO-R n=11)

3.3.4 Changes in mRNA Expression after 8 Weeks of HED

After culling, the brains from the mice in the second cohort of HED were collected and cut using the LCM method. The qPCR results showed that in the Arc there was a decrease in *npy* mRNA expression in the DIO group compared with chow-fed controls, but the reduction was not significant compared to the DIO-R group (Figure 3.7.a). There was no significant change in *pacap* or *pomc* levels. However, if the two HED groups were combined, the significant reduction seen in *npy* expression disappeared but the trend seen in *pacap* levels was confirmed as significant (Figure 3.7.c). There was still no effect seen in *pomc* expression.

In the VMN, there was a 0.5-fold increase in *bdnf* I mRNA expression in the DIO-R group compared with the chow-fed animals, but the upwards trend seen in the DIO group was not significant (Figure 3.7.b). None of the other transcripts tested showed any significant changes. However,

when the two HED groups were again combined, an increase in mRNA levels was seen for *pacap*, *bdnf* I and *bdnf* IV (Figure 3.7.d). There was no significant change in the *bdnf* IX mRNA levels, which codes for the common exon and reflects the level of total *bdnf* mRNA.

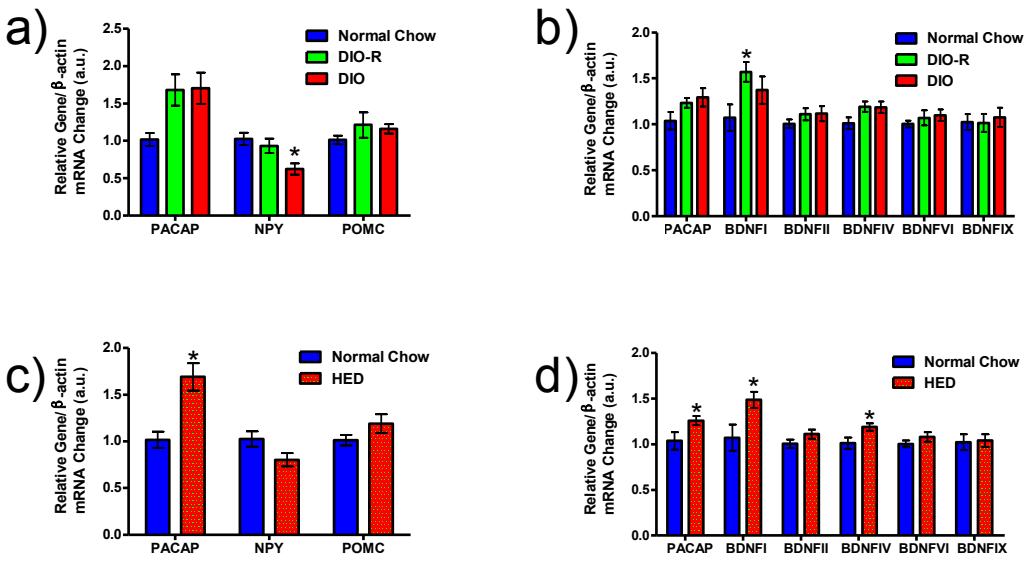

Figure 3.7 **Changes in mRNA Expression in Mice after 8 Weeks on HED (Second cohort).** The effect of HED on mRNA expression as measured by qPCR. In the Arc: *pacap*, *npy* and *pomc* (a and c) and the VMN: *pacap*, *bdnf* I, *bdnf* II, *bdnf* IV, *bdnf* VI and *bdnf* IX (b and d). In the top two graphs, the HED groups have been split into DIO and DIO-R (normal chow n=9, DIO n=8, DIO-R n=11), in the bottom two graphs the two groups have combined (normal chow n=9, HED n=19). Data are expressed as mean ± SEM. *P<0.05, **P<0.01, *** P<0.001; One-way ANOVA with Bonferroni's *post hoc* test to compare all groups at every time point (a and b); Student's unpaired *t*-test (c and d). *compared with normal chow.

3.4 Discussion

The VMN has recently emerged as one of the main nuclei in the hypothalamus responsible for energy homeostasis, though the specific neuronal types involved have yet to be identified. Both PACAP and BDNF have been implicated in body-weight regulation and there is now growing evidence that neurons in the VMN that contain these neuropeptides may be important players. As mRNA levels of both *pacap* and *bdnf* are up regulated in the VMN in diet-induced obesity-resistant mice (Hawke 2009b, Hawke et al 2009, Komori et al 2006), they are considered two likely candidates responsible for signaling in the VMN and the circuitry regulating metabolism in response to HED. To confirm this, the function of these neuropeptides in the brain needs to be better understood. Another key issue is to understand how these genes are regulated and how metabolic manipulation affects their expression. Thus, the aim of this chapter is to understand

whether these genes might have a protective role against the development of diet-induced obesity.

To investigate if *pacap* and *bdnf* transcripts are affected by metabolic manipulation, a set of mice were subjected to a period of fasting and another two sets were put on HED. After 48 hours of fasting, where the mice lost a significant amount of body weight, we examined the differences in mRNA regulation in the Arc and VMN. It is established that *npy* mRNA is up regulated following food restriction or fasting (Bi et al 2003) and was here used as a positive control. POMC is an anorexigenic peptide, and its mRNA has previously been shown to be downregulated in the Arc following fasting. The effect on *npy* was replicated in our experiment, but we did not see the expected downregulation of *pomc*. This could be due to the fact that a changes in *pomc* mRNA are not always seen when the whole of the Arc is sampled (Luckman personal observations). POMC undergoes extensive post-translational processing that is cell specific, and which can lead to the production of several different biologically active peptides. In the Arc, POMC neurons can, for example, release α-MSH, which has an anorexigenic effect by activating both melanocortin 3 and 4 receptors (Heisler et al 2003) and would most likely be inhibited by fasting. However, other Arc POMC neurons produce β-endorphin, which can induce food intake in satiated rats when infused in the hypothalamus (Grandison & Guidotti 1977). Thus, different populations of POMC neuron could be differentially regulated after fasting, hence confounding our results.

PACAP is expressed in both the Arc and the VMN (Vaudry et al 2009), and there is a possibility that these neurons may form a continuous functional group. There was no change seen in *pacap* mRNA in the Arc, but in the VMN there was a downregulation seen in *pacap* and *bdnf* transcripts I and II. These results fit with previous findings by this lab (Hawke 2009b), where *in situ* hybridization showed a reduction in *pacap* and *bdnf* mRNA following fasting, and with the fact that both PACAP and BDNF have catabolic actions when centrally administered (Mizuno et al 1998b, Morley et al 1992, Wang et al 2007). However, in our results the overall *bdnf* mRNA level (which should be indicated by the common exon, *bdnf* IX) was not significantly reduced, which could possibly be due to the concurrent upregulation seen for transcript VI. This indicates that the *bdnf* transcripts are differentially regulated following fasting.

Following 8 weeks on HED, the mice in the first cohort exhibited a larger separation in body weight between the DIO and the DIO-R group than the second cohort, i.e. the obese mice gained more weight in the first cohort. This could explain the difference in glucose tolerance seen at the final OGTT day in the two cohorts, where the higher body weight might contribute to the DIO

mice in the first cohort having a glucose tolerance curve significantly above the DIO-R group. This was not apparent in the second cohort. However, when the plasma insulin concentrations were examined in the second cohort, the DIO group had significantly higher levels than the DIO-R group, which did not differ from control levels. Indeed, the plasma insulin concentration was highly correlated with final body weight in the HED groups. In conclusion, even though the more impaired glucose tolerance seen in the DIO group in the first cohort was not repeated in the second cohort, there was still a difference seen in insulin levels with the high levels in the DIO group, which may be indicative of future insulin resistance and diabetes developing. Importantly, there is no obvious indication that the OGTT at early time points is predictive of future weight gain.

The qPCR experiments for the first cohort were not successful due to the fact that not enough tissue was collected for the detection of the mRNAs of interest. In the second cohort we had more success, so the results are shown in two ways, with one graph depicting both HED groups combined and another with the two groups separated. The reason for this is the inherent nature of the statistical tests that were used, where some changes seen did not reach significance using a one-way ANOVA for the three groups (normal chow n=9, DIO n=8, DIO-R n=11). For example, the *pacap* mRNA levels in the Arc seem to be up regulated in both of the HED groups but the effect does not appear to be significant. When the groups are combined (normal chow n=9, HED n=19) and a student's *t* test is performed the significance is there, probably due to the increased *n* number. The upregulation indicates that the Arc *pacap* neuron population may play a role in the response to HED. The *npy* mRNA level appears to not change in the DIO-R group but is reduced in the DIO animals, which fits with the fact that an orexigenic signal would be repressed with an increase in body weight and suggests that *npy* regulation follows body adiposity. No change was seen in *pomc* mRNA levels, although a positive trend is apparent. The lack of change seen in *pomc* mRNA does not exclude the possibility of an early upregulation in the mRNA that is then attenuated through the course of the 8 weeks.

The qPCR data for the VMN was less convincing, although we did see the expected upregulation in *pacap* mRNA and also an upregulation in *bdnf* transcript I and IV. However, there was no upregulation of the pan*bdnf* transcript IX, and there was no clear indication of differential regulation of the transcripts or *pacap* in DIO and DIO-R. This differs from previous data from this lab (see Figure 3.1), which was collected using semi-quantitative *in situ* hybridization and might indicate that qPCR preceded by LCM may not be the best method, as the tissue is subject to

numerous processing steps that might have a degrading effect on the RNA. Also, the split between DIO and DIO-R groups in the second cohort in terms of final body weight was not as large as previously seen in the first cohort or previously in the lab (Hawke 2009b), and might account for the smaller changes seen in gene expression. There were also limitations to our qPCR paradigm that need to be discussed. All of the expression levels measured were normalised to the expression of *β-actin*, which was used as the housekeeping gene. To further verify our results, the experiments would need to be repeated using additional housekeeping genes in order to prove the up- and downregulation results as robust. Additionally, none of the qPCR products were sequenced and it is thus not clear that the changes seen in mRNA levels were in fact the ones we were looking for, and in the future sequencing of the products should be added as a further validation step of the primers used. One further thing to keep in mind when discussing this data is the effect on these expression results of multiple OGTTs. We did not perform any recovery experiments to investigate time period required for expression levels to return to base levels, i.e. levels prior to the OGTT. It is not unreasonable to suppose that a six-hour fast followed by a high dose of glucose would affect expression levels of genes linked to energy homeostasis, and that this is something that would have to be controlled for in future experiments.

Accepting these caveats, we did show differences in *bdnf* mRNA transcript regulation after both fasting and HED, which indicates that the transcripts have different roles in the response to metabolic manipulation. This can occur if different transcripts are transported to specific subcellular compartments, for example the dendrites, where they are translated locally into protein. Aliaga et al (2008) showed that transcript VI was the only transcript present in primary dendritic processes during basal conditions in cultured hypothalamic rat neurons, using non-isotopic *in situ* hybridization, and linked this to its likely involvement in synaptic plasticity (Aliaga et al 2009). This had previously been reported by Pattabiraman et al (2005) in neurons of the visual cortex (Pattabiraman et al 2005), and fits with the fact that the hypothalamus has a high capacity for plasticity in order to respond to physiological challenges. The authors hypothesize that the mechanism for transcript VI transportation to the dendrites is dependent on specific sequence elements in transcript's 5'-UTR region that is recognized by the transport machinery, and they point out that this transcript contains the exon with the highest GC content of all the *bdnf* transcripts. This allows for a stable secondary structure formation that is crucial for messenger transportation elements (Kindler et al 2005).

The different cellular locations of the *bdnf* transcripts could be associated with their different functions. As mentioned above, transcript VI appears to be present in the dendrites and is possibly plasticity related (Kang & Schuman 1996), so the upregulation of this transcript that we saw following 48 hour fasting in the VMN might indicate dendritic changes in response to the stimulus. The same was not observed following 8 weeks on HED, although that does not exclude the possibility that we would have seen this upregulation more immediately following the diet change. 48 hour fasting is a very strong stimulus and the response seen might only be there in the acute phase in the HED experiment. The *bdnf* transcripts might be present only in other cellular compartments, such as the soma and could be involved in other functions (Guerra-Crespo et al 2001, Loudes et al 1999, Rage et al 1999). For example, BDNF peptide produced from these alternative transcripts may be destined for release from nerve terminals and be involved in intercellular communication. As BDNF is catabolic, it is possible that it is important to reduce the production of these transcripts, while still allowing for dendritic plasticity in response to the fasting response.

In the second cohort, mice placed on HED displayed an increase in the expression of *bdnf* transcripts I and IV. Publications by the Wang group also implicate transcript IV in some forms of neuronal plasticity, as it is up regulated in an activity-dependent manner (Zheng & Wang 2009, Zheng et al 2011). It had previously been shown that BDNF promotes its own transcription through the transcript IV promotor, both *in vitro* in cortical neurons (Yasuda et al 2007) and *in vivo* in the dentate gyrus of the hippocampus (Wibrand et al 2006). Thus, Wang suggests that following an upregulation due to neuronal activity, the self-stimulation of transcript IV contributes to the sustained maintenance of *bdnf* expression, which may be important in activity-dependent neuronal changes (Zheng & Wang 2009). This may be relevant to long-term plasticity in the VMN in mice maintained on HED, and presents the possibility that BDNF may be able to mediate the effects of other trophic hormones, such as leptin (Bouret, 2013) on structures of the hypothalamus.

A further complication regarding bdnf transcripts is now apparent, since all of the *bdnf* transcripts have two splice variants, one with a short (~0.4 kb) and one with a long (~2.9 kb) 3' UTR-region (Aid et al 2007, Timmusk et al 1993) due to the final exon having two alternative polyadenylation sites (see Figure 3.2). The paper by Liao et al (2012) ties together previous findings from their lab, where they show that *bdnf* mRNA with short 3' UTR is restricted to the neuronal cell bodies whereas the longer mRNAs can also localize to dendrites in cortical and hippocampal neurons (An

et al 2008), with more recent data implicating the necessity of local protein synthesis of long *bdnf* transcripts in the dendrites in energy homeostasis (Liao et al 2012). They showed that knock-out mice lacking long 3' UTR *bdnf* mRNA developed hyperphagic obesity and leptin resistance, and that both insulin and leptin could stimulate the local translation of long 3' UTR *bdnf* mRNA in cultured hypothalamic rat neurons. The authors suggest, following their results, that *bdnf* and leptin have a linked role in the control of energy balance. As leptin stimulates the translation of long 3' UTR *bdnf* mRNA through neuronal activity, it is possible that the BDNF protein translated from these transcripts is necessary to maintain leptin's further activity in other hypothalamic nuclei. Thus, if parts of BDNF signaling are disrupted, it could lead to compromised neural circuits in other areas, leading to leptin resistance and the development of obesity (Liao et al 2012).

As mentioned above, there is no clear evidence as to what regulates *pacap* and *bdnf* with changing energy status. If there is a shared input to these two neuronal types, it could be either hormonal or neuronal. Leptin is one possible hormonal input, but why would the leaner DIO-R mice respond, when it is the DIO mice with their increased white adipose tissue (WAT) that should have the higher circulating leptin? Perhaps the DIO mice have already become leptin resistant. If the input is neuronal, where does it originate? The obvious suggestion is the Arc, but our data for NPY suggests that these neurons may be followers of body weight rather than primary regulators. The VMN has all the sensing capabilities to suggest it is not receiving the control from outside, but instead it is likely to be a hub, perhaps along with the Arc.

Another possibility is that there is a 'master gene' within the VMN. For example, SF-1 is a transcription factor that is necessary for the normal development of the VMN. Kim et al (2011) showed that both pre- and post-natal VMN-specific SF-1 knockout mice were susceptible to HED-induced obesity. They also showed that these mice had decreased leptin receptor expression specifically in the VMN, which leads to leptin resistance (Kim et al 2011). This indicates a role for the SF-1 transcription factor in the coordinated control of energy homeostasis in the hypothalamus, especially following HED. However, the SF-1-driven knockout of *bdnf* did not elicit an obese phenotype, it is uncertain if BDNF is a relevant mediator in SF-1 neurons (Dhillon et al 2006). In another paper, the same group implicated another transcription factor, FOXO1, which is known to play a role in metabolic homeostasis through leptin and insulin regulation (Kim et al 2012). They show that the VMN is an important site for FOXO1 action, and that mice lacking the *foxo1* gene in SF-1 positive neurons in the VMN are lean due to an increase in energy expenditure. They also identified the *sf-1* gene as a direct FOXO1 transcriptional target in the VMN. Taken

together, it appears both SF-1 and FOXO1 are necessary to maintain energy homeostasis and both could be possible 'master-genes' controlling the expression of *pacap* and *bdnf* genes, although it is unclear what the relationship between SF-1 and BDNF is, as BDNF appear not to exert its anorexigenic effects through SF-1 positive cells in the VMN (Dhillon et al 2006).

Finally, epigenetic modulation is another possible regulatory mechanism for *pacap* and *bdnf* transcription. Epigenetic phenomena, which can be described simplistically as winding and unwinding of genomic DNA, occur when the chromatin structure is remodelled, affecting the capability of transcription factors to bind. These changes can be due to two major events: histone modification or DNA methylation. For example, the protein modifying enzyme silent information regulator 1 (SIRT1) is a nuclear metabolic sensor that detects cellular metabolic status and acts accordingly to alter chromatin structure and gene regulation, specifically through deacetylation of histones and the subsequent effects on transcription (Li 2013). The activity of SIRT1 is dependent on peripheral signals, for example nutritional, hormonal and environmental. Evidence of SIRT1 involvement in central control of metabolic homeostasis comes from studies showing that calorie restriction and fasting increases *sirt1* expression in the hypothalamus (Cakir et al 2009, Satoh et al 2010). Further, inhibition of hypothalamic SIRT1 activity increases acetylation of *foxo1*, which in turn increases *pomc* and decreases *agrp* expression in the Arc leading to a decrease in food intake and reduced weight gain (Cakir et al 2009). Furthermore, AgRP-dependent neuronal deletion of *sirt1* has a dampening effect on AgRP neuronal activity, which also leads to a decrease in food intake and reduced weight gain (Dietrich et al 2010). But if the *sirt1* gene is specifically deleted in the POMC neurons in mice, the animals exhibit a blunted response to leptin and have a higher risk of developing DIO (Ramadori et al 2010). This fits with previous reports that long-term treatment with a small molecule *sirt1* activator (resveratol) normalizes hyperglycaemia and improves hyperinsulinaemia in DIO mice (Ramadori et al 2009). Taken together, this evidence suggests an important role for SIRT1 in central regulation of nutrient sensing, and could be an epigenetic modulator of *pacap* and *bdnf* transcription.

We proceeded to investigate possible epigenetic modulation of the *pacap* and *bdnf* genes by looking, instead, at DNA methylation in CG rich sequences of the promoters of *pacap* and *bdnf*'s different transcripts in collaboration with the Babraham Institute in Cambridge. However, the techniques used by our lab for tissue collection (LCM) appeared to yield insufficient amount of DNA for reliable results following subsequent bisulphate treatment and mass spectrometry

analysis. Therefore, unfortunately, the possibility of epigenetic regulation could not be further explored in this thesis.

3.5 Summary

In conclusion, metabolic manipulation in the form of both 48-hour fasting and 8-weeks HED differentially regulates *pacap* and *bdnf* transcripts expression in the VMN of outbred mice. While the results presented here do not fully support the hypothesis that these genes have a protective role in the development of diet-induced obesity, the data do further support their position of PACAP and BDNF as candidates responsible for signaling in the VMN and in the circuitry regulating metabolism. The presence of several *bdnf* transcripts and their differential regulation in the VMN points to potentially distinct roles for the transcripts, for example in synaptic plasticity or expression maintenance, which the literature suggests is determined by the transcript size and location. It is not yet clear what regulates *pacap* and *bdnf* in the VMN, but hormonal inputs (e.g. from leptin) or neuronal inputs (possibly originating in the Arc) are likely to play a role. There could also be a 'master-gene', similar to the transcription factors SF-1 or FOXO1, which drive the expression of some genes, while inhibiting the expression of others. Finally, *pacap* and *bdnf* could be subject to epigenetic modulation, with SIRT1 being one potential candidate for the regulation of histone acetylation. Whatever the regulator, it will be interesting to determine if it is dysfunctional in individual animals that are prone to diet-induced obesity, while still effective in those that are resistant.

Chapter 4. Metabolic sensitivity of PACAP neurons in the hypothalamus

4.1 Introduction

In recent years, progress has been made in defining the roles of different cell populations in the brain and neuropeptides in the regulation energy homeostasis (reviewed by Parker & Bloom 2012). Much of the research has focused on the Arc nucleus in the hypothalamus, and the anorectic POMC-derived and orexigenic NPY peptides have been identified as two of the major signaling molecules.

When leptin and the long, signalling form its receptor (leprB) were discovered (Zhang et al 1994), mutations in their genes were identified as being responsible for the obese phenotypes seen in the naturally occurring mutant mice, *ob/ob* and *db/db*, respectively. When leptin binds to its receptor in certain parts of the brain, appetite is inhibited and energy expenditure increased (through adaptive thermogenesis). Thus, mice lacking either leptin or leprB are obese, due to hyperphagia and a reduction in energy expenditure. Interestingly, in transgenic mice in which the leprB is knocked-out specifically in POMC neurons, the obese phenotype seen is not as extreme as that observed with brain-specific knock out or total Lepr knock out (*db*/*db*) (Balthasar et al 2004). This suggests that neuronal populations other than POMC cells, perhaps also within the hypothalamus, must be involved in energy regulation and feeding.

Recently, evidence is mounting for the involvement of the VMN in energy homeostasis, which is indicated to play as big a role as the Arc. The leprB is expressed throughout the ventromedial hypothalamus, and about 50% of neurons in both the VMN and Arc respond to leptin (Irani et al 2008). Adding to the evidence, the knock out of the VMN-expressed transcription factor SF-1 prevents normal development of the VMN and the animal develops an obese phenotype in adulthood (Zhao et al 2004). When the leprB is specifically knocked out in SF-1-positive VMN cells, obesity is also induced, and when the leprB is selectively knocked out of both SF-1 and POMC positive cells it leads to an obese phenotype that is additively more severe than the two single knock outs on their own (Dhillon et al 2006).

The cellular phenotypes of the VMN are largely uncharacterized, in comparison with those in the Arc. However, PACAP has been found to be one of the peptides enriched in the VMN (Segal et al 2005). Earlier, intense PACAP expression at both the mRNA and protein level was demonstrated in rat brain using *in situ* hybridization immunohistochemistry, respectively, while a much weaker level was detected in the Arc (Hannibal 2002). More recently, Durr and colleagues (2007) sought to map the expression of PACAP, focusing more specifically within the mediobasal hypothalamus of the rat, using fluorescent *in situ* hybridisation immunohistochemistry. Here as well, they reported extensive PACAP expression in the VMN with a weaker signal detected in the Arc. Interestingly, this study found that PACAP co-localised with α-MSH in around 20% of Arc POMC neurons, pointing to the neurochemical heterogeneity of hypothalamic POMC neurons. Beyond the hypothalamus, studies have shown that PACAP is expressed extensively throughout the whole brain, supporting the many roles the peptide plays in physiology, as described previously (Vaudry et al 2009).

Our lab has investigated the role of PACAP in energy balance for a number of years, using *in vivo* pharmacology and *in situ* hybridisation to yield a number of convincing results to confirm this relationship (Hawke et al 2009). Using dual-label *in situ* hybridisation, a population was found concentrated in the dorsomedial VMN where *sf-1* and *pacap* mRNA co-localise, and where leptin signalling via leprB is required for normal PACAP expression in these cells. The leprB is richly expressed in this area, inferring that these PACAP cells are targets for leptin. To test this, *ob/ob* mice and fasted normal mice, which both have reduced *pacap* mRNA expression in the VMN, were given leptin replacement, which restored the low expression to normal levels (Hawke et al 2009). Furthermore, as seen in Chapter 3, the transcription of the pacap gene in the VMN (as well as in the Arc) is heavily dependent on energy status. In fasted mice, PACAP mRNA is down regulated in the VMN, but not affected in the Arc. Following HED, PACAP mRNA is up regulated in both nuclei, suggesting that PACAP in both Arc and VMN plays a role in the development of obesity and/or in counter regulation to prevent it.

The most important aspect in the maintenance of metabolic homeostasis is the detection of fluctuations in different metabolic signals, such as leptin and glucose, the latter being one of the most vital. The brain requires glucose to function normally and hypoglycaemia, detected by both brain and peripheral sensors, leads to the initiation of a counter-regulatory response (or CRR), involving an immediate autonomic-mediated reduction in insulin and an increase in glucagon secretion from the pancreas, along with an increase in adrenal hormones (e.g. adrenalin),

followed by a slower behavioural response of an increase in feeding (Cryer 2005). The CRR ensures an immediate release of glucose into the blood stream to redress the hypoglycaemia. The ventromedial hypothalamus has been established as a centre for glucose detection controlling CRR. Evidence includes the selective chemical destruction of the VMN in rats, which results in a 75% reduction in the endocrine CRR (Borg et al 1994). Furthermore, local perfusion of the VMN with 2-deoxy-D-glucose (or 2DG), a non-metabolisable form of glucose that effectively causes local glucoprivation, stimulates the CRR (Borg et al 1995), while the local perfusion of the VMN with glucose during systemic hypoglycaemia markedly suppresses the CRR (Borg et al 1997).

The hypothalamus experiences a range of glucose *in vivo* of 0.5mM (fasted levels) to 2.5mM (post-prandial levels) (Burdakov et al 2005a). Besides a high density of glucose sensing neurones in the VMN, the other main areas containing these neurons are the lateral hypothalamus and the brainstem nucleus of the tractus solitarius (Burdakov et al 2005a). Although the phenotypes of the glucose-sensing neurones of the VMN remain uncharacterised, unpublished data from our lab show that SF-1 positive VMN cells are sensitive to physiological changes in glucose (Belle, Piggins and Luckman, unpublished). SF-1-positive neurones may be a mixed population of cells and could contain neurones that are glucose excited (GE) or glucose inhibited (GI). And as mentioned above, most SF-1-positive neurones in the dorsomedial region of the VMN contain PACAP, making the peptide a candidate for characterisation of these glucose-sensing neurones.

Electrical stimulation of the VMN, or the local release of glutamate, increases glycogenolysis and hepatic glucose production (Takahashi et al 1997, Tong et al 2007), while PACAP (from an unknown source) acts through the paraventricular nucleus (PVN) to activate the sympathetic pathway also leading to an increase in hepatic glucose production (Yi et al 2010). Taken together, we hypothesised that VMN PACAP neurons are involved in glucose sensing, and that they are likely to be GI (i.e. when glucose levels fall, PACAP neurons projecting to the PVN are activated to induce the endocrine CRR).

In this chapter, we aimed to establish whether PACAP neurones in the VMN are involved in metabolic sensing of circulating leptin and glucose, through the use of transgenic mouse models, immunohistochemistry, electrophysiology and Ca^{2+} imaging.

4.2 Methods

4.1.1 Animals and *in vivo* work

Several transgenic mice lines were used in this chapter, including Adcyap1-eGFP, Pacap-i-Cre x Z/EG and Pacap-i-cre x Lepr flox. For breeding schedules see Chapter 2.

- **Growth curve and OGTT:** The body weights of Pacap-i-cre X Lepr flox mice were recorded once a week from 3 to 20 weeks of age ($cre^{-/-}$ $flox^{-/-}$ male n=7, female n=4; $cre^{-/+}$ $flox^{-/-}$ male n=9, female n=7; $cre^{-/-}$ $flox^{+/+}$ male n=8, female n=7; $cre^{-/+}$ $flox^{+/+}$ male n=12, female n=9). An OGTT was performed on all mice at 18 weeks of age, as described in Chapter 2.
- **Leptin intraperitoneal injection:** A nocturnal feeding study with a cross-over design was performed using Pacap-i-cre X Lepr flox mice ($cre^{-/+}$ $flox^{+/+}$ n=10, $cre^{-/-}$ $flox^{+/+}$ n=10) at 8 weeks of age, where mice received either saline (0.9% NaCl) or 5mg/kg body weight leptin (PeproTech, UK) on day 1 of the crossover and the other treatment on day 2 a week later. Food intake was measured at 2, 4 and 12 hours after injection.
- **2DG intraperitoneal injection:** A daytime feeding study was performed using Adcyap1-eGFP mice (40 ± 3g), where the mice were randomly assigned to receive either saline (0.9% NaCl) (n=6) or 600mg/kg 2DG (Sigma-Aldrich Corp. Ltd., UK) (n=6) intraperitoneously. Food intake was measured 90 minutes after injection, followed by transcardial perfusion. The perfused brain was then used for immunohistochemistry.

4.1.2 Immunohistochemistry

Following transcardial perfusion, the brains were cut into sections starting from 1.22mm through to 2.30mm caudal of bregma (Franklin & Paxinos 2008), encompassing the VMN, Arc and the PVN. Two MRes students in our lab, Holly Hopkins and Kate Merritt, performed these staining protocols supervised by and after being trained by the author.

PACAP antibody testing

The standard fluorescent immunohistochemistry protocol (described in Chapter 2) was used to visualise the expression of PACAP in Adcyap1-eGFP and PACAP-Cre X Z/EG mice. Previous attempts at this staining were unsuccessful, so an antigen retrieval protocol was performed before the blocking step, by incubating the sections in citrate buffer (10mM Tri-sodium citrate

(Fisher Scientific) at 80^{o}C for 30 min, before cooling and three washes in PB. This treatment breaks the cross-links formed by formalin fixation and allows the antigenic epitope to be better exposed. The primary antibody, PACAP (C-19) goat polyclonal IgG (sc-7840; Santa Cruz Biotechnology, USA), was diluted 1:100 in 1% NDS. The secondary antibody, Cy3-conjugated donkey anti-sheep IgG (Millipore, CA, USA), was diluted 1:500 in 5% NDS.

GFP immunostaining

The primary chicken anti-eGFP polyclonal antibody (Millipore, CA, USA), was diluted 1:1000 in 1% NDS. The secondary antibody, donkey anti chicken IgG conjugated with Cy3 (Millipore, CA, USA), was diluted 1:500 in 5% NDS.

c-Fos immunostaining

The primary antibody, rabbit anti-c-Fos (Calbiochem, Ca, USA), was diluted 1:8000 in 1% NGS. The secondary antibody, Cy3-conjugated goat anti-rabbit (Jackson ImmunoResearch Laboratories Inc., PA, USA), was diluted 1:500 in 5% NGS.

4.1.3 Imaging

The imaging protocols in his chapter was developed and performed with Dr Mino Belle, current post-doc in Professor Hugh Piggins lab.

Patch clamp electrophysiology

An Adcyap1-eGFP mouse aged 4 weeks was used for the patch clamp recordings, as described in Chapter 2.

Cell dissociation and Ca^{2+} imaging

PACAP-Cre X Z/EG mice aged 10-14 days were used for Fura-2 Ca^{2+} imaging, following cell dissociation of their ventromedial hypothalamus, both as described in Chapter 2.

4.3 Results

4.1.4 Testing a PACAP antibody for immunohistochemical staining

In order to establish whether our two reporter strains, the Adycyap1-eGFP and Pacap-i-Cre-GFP mice, have cell-specific expression of eGFP, we attempted to utilise an antibody that reportedly

stains for the PACAP protein. Previous work has gone into optimisation of an immunohistochemical staining protocol for PACAP, but staining has been problematic. Here we included antigen retrieval in an effort to expose more of the PACAP epitopes in our brain sections, and the new protocol appeared be more successful when tried on slices obtained from wild-type littermates of Adcyap1-eGFP mice. However, we only saw weak staining in the VMN and Arc at the lowest dilution of 1:100 of the antibody. Also, we were unable to replicate this staining in the Adcyap1-eGFP and Pacap-i-Cre x Z/EG transgenic mice. Taken together this might indicate that the antibody is unreliable rather than there being a problem in PACAP synthesis in the transgenic mice.

4.1.5 Expression of eGFP in two transgenic strains.

As our attempts to co-visualise the endogenous GFP expressed in our two transgenic mice with a PACAP antibody were unsuccessful, we decided to compare the expression of eGFP in the two mice and in that way discover whether they overlap. If they do, it is a good indicator that the eGFP positive cells are indeed PACAP-containing cells.

The purpose of us obtaining these reporter lines was so that we could utilise them to study PACAP positive cells more closely in our areas of interest in the hypothalamus; the VMN, Arc and PVN. While the endogenous fluorescence of the eGFP was visible in both mouse lines using the FITC filter (excited 450-490nm, emission 515-565nm) on the microscope, and expression was seen in the cortex, habenula and hippocampus, the fluorescent signal was relatively weak in the hypothalamus. However, the signal in the hypothalamus would be enough for isolation of single neurons in acute slices for use in electrophysiological patch-clamping experiments.

But we were also hoping to carry out co-localisation studies and/or functional cell activity staining (e.g. for immediate early gene c-Fos (Luckman et al 1994), and for that we would need to amplify the hypothalamic signal by performing an immunohistochemical stain for GFP. However, first we determined that the eGFP fluorescence signal co-localised with the immunohistochemical one.

In the Adcyap1-eGFP mice, PACAP cells were observed in the VMN and PVN but not in the Arc (Figure 4.1). In the Pacap-i-Cre x Z/EG mice, PACAP cells were observed in the VMN spreading into the Arc, as well as in the PVN (Figure 4.2). In both of these strains, eGFP immunofluorescence was found in cells in the ventrolateral and central region of the VMN more than dorsomedially.

The co-localisation (yellow) of endogenous eGFP (green) and Cy3 labelled eGFP (red) is comprehensive in all images when the images are combined, showing that that the eGFP antibody is suitable for identification of cells expressing the eGFP.

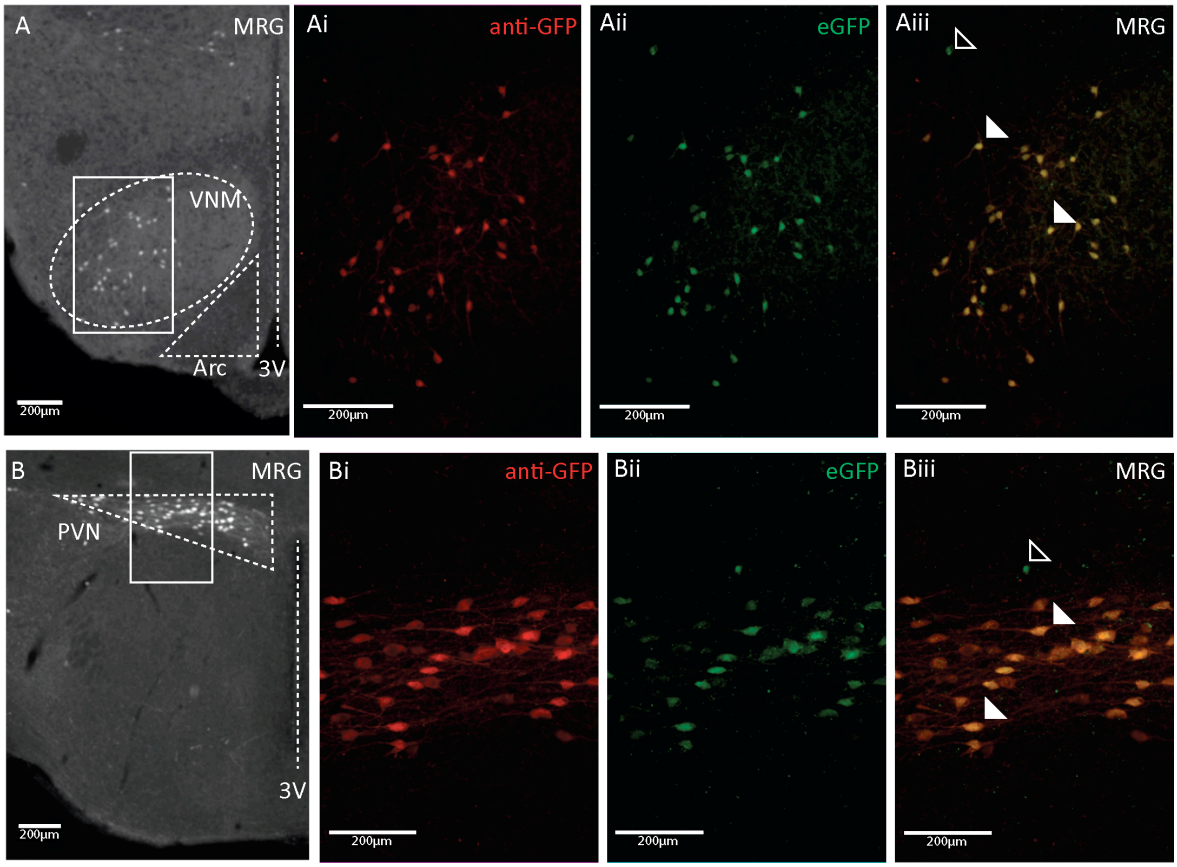

Figure 4.1 Expression of eGFP in Adcyap1-eGFP mice. Immunohistochemistry was performed to stain eGFP using a Cy3-conjugated antibody. Endogenous eGFP was visualised using a FITC filter. A: x4 objective image of VMN and Arc using combined Cy3 and FITC channels; signal present in the ventrolateral and central VMN, none in Arc; magnification square indicated. Ai: x10 objective image of lateral VMN using Cy3 channel, showing antibody labelled GFP. Aii: x10 objective image of lateral VMN using FITC channel, showing endogenous GFP. Aiii: combined Cy3 and FITC channels, white open arrows indicate single green eGFP-expressing cell bodies, and filled white arrows show co-localised eGFP cell bodies and GFP antibody staining. B: x4 objective image of PVN using combined Cy3 and FITC channels; magnification square indicated. Bi: x10 objective image of PVN using Cy3 channel, showing antibody labelled GFP. Bii: x10 objective image of PVN using FITC channel, showing endogenous GFP. Biii: combined Cy3 and FITC channels, white open arrows indicate single green eGFP-expressing cell bodies, and filled white arrows show co-localised eGFP cell bodies and GFP antibody staining.

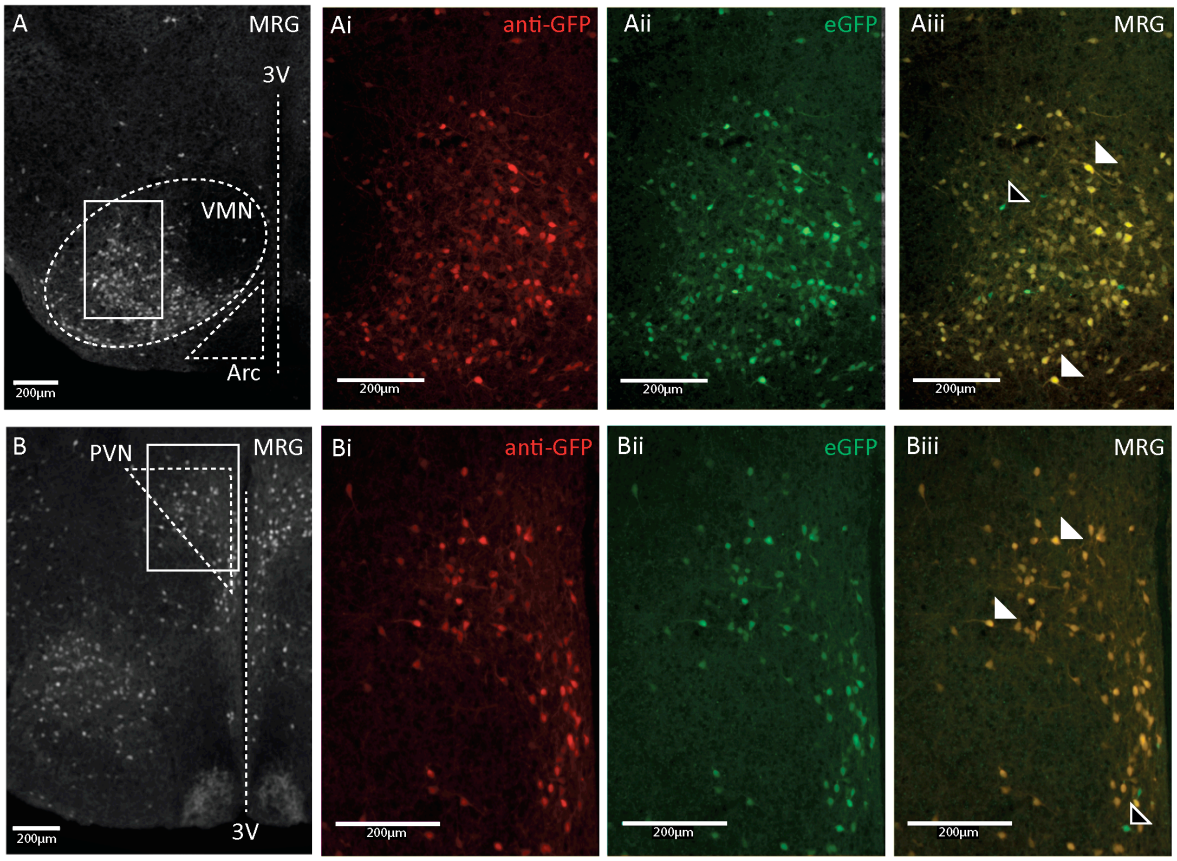

Figure 4.2 Expression of eGFP in Pacap-i-Cre X Z/EG mice. Immunohistochemistry was performed to stain eGFP using a Cy3-conjugated antibody. Endogenous eGFP was visualised using a FITC filter. A: x4 objective image of VMN and Arc using combined Cy3 and FITC channels; signal present in the ventrolateral and central VMN; magnification square indicated. Ai: x10 objective image of lateral VMN using Cy3 channel, showing antibody labelled GFP. Aii: x10 objective image of lateral VMN using FITC channel, showing endogenous GFP. Aiii: combined Cy3 and FITC channels, white open arrows indicate single green eGFP-expressing cell bodies, and filled white arrows show co-localised eGFP cell bodies and GFP antibody staining. B: x4 objective image of PVN using combined Cy3 and FITC channels; magnification square indicated. Bi: x10 objective image of PVN using Cy3 channel, showing antibody labelled GFP. Bii: x10 objective image of PVN using FITC channel, showing endogenous GFP. Biii: combined Cy3 and FITC channels, white open arrows indicate single green eGFP-expressing cell bodies, and filled white arrows show co-localised eGFP cell bodies and GFP antibody staining.

4.1.6 Generation of Pacap-i-cre X Lepr flox mice: growth curve, OGTT and leptin ip

Pacap-i-cre X Lepr flox mice were generated to investigate what effect the knock-out of the leptin receptor in PACAP cells only would have on growth curves, glucose tolerance and systemic leptin response. A group of both male and female mice were weighed weekly from weaning at 3 weeks of age. There was no difference seen in weight accumulation between the transgenic mice, the cre$^{-/+}$ flox$^{+/+}$, and the three control genotypes up to 20 weeks of age; the cre$^{-/-}$ flox$^{-/-}$ being the full wild type, the cre$^{-/+}$ flox$^{-/-}$ only being positive for the cre and the cre$^{-/-}$ flox$^{+/+}$ only carrying the floxed gene (Figure 4.3).

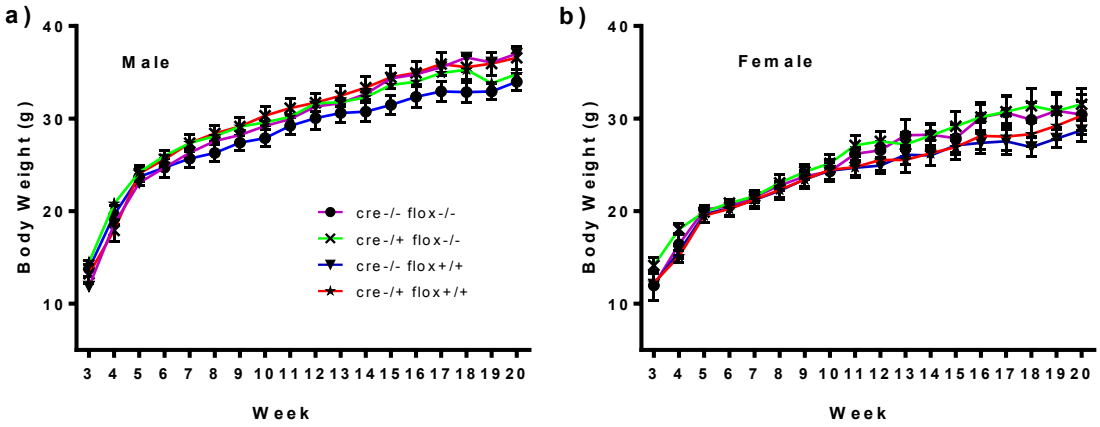

Figure 4.3 **Growth curves of male and female Pacap-i-cre X Lepr flox mice.** Body weight data was collected from the mice from the age of 3 weeks up until 20 weeks of age. a) Showing the male growth curve and b) showing the female. The cre$^{-/-}$ flox$^{-/-}$ represents the full wild-type (male n=7, female n=4), the cre$^{-/+}$ flox$^{-/-}$ is only positive for the cre insertion (male n=9, female n=7), the cre$^{-/-}$ flox$^{+/+}$ is homozygous for the floxed leptin receptor gene only (male n=8, female n=7), and the cre$^{-/+}$ flox$^{+/+}$ is the transgenic animal positive for both the cre insertion and homozygous for the floxed leptin receptor gene (male n=12, female n=9). Data is expressed as mean ± SEM.

At 18 weeks of age, the same male and female mice were tested for differences in glucose tolerance. In the male mice there was a slight variation seen between the different genotypes (Figure 4.4.a), and the area-under the curve analysis was included to investigate if this was significant (Figure 4.4.b), which it was found not to be. The OGTT results show no difference in the glucose tolerance curve in the different genotypes of the female mice (Figure 4.4.c).

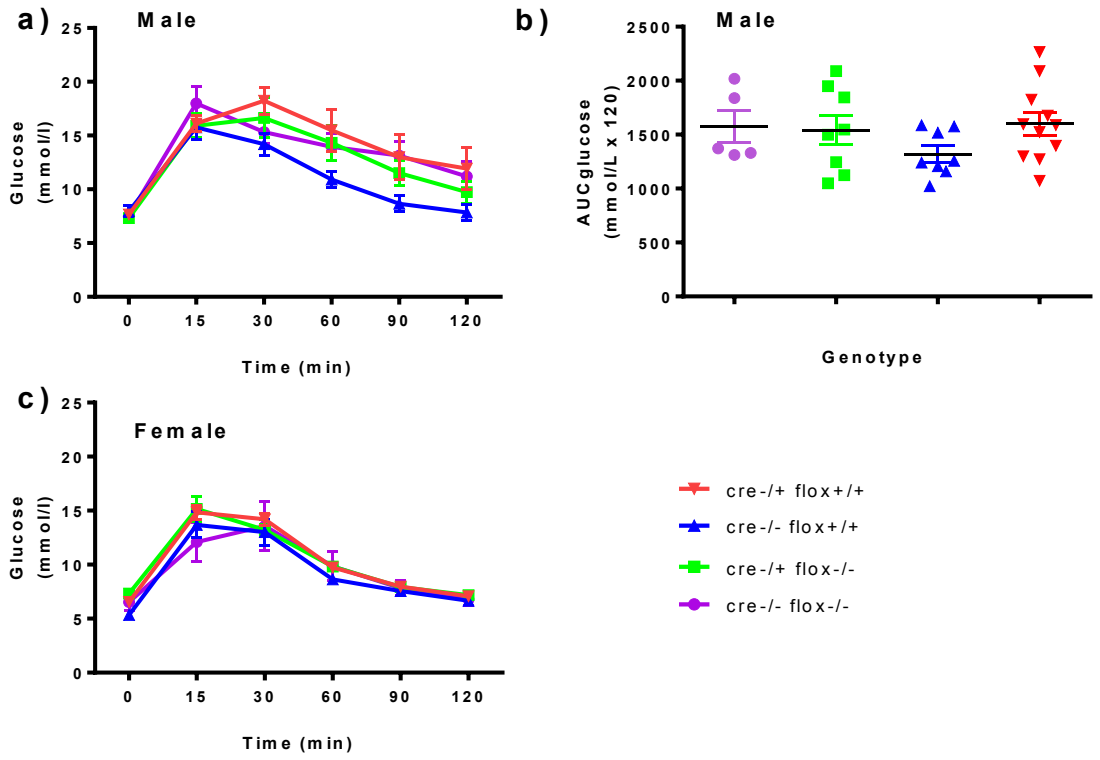

Figure 4.4 **Glucose tolerance testing of male and female Pacap-i-cre X Lepr flox mice.** An OGTT was performed on the mice at 18 weeks of age. a) Showing the glucose tolerance curve, b) shows the male AUC graph and c) showing the female. The cre$^{-/-}$ flox$^{-/-}$ represents the full wild-type (male n=7, female n=4), the cre$^{-/+}$ flox$^{-/-}$ is only positive for the cre insertion (male n=9, female n=7), the cre$^{-/-}$ flox$^{+/+}$ is homozygous for the floxed leptin receptor gene only (male n=8, female n=7), and the cre$^{-/+}$ flox$^{+/+}$ is the transgenic animal positive for both the cre insertion and homozygous for the floxed leptin receptor gene (male n=12, female n=9). Data is expressed as mean ± SEM.

A different cohort of male Pacap-i-cre X Lepr flox mice were given an intraperitoneal injection of leptin (5mg/kg body weight) in a crossover night-time feeding study at 8 weeks of age to. Only the cre$^{-/+}$ flox$^{+/+}$ (where the leptin receptor is knocked out of pacap positive cells)(n=10) and the cre$^{-/-}$ flox$^{+/+}$ (where the leptin receptor gene is floxed but the cre is missing from the pacap cells)(n=10) was included in this experiment as the previous results showed that the other two control genotypes did not appear to exhibit a different metabolic phenotype. The female mice were excluded as well. Exogenous leptin is known to reduce food-intake (Murphy et al 2006, Pelleymounter et al 1995b, Rentsch et al 1995) in mice at 2 hours post injection, and we were thus expecting a similar result in the cre$^{-/-}$ flox$^{+/+}$ mice. However, in our experiment the two-way ANOVA did not deem the reduction in food intake seen at 2 and 4 hours as significant, but only registered a significant reduction at 12 hours in our control group (Figure 4.5). On the other hand, the mice lacking the leptin receptor in PACAP cells showed no reduction in food intake at any of the time points.

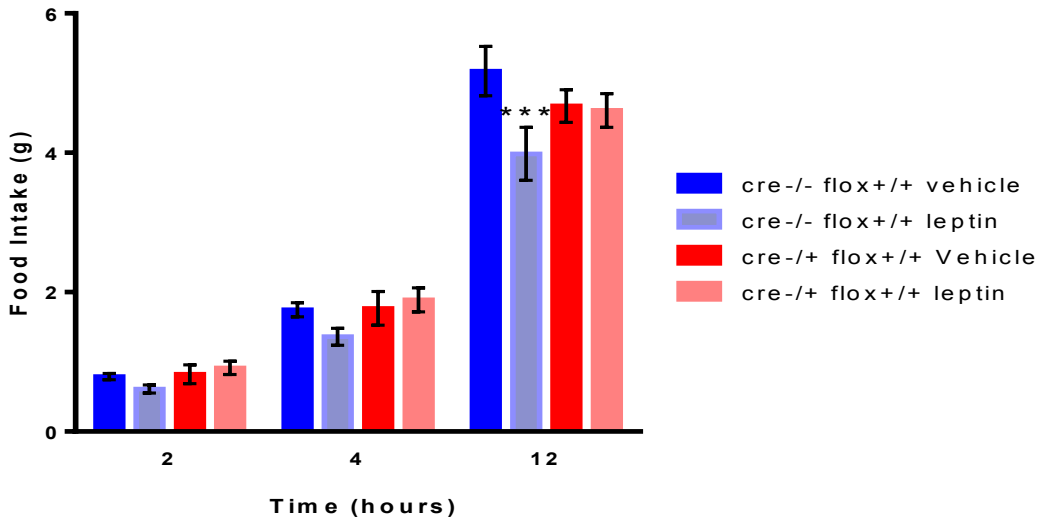

Figure 4.5 **Effect of systemic leptin injection in male Pacap-i-cre X Lepr flox mice.** A group of 8-week-old mice were given a dose of either intraperitoneal saline or leptin (5mg/kg body weight) following a 6 hour fast right before lights-off. This was done in a crossover fashion, where the mice received one of the treatments on day 1 and a week later the other treatment on day 2. The food intake data is expressed as mean ± SEM. *** P<0.001; Two-way ANOVA with Bonferroni's *post hoc* test to compare all groups. *compared with cre$^{-/-}$ flox$^{+/+}$ saline treatment. (cre$^{-/+}$flox$^{+/+}$ n=10, cre$^{-/-}$flox$^{+/+}$ n=10)

4.1.7 Response of PACAP neurones to systemic hypoglycaemia

To test how PACAP neurons respond to glucoprivation, we injected non-fasted Adcyap1-eGFP male mice intraperitoneally with either 2DG (n=6) or saline (n=4) as a control. In order to confirm that the mice exhibited a hypoglycaemic response, the food intake of the mice was measured 90 minutes post injection. The Adcyap1-eGFP mice with the 2DG treatment showed a significant increase in food intake compared to controls (Figure 4.6), meaning that they are indeed hypoglycaemic and that 2DG treatment is a viable method of inducing hypoglycaemia in these mice.

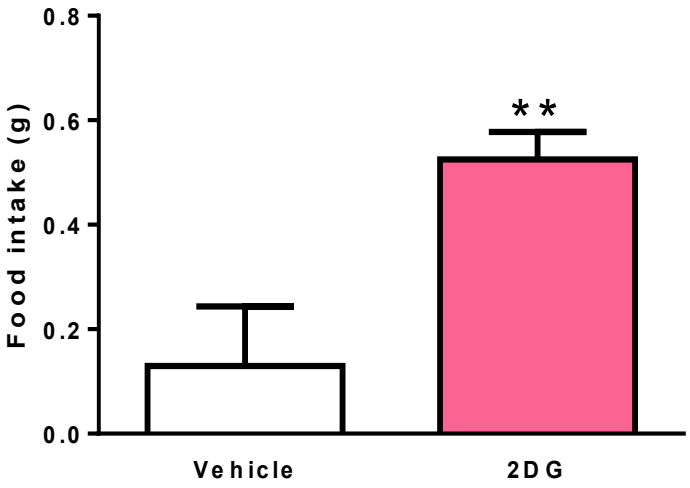

Figure 4.6 Total food intake of ADCYAP-eGFP mice at 90 minutes post 2DG or saline intraperitoneal injection. A student t-test showed that 2DG treatment significantly increases food intake in comparison to saline. Data is expressed as mean ± SEM. **P<0.01; Student's unpaired *t*-test. (vehicle n=6, 2DG n=6)

Following transcardial perfusion at 90 minutes post injection, the brains of the mice were stained for c-Fos, to visualise cell activation, and GFP to amplify up the endogenous green cells. Two representative images of a number of cells positively stained for c-Fos, GFP and their co-localisation in the lateral hypothalamus and the dorsomedial hypothalamic nucleus are shown in Figure 4.7.

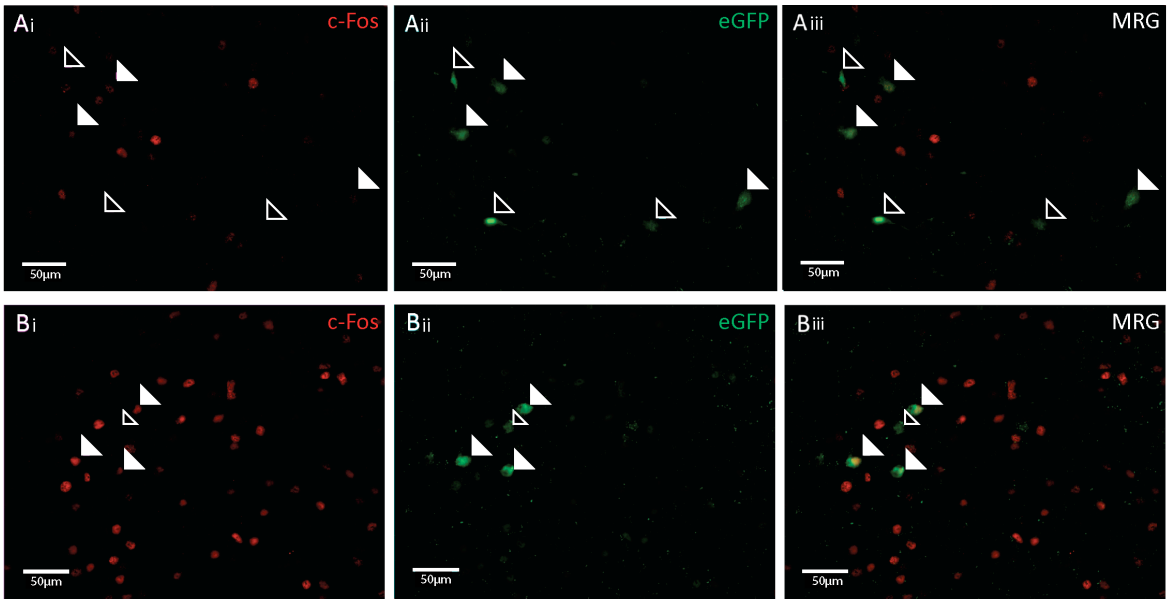

Figure 4.7 Representative fluorescence microscope images of c-Fos immunostaining and direct visualisation of eGFP-expressing cells at 20x magnification. Single c-Fos staining can be seen as red fluorescent nuclei, white open arrows indicate single green eGFP-expressing cell bodies, and filled white arrows show co-localised eGFP cell bodies and c-Fos staining. Image series A shows the lateral hypothalamus and image series B shows the dorsomedial hypothalamic nucleus. Ai: image using Cy3 channel, showing c-Fos antibody labelled cells. Aii: image using FITC channel, showing endogenous GFP. Aiii: combined Cy3 and FITC channels. Bi: image using Cy3 channel, showing c-Fos antibody labelled cells. Bii: image using FITC channel, showing endogenous GFP. Biii: combined Cy3 and FITC channels.

After the cells were counted, statistical testing show that 2DG treatment had no effect on the number of c-Fos positive cells, eGFP expressing cells or their co-localisation in the hypothalamus, except in the VMN and the lateral hypothalamus Figure 4.8. In the VMN, there were significantly more eGFP-expressing cells in the 2DG treated animals compared to the saline controls. When the VMN was divided into its ventrolateral and dorsomedial aspects, it was found that significantly more eGFP-expressing cells lie within the ventrolateral part in 2DG treated mice compared with saline controls. In the lateral hypothalamus, significantly less c-Fos positive cells were found in 2DG treated mice in comparison with saline treatment, indicating a suppression of non-PACAP cells in this area in response to glucoprivation.

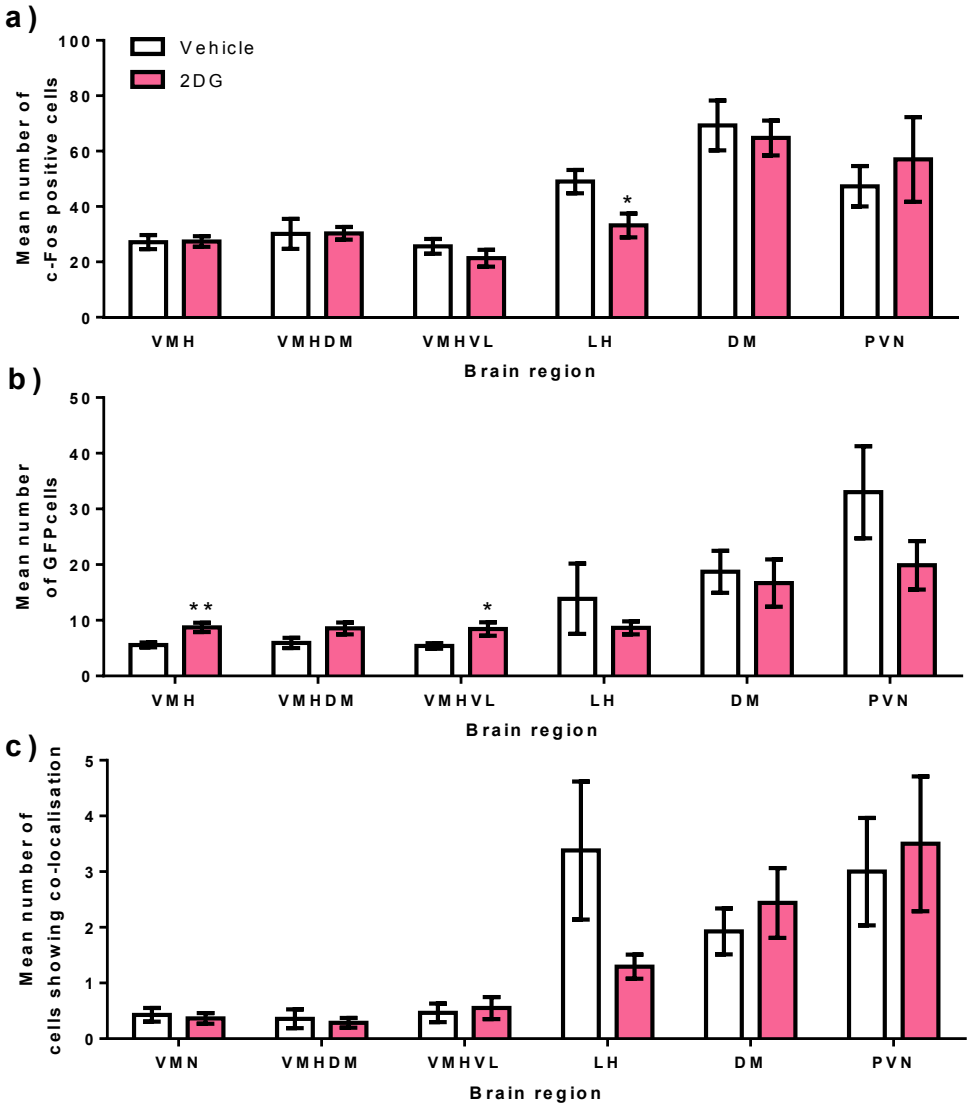

Figure 4.8 Graph illustrating the mean number of c-Fos and eGFP-expressing cells, and their co-localisation, in different hypothalamic nuclei in ADCYAP-eGFP mice treated with 2DG or saline. Following intraperitoneal injection of either 2DG or saline, the brains were stained for c-Fos and GFP and the number of immunoreactive cells were counted in the hypothalamus. a) shows number of c-Fos positive cells, b) GFP positive cells and c) shows their co-localisation. The areas of the hypothalamus included: ventromedial nucleus (VMN), dorsomedial VMN (VMHDM), ventrolateral VMN (VMHVL), lateral hypothalamus (LH), dorsomedial nucleus (DM) and the paraventricular nucleus (PVN). The data is expressed as mean ± SEM. *P<0.05, **P<0.01; Student's unpaired *t*-test. (vehicle n=6, 2DG n=6)

4.1.8 Acute response of PACAP neurones to changes in glucose.

To investigate the direct response of PACAP neurons to changes in glucose, we used two different techniques. First we obtained some preliminary data from patch clamp electrophysiology of eGFP-expressing PACAP neurons in the VMN, and then we went on Ca^{2+} imaging recording from dissociated ventromedial hypothalamic neurons.

Patch clamping electrophysiology

Figure 4.9 shows the recording of an Adcyap1-eGFP VMN cell expressing eGFP, with the position of the patch pipette shown in d. Following a 10pA depolarising current, the cell depolarises and exhibits no spike-rate adaptation (a), while a 10pA hyperpolarising current hyperpolarises the cell and gives rise to a low-threshold rebound spike on recovery (b). When the glucose concentration in the recording bath was raised from 1mM to 5mM the cell was hyperpolarised and reduced its firing rate (c), showing that the cell is GI.

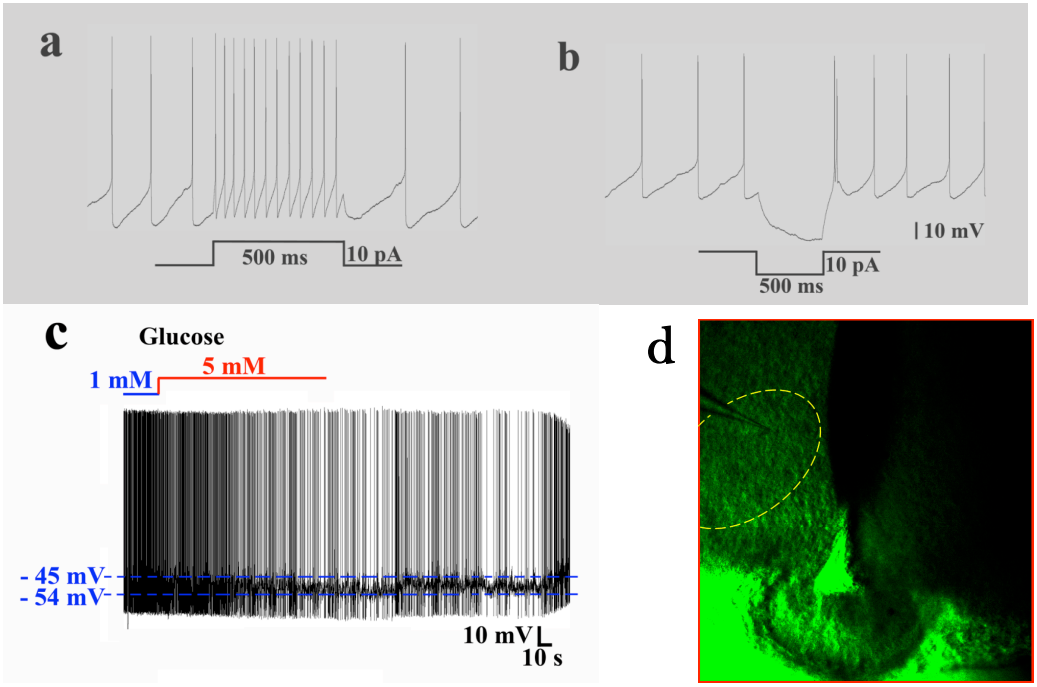

Figure 4.9 **Characterisation of an Adcyap1-eGFP VMN cell.** In (a) action potentials induced by a 10pA depolarising current pulse but no spike-rate adaptation occurs during depolarisation. And (b) shows a low-threshold rebound spike on recovery from 10pA hyperpolarisation current pulse. The cell reduces its firing rate and hyperpolarises when glucose in the bathing medium changes from 1mM to 5mM (c). The GI cell is located in the VMN as shown in (d) at 10x magnification.

Calcium imaging

Dissociated ventromedial hypothalamic neurons were obtained from Pacap-i-Cre x Z/EG transgenic mice age 10-14 days old. In the first experiment, we selected a field with two viable cells (Figure 4.10). The cells were acclimatised in aCSF containing 10mM glucose, and following recording initiation the initial aCSF was replaced with one of decreasing concentrations of glucose: 5mM at 200 seconds, 1mM at 400 seconds, 0.1mM at 800 seconds. The fura ratio for cell 1 increased as the glucose concentration decreased, indicating calcium influx to the cell and hence, the cell's activation. For cell 2, the fura ratio remained relatively stable throughout the recording period, not differing from the control region. Cell 1 remained activated until 2000 seconds, following the glucose concentrations returning to 10mM, exhibiting a slow adaptation to the glucose environment. As the glucose concentration of 10mM was again inhibiting the cell, there was a much more rapid efflux of calcium from the cell and the fura ratio reduced to a level below that at the beginning of the recording.

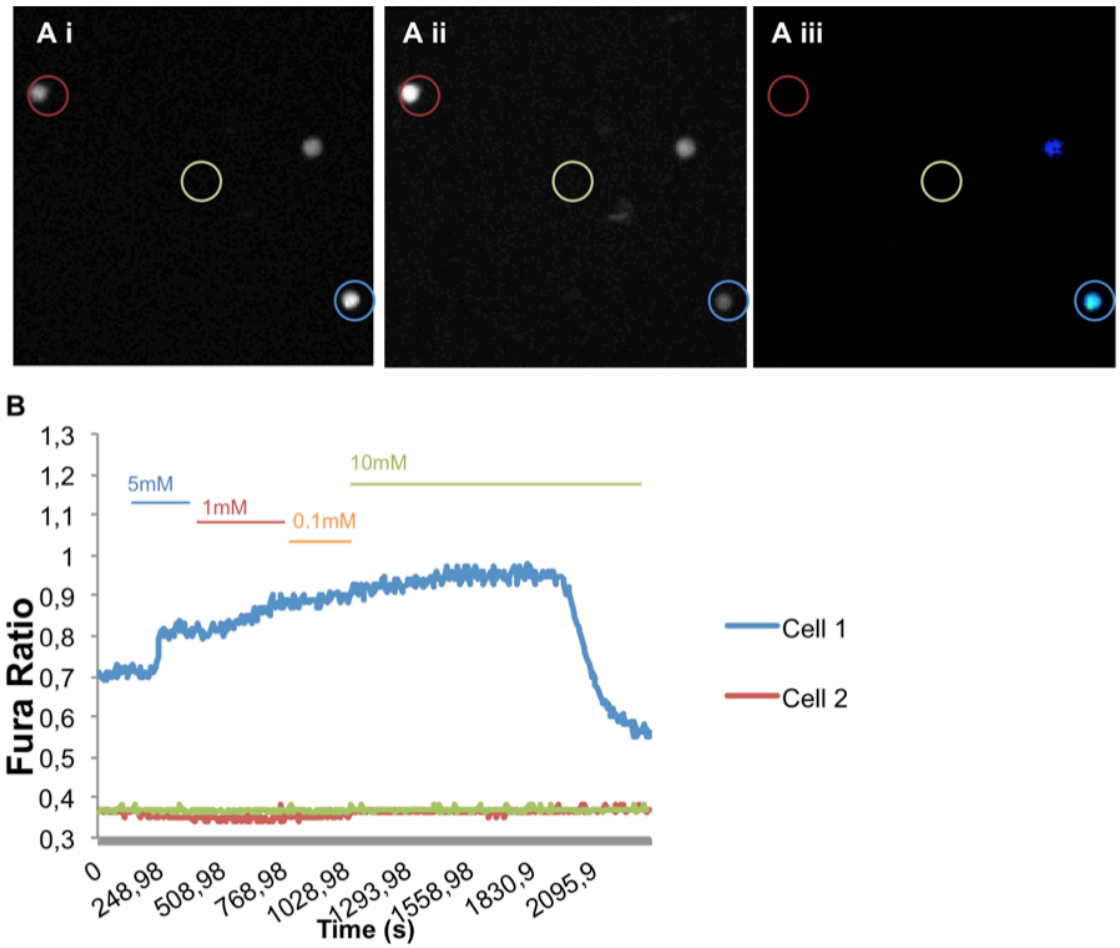

Figure 4.10 **Dissociated dorsomedial hypothalamic cells can be glucose inhibited.** Calcium imaging of two dissociated dorsomedial hypothalamic cells were recorded in different glucose concentrations. Calcium influx was activated in cell 1 by decreasing concentrations of glucose. a) Images collected at 608s of time course. i) 365nm bound fura. Regions of interest around each cell and control region are shown. ii) 385nm unbound fura. iii) Ratio of 365/385. b) Activity of cells throughout the time course of recording.

In a second experiment, we recorded from another field containing four viable cells (Figure 4.11). This recording showed individual cells with different responses to changes in glucose. Again, the culture was acclimatised in 10mM glucose before decreasing glucose concentrations was initiated: 5mM at 200 seconds, 1mM at 700 seconds and returning to 10mM at 1500 seconds. The initial decrease to 5mM glucose did not have an effect on any of the cells, but at 1mM cell 3 had a rapid and short activation, whereas cell 4 had a slower onset but sustained activation (similar to that seen in Cell 1 in the previous field; Figure 4.10). And again, this slower reacting cell 4 showed a delay in inhibition following the increase of glucose back to 10mM. Cells 1 and 2 appeared not to be affected by changes in glucose concentration and remained as stable as the control region.

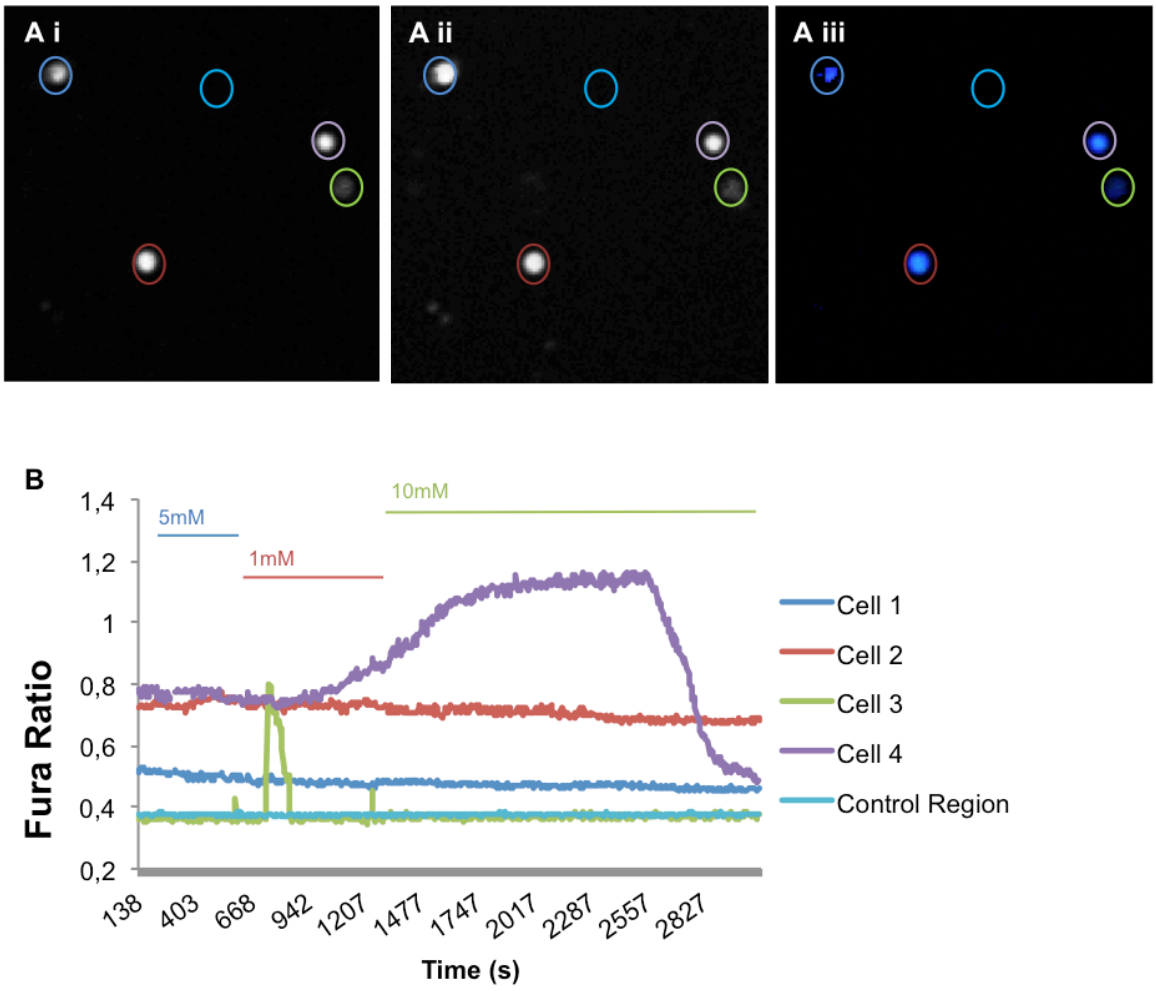

Figure 4.11 **Select dissociated dorsomedial hypothalamic cells are glucose inhibited at different rates.** Calcium imaging of four dissociated dorsomedial hypothalamic cells were recorded in different glucose concentrations. Cell 3 had a fast and short response to low glucose, whereas cell 4 had a slow sustained response. a) Images collected at 802s of time course. i) 365nm bound fura. Regions of interest around each cell and control region are shown. ii) 385nm unbound fura. iii) Ratio of 365/385. b) Activity of cells throughout the time course of recording.

In a final experiment, we recorded from a field containing 3 cells. This time the changing glucose concentrations were administered slightly differently: following acclimation in aCSF containing 10mM glucose, the concentration was lowered to 5mM at 100 seconds, then returned to 10mM at 300 seconds, then lowered to 1mM at 600 seconds, and finally returned to 10mM at 700 seconds again. All three cells responded to both the 5mM and 1mM applications, with cell 2 showing the largest fura ratio change and hence the largest change in activation. Cell 3 showed the least change in activation. Cell 1 had the fastest response to all changes in concentration, except the last application at 700 seconds. Cell 1 and 2 responded more to the 1mM concentration than the 5mM, cell 3 showed no difference in amplitude. All three cells were inhibited by the first re-application of 10mM glucose concentration with activity returning to baseline, but at the second cell 1 failed to adapt while cell 2 and 3 again returned to baseline. The control region remained stable throughout the recoding.

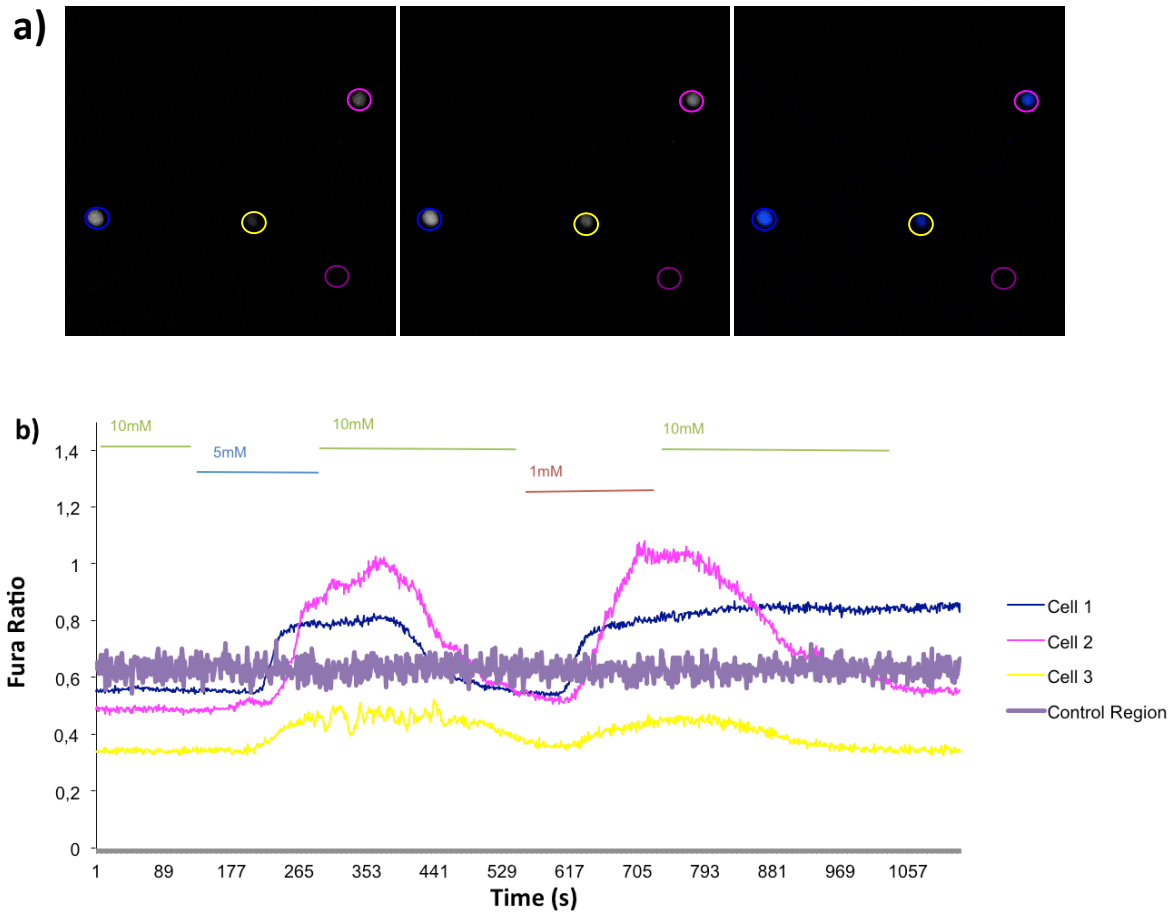

Figure 4.12 Select dissociated dorsomedial hypothalamic cells are glucose inhibited at different magnitude. Calcium imaging of four dissociated dorsomedial hypothalamic cells were recorded in different glucose concentrations. Cell 1, 2 and 3 all responded to a lowering of glucose concentration, but cell 2 responded with the largest increase in activation, cell 1's reaction was slightly smaller and cell 3 showed the smallest response. Cell 2 and 3 showed faster adaptation to the final return to 10mM concentration, while cell 1 showed very slow adaptation a) Images collected at

802s of time course. i) 365nm bound fura. Regions of interest around each cell and control region are shown. ii) 385nm unbound fura. iii) Ratio of 365/385. b) Activity of cells throughout the time course of recording.

4.4 Discussion

The VMN is established as having an important role in energy homeostasis, whether in the CRR to cause rapid changes in glucose or the longer term effects on body weight and food intake influenced by leptin. With such an integral part to play, it is likely that disruption in signalling in the VMN is a mediating factor in the development of metabolic diseases such as obesity and diabetes. Further discoveries are hampered by the lack of identified neurochemical phenotypes of the VMN neurons, as relevant neurotransmitters would provide markers for additional investigations into how these neurons are altered in response to metabolic disease. This would also allow for genetic targeting of specific populations of the VMN, by selective expression or blocking of that transmitter. As described previously, one strong potential candidate for VMN phenotyping is PACAP. In this chapter, we aimed to establish whether PACAP neurones in the VMN are involved in metabolic sensing of circulating leptin and glucose, through the use of transgenic mouse models, immunohistochemistry, electrophysiology and Ca^{2+} imaging.

To facilitate these experiments, two transgenic mouse lines were obtained, both with an eGFP signal present in PACAP-positive cells. In order to confirm the correct insertion of the IRES-Cre-recombinase into the genome, and that its expression is indeed driven by PACAP expression in the Pacap-i-cre mouse, we attempted to co-localise PACAP antibody staining with eGFP in our reporter strain Pacap-i-Cre x Z/EG. This test would also be necessary for the other reporter strain Adcyap1-eGFP, to confirm definite co-localisation. However, the experiment was not successful and the antibody failed to work in the eGFP positive Pacap-i-Cre x Z/EG mouse. There are only limited commercially available PACAP antibodies on the market, and the Santa Cruz product used in this study is considered the most effective, although here found to be unreliable. An alternative could have been the PACAP antibody used in the Hannibal and Durr publications, which have been synthesised in house by the laboratory of Dr Jens Hannibal, University of Copenhagen (Hannibal et al 1995), but this antibody is not commercially available at this time. Although the co-localisation of a PACAP antibody with the eGFP would ensure that there was no doubt that eGFP could be unquestionably used as a marker of PACAP cells in these mice, for the time being, we decided to work under the assumption that eGFP fluorescence in these transgenic animals is indicative of PACAP cells. There have been examples of publications using similar transgenic animals without explicit evidence that the target gene and eGFP are co-localised (Bouyer et al

2007). Bouyer and colleagues used the GHRH-eGFP transgenic mouse to detect if 'GHRH cells' co-localised with peptides including galanin, neurotensin and tyrosine hydroxylase. However, in the future *in situ* hybridisation techniques may be utilised to confirm co-localisation. In fact, since we carried out these experiments, we have had confirmation from the Lowell laboratory that eGFP in the PACAP-i-cre reporter crosses, shown with immunohistochemistry, does co-localise with PACAP mRNA, as shown by concomitant *in situ* hybridisation (personal communication).

To visualise the PACAP positive cells in the hypothalamus, we amplified the eGFP signal by immunostaining for GFP. In the VMN the GFP staining is particularly striking in both of our transgenic reporter lines, confirming a definite population of PACAP cells within this region. Here, we found most of the staining in the ventrolateral and central part of the VMN, with the dorsomedial region almost completely lacking any immunostaining. This finding is in contrast to previous *in situ* hybridisation, where *pacap* mRNA was found throughout the VMN (Durr et al 2007, Hannibal 2002). Not enough is known of the physiology and neurochemistry of the VMN to determine why there would be differences in distribution of mRNA and protein positive PACAP cells in the nucleus, but one possible explanation is that there is incomplete expression of cre in the PACAP cells in that region.

In the Arc, the presence of PACAP positive cells varied in the two transgenic lines, with no occurrence apparent in the Adcyap1-eGFP mice while in the Pacap-i-cre there was a small population present in the dorsolateral part of the Arc. This population appeared to be continuous with the one in the VMN, suggesting that although the VMN and Arc are defined as anatomically separate, the PACAP cells in the VMN and Arc could still be part of the same population physiologically and functionally. In the literature, there are disparate accounts of whether *pacap* mRNA is present in the Arc. Durr et al (2007) found presence of mRNA in the nucleus, while Hannibal (2002) did not; both of these studies were performed in rats. However, in Chapter 3 we found *pacap* mRNA in the Arc of CD1 mice. Taken together, it is clear that further characterisation of the Arc is needed to confirm the presence of PACAP-positive cells in the nucleus. One possible explanation for the differing accounts is that there could be species (rat/mouse) and strain (Adcyap1-eGFP / Pacap-i-Cre x Z/EG) differences in the expression of PACAP.

In a separate experiment we generated a mouse line where the leptin receptor has been knocked out of PACAP-positive cells, the Pacap-i-cre X Lepr flox. There appeared to be no effect of the lack of the leptin receptor on the body weight accumulation of the mice up to 20 weeks of age. In comparison, the full leptin receptor knock out *db*/*db* has an extreme obese phenotype, and a

knock out specifically in POMC neurons also exhibits an obese phenotype, albeit one that is less severe (Balthasar et al 2004). The latter suggests that neuronal populations other than POMC cells, perhaps also within the hypothalamus, must be involved in the development of the obesogenic phenotype in the *db*/*db*, but from our findings it would appear that PACAP cells are not among them. However, we have previously shown in the lab that PACAP strongly co-localise with SF-1 (Hawke et al 2009), and when the leprB is specifically knocked out in VMN specific SF-1 cells, obesity is induced (Dhillon et al 2006). Hence, one could infer that our transgenic Pacap-i-cre X Lepr flox mouse should also have an obese phenotype. Again, one possible explanation is that we are getting incomplete expression of cre in the PACAP cells in the VMN, which might also explain our next finding. The *db*/*db* is also characterised by fasting hyperglycaemia and insulin resistance (Hummel et al 1966) and we investigated whether the Pacap-i-cre X Lepr flox mouse would exhibit an abnormal response to a glucose tolerance test, which was not the case. Taken together, the usefulness of our Pacap-i-cre X Lepr flox mouse is questionable when studying the effect of a specific knockout of the leptin receptor in PACAP neurons.

Although leptin is generally believed to exert its effects on body weight over the long term, acute administration is known to have drastic negative effect on food intake in both lean and obese animals (Halaas et al 1995, Pelleymounter et al 1995a, Rentsch et al 1995). Hence, when we tested the feeding response of our Pacap-i-cre X Lepr flox mice to a systemic injection of leptin, we expected to see an early reduction in food intake in our control mice as we have seen previously in the lab (Hawke et al 2009). However, the statistical test we used did not show significance of the reduction until the 12-hour time-point. Importantly we did not see any effect of leptin in the floxed mice, and although potentially problematic because of the incomplete cre expression, this finding supports the role PACAP neurons play in leptin's anorectic effects.

Taken together, our results do not completely clarify whether leptin is having a physiological role through PACAP neurons, which led us to question what other roles pacap neurons in the VMN play in terms of metabolism.

Hence, we investigated the response of PACAP neurons to systemic hypoglycaemia. PACAP (from an unknown source) is known to act through the PVN to activate the sympathetic pathway leading to an increase in hepatic glucose production (Yi et al 2010), and we hypothesised that it was PACAP from the VMN mediating the CRR to hypoglycaemia. We investigated this by inducing glucoprivation by 2DG injection in Adcyap1-eGFP mice, and then performing an immunohistochemical stain for c-Fos, which we used as a neuronal activity marker (Luckman et al

1994). Disappointingly, 2DG did not induce c-Fos in eGFP positive cells, making it hard to infer anything about whether hypoglycaemia does activate PACAP neurons in the hypothalamus of these mice. It is possible that the 2DG dose used was insufficient to induce hypoglycaemia, which is supported by the relatively small, but significant, increase in feeding observed in these mice. In fact, a study by Lewis et al (2006) comparing different mouse strains' feeding response to 2DG observed that the Swiss Webster mouse, which is the background of the Adcyap1-eGFP, did not increase its food intake in response to glucoprivation (Lewis et al 2006). However, while in the Lewis study the Swiss Webster only had a food intake increase of 0.01g, in this study our Adcyap1-eGFP had an increase of 0.3g, which is smaller than what we have observed in the lab in CD1 mice (1.5g, unpublished) but still significant. As the behavioural response is intact in our case, we have to infer that the dose of 2DG was sufficient to induce hypoglycaemia, and that the c-Fos results are therefore reliable.

We would expect to see an activation in the VMN, as unpublished data from our lab show that SF-1 positive VMN cells, which have previously been shown to express *pacap* mRNA (Hawke et al 2009), are sensitive to physiological changes and decreases in glucose (Belle, Piggins and Luckman, unpublished). However, not all cells express c-Fos when they are electrically activated. Hence, it would be required to further verify the induction of hypoglycaemia and CRR in the Adcyap1-eGFP mice by measuring blood glucose, insulin, glucagon and adrenaline in order to clarify these results. As an alternative, insulin treatment could be used instead of 2DG and in that way induce glucoprivation, or glucose administration could be used to determine whether PACAP neurons are glucose activated. But the best way to further investigate c-Fos activation in PACAP neurons following glucoprivation by 2DG would be to not use the Adcyap1-eGFP mouse but the Pacap-i-Cre x Z/EG, which is on a C57BL/6 background and not the problematic Swiss Webster. However, the Pacap-i-Cre x Z/EG mouse was not available when these experiments were conducted.

While no increase in c-Fos induction was observed, we did see an increase in the number of eGFP-positive cells in the VMN in response to glucoprivation, particularly in the ventrolateral part. It is unknown if 90 minutes for the cull post injection in this experiment is enough for 2DG to induce maximal changes in PACAP expression, but from these results it suggests that this can occur and that 2DG can induce PACAP expression. If so, this could infer a modulatory role of PACAP in glucose regulation. As we have seen in Chapter 3, and as previously reported by Hawke et al (2009), *pacap* mRNA is regulated in response to fasting and obesity, but we have not investigated

this in the context of short-term hypoglycaemia. If *pacap* mRNA can be proven to be up regulated in response to hypoglycaemia, it would support the possible role PACAP plays in glucose detection, but it would still not be clear how it mediates homeostatic effects.

In order to further characterise the VMN PACAP neurons and their involvement in glucose sensing, we performed an initial patch clamp electrophysiology experiment. VMN neurons positive for the transcription factor SF-1 had already been seen to be glucose sensitive by our lab, and if our hypothesis that PACAP neurons are involved in the CRR to hypoglycaemia held true, the eGFP expressing PACAP neurons in the VMN of the Pacap-i-Cre x Z/EG mouse was likely to be part of this glucose sensing population. Preliminary data from our recording of electrical responses of eGFP-PACAP neurons found that the majority of the cells were found to be glucose inhibited, while some were non-responsive. The glucose inhibited cells were hyperpolarised and silenced, or exhibited a reduction in firing frequency, in response to an increase in glucose concentration from 1mM to 5mM. These neurons display a specific electrophysiological fingerprint that has previously been seen in glucose responsive orexin neurons in the lateral hypothalamus (Burdakov et al (2005). When receiving a depolarising current these cells exhibit an increase in firing rate with no spike adaptation, and when receiving a hyperpolarising pulse, a quick off response is observed, i.e. the cells produce an action potential when the current is reverted (Burdakov et al 2005a). Importantly, this part of the project has been picked up by a new post-doc in the laboratory (Dr Nicholas Nunn), who has increased the number of PACAP neurones recorded inside the VMN or just outside its anatomical bounds. At the time of writing, 6/6 PACAP neurones within the VMN are GI, while 0/6 outside the VMN are glucose responsive. From these results we can assume that PACAP VMN neurons are activated by a reduction in glucose concentration (i.e. glucose inhibited and, in that way, may form part of the response to hypoglycaemia.

To investigate this further, we attempted to record glucose responses from dissociated ventromedial hypothalamic neurons using Ca^{2+}-imaging. We used the Pacap-i-Cre x Z/EG mouse for these experiments, but did not obtain recordings from eGFP positive cells, due to the low number of cells remaining in our cultures following dissociation. Whether this is due to experimental variation, in that we did not get any eGFP cells to adhere to the prepared coverslips, or due to poorly designed procedure, is unknown. One possibility is that the eGFP fluorescence was bleached during the process, or that its expression was affected by the relatively toxic incubation with the Fura-2 dye. We also had issues obtaining healthy cultures that would produce reliable results when recorded from the day after plating, as was our initial plan. Instead, we

recorded immediately following dissociation when the cultures were healthiest, and up to 5 hours after. The cause of the problems with unhealthy cultures might be that the recipe for aCSF was taken from a protocol for dissociating rat cortical neurons. In fact, most publications using Ca^{2+}-imaging are in rat. In the future, it might be advisable to adjust the molarity of salts and sugars to promote hyperpolarisation and reduce cell firing, which may protect the cells after the unsettling process of dissociation and allow them to survive for longer.

From our Ca^{2+}-imaging recordings, it appears that some dissociated ventromedial hypothalamic neurons are glucose inhibited, while some are non-responders. When the glucose concentration was decreased, these cells were depolarised by an influx of calcium, calculated by the ratio of bound: unbound Fura-2. These glucose-induced changes in Ca^{2+} oscillations are qualitatively similar to glucose-induced responses of VMN glucose sensing neurons in slice preparations (Silver & Erecinska 1994, Song et al 2001). When the glucose concentration was increased, most of the cells showed an efflux of calcium, likely resulting in hyperpolarisation, although the cells varied in the swiftness of response. One cell showed a rapid and short-lived glucose-inhibited response, while most others showed glucose-inhibited response of varied delay and sustainability. This heterogeneity in the responses is expected, as different subtypes of glucose-inhibited neurons are most likely necessary to fine tune the response to a changing glucose environment and energy state.

However, as stated above, we have no way of proving that the cells recorded from in these Ca^{2+}-imaging experiments are PACAP-positive, or that they are definitely VMN cells. Hence, in future experiments it might wiser to modify the Ca^{2+}-imaging recording protocol to be used in brain slices, circumventing the damaging dissociation step. Then the cells would be *in situ*, and the exact anatomical position of the neurons would be defined. However, while dissociated cells do not have their activity affected by pre-synaptic inputs, this would have to be taken into consideration when recording from slice preparations (Song et al 2001).

Song et al (2001) reported findings of a heterogeneous population of glucose sensing neurons in the VMN using patch clamp electrophysiology, which included a large population of glucose-excited neurons, but they also identified a population of glucose-inhibited neurons. If our conclusions are correct, this would imply that the glucose-inhibited neurons are PACAP cells and that signalling in the glucose-excited neurons may be mediated by other factors with distinct physiological function. Going forward, it will be imperative to further define and characterise the recording parameters of VMN cells, as cell populations throughout the brain differ in their

response to stimuli and the signature of VMN cells needs to be determined. It is also important to study responses of VMN cells, either dissociated or in slice preparation, using Ca^{2+}-imaging or patch clamp electrophysiology, to changes in physiologically relevant glucose levels (normal levels 1.0-2.5mM, sever hypoglycaemia at 0.2mM) to mimic an *in vivo* situation.

As a final comment, it can be said that while the CRR to hypoglycaemia is sufficient to normalise glucose levels in healthy individuals, repeated bouts of severe hypoglycaemia can reduce the response to glucose (Borg et al 1999, Cotero & Routh 2009, Kang et al 2008, Song & Routh 2006), and can have a significant deleterious effect on subsequent endocrine CRR in both rats and humans (Davis & Shamoon 1991, Powell et al 1993). The condition is known as hypoglycaemia associated autonomic failure (or HAAF), and this is an extremely serious phenomenon when occurring in diabetic patients who receive insulin replacement, who are already particularly sensitive to hypoglycaemia (Cryer 2005). If the results shown here are reliable, they would imply that glucose-inhibited PACAP neurons in the VMN are involved in the CRR to hypoglycaemia, and further investigation would be warranted in order to attempt to elucidate how repeated hypoglycaemia affects the properties of these cells in an attempt to elucidate how the CRR becomes impaired in HAAF.

4.5 Summary

The VMN plays a crucial part in the regulation of appetite, body weight and glucose homeostasis (Borg et al 1997, Zhao et al 2004). However, the mechanism by which this is mediated is still unknown, but candidates include PACAP and leptin. From our findings, it is not clear whether leptin is having a physiological role through PACAP neurons, which begs to question what are the roles of PACAP neurons in the VMN in terms of metabolism. Attempts have been made in this chapter to confirm that a subtype of VMN neurons contain PACAP using the Adcyap1-eGFP and PACAP-i-cre X Z/EG transgenic mouse lines, and progress has been made in both experimental procedures and findings that will work towards characterisation of the VMN in relation to energy homeostasis. Electrophysiological findings in this study indicate that PACAP-positive cells in the VMN are glucose inhibited, although these results could not be confirmed using *in vivo* techniques, as induced hypoglycaemia was not found to produce c-Fos in VMN neurons. However, important steps forward have been made in elucidating the phenotype of VMN PACAP cells by electrophysiological and Ca^{2+}-imaging techniques, highlighting the value of our two transgenic reporter strains. Further work confirming the hypothesis that PACAP VMN neurons are glucose

inhibited is warranted, and is required to fully clarify the role of PACAP in the CRR to hypoglycaemia. Such work could lead to better understanding of the pathogenesis of HAAF in diabetic patients.

Chapter 5. The anorectic effects of PACAP and downstream targets

5.1 Introduction

PACAP has multiple functions in the brain, which have been extensively reviewed in the literature (Vaudry et al 2009). Notably, there is convincing evidence indicating an important role for PACAP in the regulation of energy homeostasis. When administered into the brain, PACAP reduces food intake in rodents (Hawke et al 2009, Mizuno et al 1998b, Morley et al 1992, Mounien et al 2008, Resch et al 2011), while fasting lowers levels of PACAP mRNA in the ventromedial nucleus (VMN), as seen in Chapter 3 and in Hawke et al (2009). In addition, genetic impairment of PACAP signaling disrupts carbohydrate and lipid metabolism, glucose handling and brown adipose tissue thermogenesis (Adams et al 2008, Gray et al 2001, Gray et al 2002, Hashimoto et al 2000). As yet, it is unknown through which receptors these effects are mediated.

To date, three receptors have been cloned, for which PACAP and the related VIP are ligands: the PACAP-specific PAC_1 receptor (gene name *Adcyap1r1*), and the $VPAC_1$ and $VPAC_2$ receptors (gene names *Vipr1* and *Vipr2*) that are activated by both PACAP and VIP, though affinities vary (Vaudry et al 2009). All three receptors are expressed widely in the brain, including regions that influence energy balance. Previous studies have demonstrated that PACAP-induced anorexia and thermogenesis can be blocked by co-administration of the synthetic PACAP analogue $PACAP_{6-38}$ (Hawke et al 2009, Mounien et al 2008, Resch et al 2011), which has high affinity for the PAC_1 and $VPAC_2$ receptors, but demonstrates only negligible binding at $VPAC_1$ (Gourlet et al 1995). This suggests that the acute metabolic effects exerted by PACAP are mediated by PAC_1 or $VPAC_2$. The striking similarities in the metabolic profiles of PAC_1 and PACAP null mice implicate the PAC_1 receptor as being of prime importance. However, the $VPAC_2$ receptor increases endogenous hepatic glucose production after central infusion of PACAP in rats (Yi et al 2010) and, thus, cannot be discounted as being possibly involved in other metabolic effects.

Like PACAP itself, the expression of the different receptors is widespread throughout the brain, including regions that have been implicated in energy regulation (Joo et al 2004). While several groups have examined specific target sites such as the hypothalamic paraventricular nucleus (PVN)(Agarwal et al 2005, Legradi et al 1998), the hypothalamic arcuate nucleus (Arc)(Mounien et

al 2006, Mounien et al 2008), and the midbrain periaqueductal grey (PAG)(Maekawa et al 2006), amongst others, more extensive studies have not yet been described.

Since forebrain ventricular injection of PACAP reduces fast-induced re-feeding (Mizuno et al 1998b, Morley et al 1992, Mounien et al 2008), and the anorectic actions of both PACAP and leptin on normal, night-time feeding are blocked by $PACAP_{6-38}$ (Hawke et al 2009), understandably interest has focused on the hypothalamus and its connections. The Arc and PVN are key regulatory nuclei that have reciprocal connections with the VMN, where the majority of hypothalamic PACAP-expressing neurons are found and where PACAP expression is regulated in a leptin-dependent fashion (Hawke et al 2009). The injection of PACAP directly into the VMN, albeit at relatively high concentrations, can reduce feeding (Resch et al 2011). Mounien and colleagues have highlighted a potential downstream role for Arc POMC neurons, since the anorectic effects of PACAP were reversed by the melanocortin receptor antagonist, SHU9119 (Mounien et al 2006, Mounien et al 2008). However, this pathway is further complicated by the localisation of PACAP in a subset of POMC neurons in the Arc itself (Durr et al 2007). In contrast, PACAP is released by stress in the PVN, where it can activate neurons that contain corticotrophin-releasing hormone (CRH), and so may be part of a more general stress response that includes reduced feeding (Agarwal et al 2005, Legradi et al 1998). While the ventromedial hypothalamus is an important source of PACAP, we cannot ignore the potential role of PACAP-containing neurons from outside the hypothalamus. Indeed, PACAP innervation of the PVN comes from many extra hypothalamic areas (Das et al 2007). Our laboratory has re-evaluated the role of melanocortin receptors in mediating the anorexic effects of PACAP, and has shown that they probably are not involved. Instead, we have evidence that downstream signaling may require CRH receptors (unpublished). Here, we also aim to determine the potential role of oxytocin signaling.

5.2 Methods

5.2.1 Animals

CD1 mice were cannulated with the cannulae inserted into the lateral ventricle and were given an intracerebroventricular (i.c.v.) injection of drugs in a volume of 2µl of sterile isotonic saline vehicle (B. Braun Medical Ltd., UK).

5.2.2 i.c.v. PACAP or VIP in CD1 mice

Daytime fast-induced re-feeding assessment: following an overnight fast, pre-weighed food was returned to the mice immediately after injection and intake was measured at the time points 1, 2 and 4 hours later. For the initial comparative study in CD1 mice, groups received saline vehicle, 30 or 60 pmol PACAP, 30 or 60 pmol VIP (Bachem, Germany).

5.2.3 i.c.v. PACAP and antagonist

For the nocturnal re-feeding studies using the receptor 'antagonists', treatment groups were as follows: saline vehicle; 30 pmol PACAP only; 30 pmol PACAP + 'antagonist'; 'antagonist' only (n=5-14 per group). The dose of 9 nmol of the oxytocin receptor antagonist ([d(CH2)51,Tyr(Me)2,Orn8]-oxytocin) was based on previous work by the lab (Bechtold & Luckman 2006).

5.3 Results

5.3.1 Effect of PACAP and VIP on food intake

PACAP administered i.c.v. dose-dependently reduced food intake at 1, 2 and 4 hours after injection in a fast-induced re-feeding paradigm (Figure 5.1). By contrast, equimolar doses of VIP had little effect on food intake. 30 pmol of VIP failed to alter food intake at any time point, and 60 pmol VIP caused only a small decrease in food intake, and only at the 2-hour time point (**Error! Reference source not found.**).

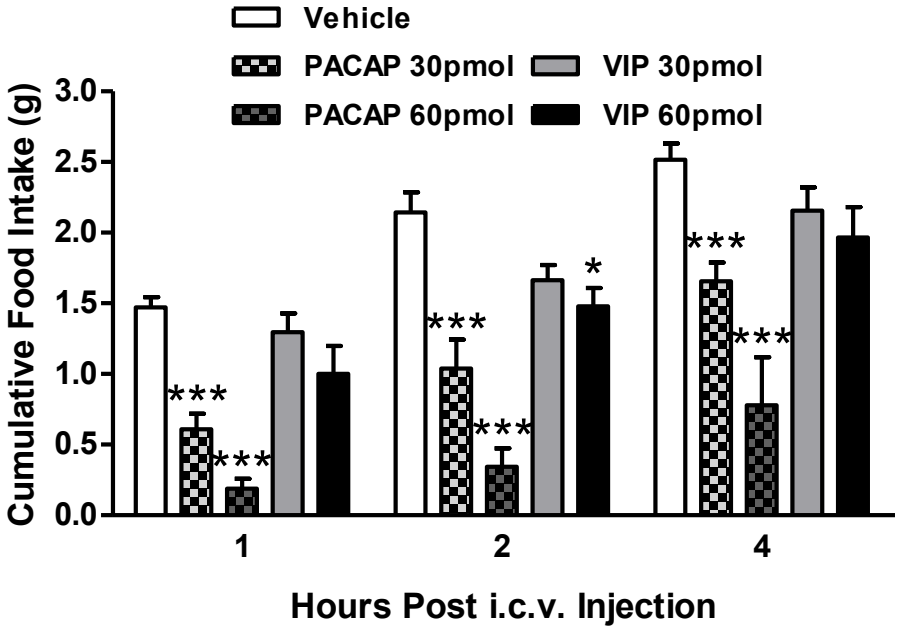

Figure 5.1 **Effect of equimolar PACAP and VIP on fast-induced re-feeding**. Food intake was measured at 1, 2 and 4h after i.c.v. injection of saline vehicle, 30 pmol PACAP, 60 pmol PACAP, 30 pmol VIP, 60 pmol VIP (n=6-7 per group). Bars represent mean ± SEM. *P<0.05, ***P<0.001 compared with vehicle; one-way ANOVA with Bonferroni's *post hoc* test.

5.3.2 Co-administration of an oxytocin receptor antagonist with PACAP

9 nmol oxytocin antagonist ([d(CH2)51,Tyr(Me)2,Orn8]-oxytocin) did not reduce the hypophagic effect of PACAP. This dose of the antagonist has been shown to be effective in our hands in previous experiments (Bechtold & Luckman 2006).

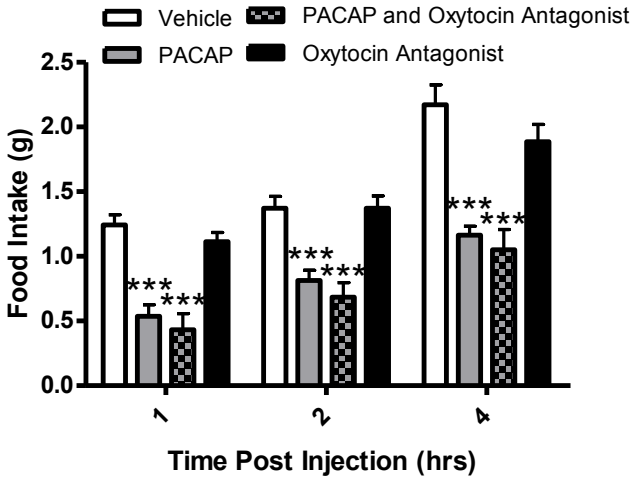

Figure 5.2 **Oxytocin antagonist effect on PACAP-induced anorexia.** The effect of administration of 9 nmol oxytocin receptor antagonist, [d(CH2)51,Tyr(Me)2,Orn8]-oxytocin, on hypophagia induced by 30 pmol PACAP at 1, 2 and 4h after injection. Groups were saline vehicle, PACAP alone, PACAP + d(CH2)51,Tyr(Me)2,Orn8]-oxytocin, d(CH2)51 and Tyr(Me)2,Orn8]-oxytocin alone (n=7-8 per group). ***P<0.001 compared with vehicle; two-way ANOVA with Bonferroni's *post hoc* test.

5.4 Discussion

PACAP has a well-established anorexic action when administered centrally, though the receptors and downstream effectors, or how it relates to normal physiology is currently unknown. Here we attempted to dissect the target pathways through which the effect of PACAP is propagated. Firstly, there are three G protein-coupled receptors with which PACAP binds with equal affinity, and two of which also bind VIP (Vaudry et al 2009). Knock-out of the PAC_1 (*Adcyap1r1*) receptor produces a very similar metabolic phenotype as the PACAP knock-out mouse (Adams et al 2008, Gray et al 2001, Gray et al 2002, Hashimoto et al 2001) and, thus, this lessens the potential role for VIP being the endogenous regulating peptide, and makes this receptor the likely candidate to mediate the anorectic response to endogenous PACAP. By comparison, the $VPAC_1$ (*Vipr1*) knock-out mouse has no obvious metabolic phenotype (personal observation) and, although the VPAC2

(*Vipr2*) knockout mouse displays a dampening of feeding patterns, this phenotype is related more to VIP signaling in the suprachiasmatic nucleus and an advancement of daily rhythmic behaviours (Bechtold et al 2008). The shortened peptide, $PACAP_{6-38}$, acts as a receptor antagonist, and has been shown previously to abolish PACAP-induced hypophagia (Hawke et al 2009, Mounien et al 2008, Resch et al 2011). However, $PACAP_{6-38}$ binds to both PAC_1 and $VPAC_2$ receptors, and so it does not fully distinguish the endogenous peptide or receptor involved. To further clarify the situation, we first tested whether equimolar doses of centrally injected VIP and PACAP had the same hypophagic effect. PACAP's actions were robust at lower doses and displayed a definite dose-dependent effect. We found that VIP elicited a small reduction in food intake, and only at the higher dose. This again indicates that VIP and the two VPAC receptors are less likely to be involved in central anorexic pathways. Previous experiments in the lab tested this by centrally injecting PACAP into $VPAC_1$ and $VPAC_2$ receptor knockout mice (unpublished). PACAP elicited the same effect as in wild-type controls in both the receptor knockout strains. This finally implicates the PAC_1 receptor in PACAP's effect on feeding, and complements our earlier additional findings that the effect of PACAP to induce thermogenesis and mediate some of the metabolic actions of leptin, are also dependent on PAC_1 signaling (Hawke et al 2009). This is an interesting contrast to another metabolic action in the hypothalamus, whereby PACAP increases endogenous glucose production through an action on the $VPAC_2$ receptor (Yi et al 2010).

Following on from our hypothesis that the hypophagic response of PACAP is mediated by the PAC_1 receptor, previous experiments in the lab went on to investigate which areas of the brain might be targeted. In a functional mapping study (unpublished), we found that central PACAP injection caused substantial c-Fos induction in the PVN and CeA, the two major brain areas that express CRH (Makino et al 1994). Cells of the PVN and CeA strongly express the PACAP-specific, PAC_1 receptor (Hashimoto et al 1996, Joo et al 2004, Nomura et al 1996) and dense PACAP-immunopositive terminals innervate these areas (Koves et al 1991, Legradi et al 1997, Piggins et al 1996).

Oxytocin neurons in the PVN are activated by satiety signals from the gut, but also by overeating or nauseous stimuli (Ho & Blevins 2013, Olszewski et al 2010). Thus, they may represent the convergence of a number of central pathways that lead to a reduction in food intake. Recent investigation of a hypothalamic feeding circuit demonstrated that feeding in response to the activation of AgRP neurons in the Arc leads to an inhibition of PVN oxytocin neurons (Atasoy et al 2012). Since AgRP reversed the hypophagia produced by PACAP, could oxytocin neurons be the

common downstream target of PACAP/AgRP signaling? Oxytocin acts through a single G-protein-coupled receptor, and so we used the same antagonist, d(CH2)51,Tyr(Me)2,Orn8]-oxytocin, which we had shown previously to affect satiety signaling by a cholecystokinin-vagal-NTS-prolactin-releasing peptide pathway (Bechtold & Luckman 2006). However, d(CH2)51,Tyr(Me)2,Orn8]-oxytocin, was unable to attenuate PACAP-induced hypophagia, suggesting oxytocin neurons do not have a role in mediating the effects of PACAP on food intake.

Central PACAP injection alters the expression levels of CRH mRNA in the PVN of both rats (Grinevich et al 1997) and mice (Mounien et al 2008). This anatomical and histological evidence suggests a physiological connection between the PACAP and CRH systems. In a previous experiment in the lab PACAP was co-administered with the CRH antagonists α-helical CRH and astressin, and we found that both antagonists partially attenuated the hypophagic effect of central PACAP (unpublished). Although these various findings support the hypothesis that CRH cells of the PVN are an important target for PACAP, we cannot discount the fact that PACAP also activates the CeA, which is another major source of CRH. Furthermore, because the *in vivo* effects of PACAP were only attenuated and not completely abolished by either CRH antagonist, we need to include the involvement of other neural substrates in mediating PACAP-induced hypophagia.

Other groups have highlighted a role for a PACAP projection from the VMN to POMC neurons in the hypothalamic arcuate nucleus (Mounien et al 2006, Mounien et al 2008, Resch et al 2011). In a previous functional mapping study we found no significant change in c-Fos immunopositive cells in the Arc following 30 pmol PACAP, though there was a trend towards an increase, but expression was seen in regions known to govern food intake including the PVN (unpublished). The MC_4 receptor is expressed on POMC neurones and we investigated the involvement of the melanocortin system in PACAPs anorectic effect in a previous experiment by co-administering Mc_4R antagonist SHU9119 and inverse agonist AgRP. We found that SHU9119 does not block PACAPs effects while AgRP completely blocks the reduction in food intake. There is strong evidence that AgRP, in contrast to SHU9119, functions independently as an inverse agonist, causing active downregulation of receptor tone. While anorectic peptides such as CRH, α-MSH and evidently PACAP all stimulate cAMP production in target cells, AgRP causes an active decrease in such intracellular events upon binding to melanocortin receptors, rather than purely blocking receptor activation (Chai et al 2003, Ollmann et al 1997).

Interestingly, and unlike any of the antagonists we have tested in the lab, AgRP was able to fully reverse the effects of PACAP on feeding in our previous study. However, considering our earlier

SHU9119 data, we do not judge that a direct relationship between PACAP and POMC neurons/peptides should necessarily be inferred from this result. Instead, we propose an alternative hypothesis, whereby actions of exogenous AgRP and PACAP converge on common metabolic target cells, resulting in 'cancelling out' of the anorexic effect. We believe these pathways are convergent, rather than independent, since the pre-fast will have reduced the tone on anorexic pathways, meaning AgRP would have little further effect if acting on non-PACAP targets. In support of this, AgRP alone under these conditions did not increase food intake. Therefore, we suggest that AgRP decreases the activation of melanocortin receptor-expressing cells, which also respond to PACAP, resulting in a zero net effect on food intake.

The physiological role of PACAP, notably that produced in the ventromedial hypothalamus, remains enigmatic. The expression of *Pacap* mRNA in the VMN is regulated by leptin according to nutritional status (Hawke et al 2009). Although central injection of exogenous PACAP acts as a powerful anorexigen (Hawke et al 2009, Mizuno et al 1998b, Morley et al 1992, Mounien et al 2008), this may not be a normal physiological function. Indeed, we have shown that high doses of exogenous PACAP cause non-appetitive behaviours (Hawke et al 2009), which could indicate nausea or aversion. This might be supported by our previous finding that PACAP-induced hypophagia is at least partially dependent in CRH receptor signalling (unpublished), which could indicate non-selective activation of the HPA axis. Furthermore, the *in vivo* evidence for a role of POMC cells/melanocortin signalling downstream of PACAP remains ambiguous. Genetic work carried out by Lowell and colleagues demonstrates that the effect of leptin on VMN neurons, which co-express PACAP and steroidogenic factor 1 (SF-1) (Hawke et al 2009), and that on Arc neurons which express POMC are non-convergent, since knock-out of the leptin receptor in both cell types have an additive effect on the obesity phenotype compared with knock-out in either cell type alone (Dhillon et al 2006). Given that impairment of PACAP signalling disrupts carbohydrate and lipid metabolism, glucose handling and brown adipose tissue thermogenesis (Adams et al 2008, Gray et al 2001, Gray et al 2002, Hashimoto et al 2000), a leptin-sensitive role in these metabolic functions may be more important physiologically than appetite regulation.

Chapter 6. Diet-induced obesity in recombinant inbred mouse strains

6.1 Introduction

Obesity is a complex disease that develops from an imbalance in energy homeostasis where the relationship between energy intake and expenditure has been disrupted. The upset to the equilibrium usually stems from a disruption in the complex interaction between genes and environment. The predisposition for developing metabolic syndrome, like obesity, is not inherited in the classical Mandelian fashion (one gene-one phenotype), but has instead a pathogenesis based on genetic heterogeneity and complex gene-by-environment interactions. Attempts to untangle the genetic basis of obesity by utilizing single gene analysis, as in mice knock-out studies where a gene mutation's effect on the response to an inappropriate environment (e.g. HED) is investigated, fails to recognize underlying polygenic networks of genes and gene-by-environment interactions (Andreux et al 2012, Auwerx et al 2004). Genome-wide analyses studies (GWAS), where genetic variants are identified that contain risk factors for developing metabolic disease in humans, has had more success in finding both genetic (e.g. mutations in the *fto* gene (Dina et al 2007)) and environmental causes (e.g. lack of exercise (Warden & Fisler 2008)). But again, these studies have difficulty defining gene-by-environment interactions as they struggle to control for cohort, environment and admixture effects, which is a recurring problem in human studies along with the inability to obtain certain molecular or physiological data (Andreux et al 2012). So, neither single-gene nor genome-wide analyses are able to identify the networks of genes or the phenotypes they modify, which together underlie metabolic disease.

Metabolic syndrome develops through the additive effect of several intermediate phenotypes, for example glucose intolerance and body fat composition, which are modulated by genetic and environmental factors. These intermediate obesity traits, or quantitative traits, also influence each other rendering causality hard to determine. By utilizing a systems genetics approach, and with the development of murine genetic reference populations, these obstacles can be circumvented. The underlying principle of these powerful genetic model systems is to use multiple-genes to multiple phenotype analysis to investigate causal interactions between sets of traits, gene-networks or environmental conditions (Williams et al 2001). The recombinant inbred

strains offer compelling advantages for mapping complex genetic traits and in integrative genomics research (Chesler et al 2005), in particular those that have modest heritability (Williams et al 2001) as they create an immortalized mapping population that allows researchers to phenotype as many animals per line as desired over extended periods of time, reducing the effect of environmental noise (Peirce et al 2004). The BXD is such a system, with a recombinant inbred model of over one hundred genetically defined lines that initially was produced by crossing two well characterized progenitors: C57BL/6J (B) and DBA/2J (D), hence BXD.

The Jackson Laboratory first generated the BXD recombinant inbred model in the mid 1970s. Following the parental cross, the F1 generation is crossed again to produce the F2 generation, which in turn is then inbred for at least 20 generations. This continuous inbreeding within each family generates a 'frozen' recombinant pattern that is specific for that particular line, and that is homozygous for one of only two possible alleles (either from B or D) at every genetic locus (Figure 6.1). As both parental mice have been fully sequenced, it has been possible to determine that these two strains differ at approximately 4.8 million segregating single nucleotide polymorphisms (SNPs), and varies by 500,000 insertions and deletions (www.genenetwork.org/mousecross.html). This means that the BXD model captures a vast amount of genetic variation and reaches the complexity of the human population (Andreux et al 2012). It also means that the efficiency of positional candidate gene evaluation is greatly increased (Chesler et al 2005). And, because each recombinant line is genetically fixed, data collected in separate experiments across time and location can be analyzed in conjunction, as the genetic variation remains the same and variation associated with environmental factors and technical errors can be suppressed to low levels (Williams et al 2001). Data for hundreds of phenotypes, including gene expression data for over 30 body tissues, have been acquired over nearly a 40-year period (Chesler et al 2005), making the BXD model the largest genome, transcriptome and phenome dataset available for a mammalian model system (Andreux et al 2012). Furthermore, as the BXD panel has been so extensively studied, it lends itself to the efficient construction of pleiotropic relations and genetic networks (Chesler et al 2005). Most studies to date utilising the BXD model has been designed to investigate the genetics of immune function and infectious disease (Bystrykh et al 2005, Miyairi et al 2007) and in behavioural and neuropharmacological research (Chesler et al 2005, Gaglani et al 2009, Laughlin et al 2011, Philip et al 2010), but besides a paper by Andreux et al 2012, few studies have looked at the development of metabolic phenotypes.

A systems-genetics approach was used here in a pilot experiment to investigate the effect of HED on recombinant BXD mice and the interactions between three levels: genetic variation that occurs across the lines in terms of their DNA sequence, intermediate phenotype (e.g. adiposity, glucose tolerance) and systems level phenotype (e.g. body weight gain and metabolic syndrome). Moreover, we used a novel approach to apply variation in the mRNA expression of key regulatory genes across mice for additional quantitative trait analysis.

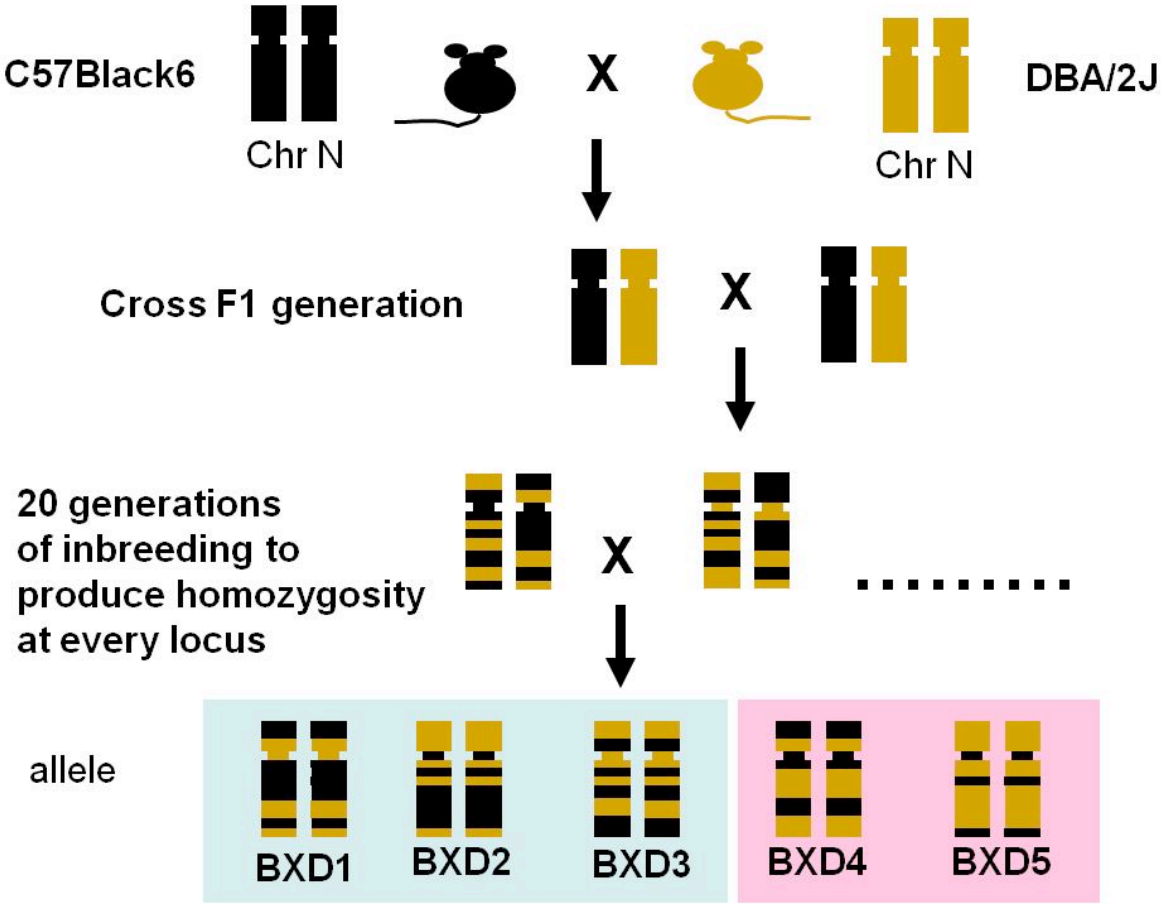

Figure 6.1 **A diagrammatic representation of the recombinant inbred BXD lines.** Following the initial cross of the parental strains of C57BL/6 and DBA/2J that produces the F1 generation, the F2 offspring are inbred for at least 20 generations, which fixes every gene locus homozygous for either the original C57BL/6J or DBA/2J.

6.2 Methods

6.2.1 BXD experiment

The BXD experiments were performed using male mice that, at beginning of experiments, were 6 weeks of age (bred at the University of Manchester by our collaborator, Dr Reinmar Hager). A total of fifty mice were chosen from 16 different lines with up to four littermates per line. Due to

there being only one littermate from some lines, all the mice were single housed to reduce confounding factors such as food competition. The mice were kept on HED for 8 weeks, and their body weight was recorded once a week.

At week 7 of the BXD experiment (13 weeks of age), the mice underwent an OGTT, as described in Chapter 2, with the exception that the mice were subjected to a longer fast (10 instead of 6 hours of daytime fast) with the tail first clipped 90 min before lights out. Representative results are expressed as area under the curve (AUC) calculated using the lowest value recorded during the OGTT as the baseline.

At week 8 of the BXD experiment, or at 14 weeks of age, the animals were culled and the following tissues were collected: blood plasma, hypothalamus, brainstem, pancreas, liver, interscapular brown adipose tissue and heart. Three white adipose tissue deposits were dissected and weighed before, including epididymal, peri-renal and mesenteric fat pads. The % body fat was calculated total fat pad weight by body weight at week 8.

6.2.2 C57 experiments

A single C57 mouse was culled at 8 weeks of age to collect tissues for gene distribution studies, and the following tissues were collected: hypothalamus, brainstem, brown adipose tissue, white adipose tissue, adrenal gland, heart, kidney, liver and skeletal muscle.

For the experiments using C57 mice (Harlan, UK) on HED, 10 animals were put on HED at 6 weeks of age and 10 were kept on the normal control diet. Their body weight was recorded once a week, starting at week 0 and finishing at week 8.

In the C57 HED experiment, the animals were culled at week 8, or 14 weeks of age, and the following tissues were collected: hypothalamus, brown adipose tissue, inguinal white adipose tissue, epididymal white adipose tissue, heart, kidney, liver, and skeletal muscle

Blood plasma was collected at culling and processed as described in Chapter 2. After thawing, the plasma glucose level was tested using the same equipment as for the OGTT.

6.2.3 QTL and Correlational analyses

The following analyses were performed by Beatrice Gini in the Hager lab at the University of Manchester as previously described in chapter 2. The quantitative traits analysis (done using GeneNetwork WebQTL) at the time of writing were: body weight gain, white adipose tissue pad

weight (adjusted for body weight), fasting glucose and glucose tolerance (OGTT AUC). For the correlational analyses, the above traits were used, together with traits collected by other labs and obtained from the online BXD database (www.genenetwork.org).

6.2.4 RNA extraction, reverse transcription and qPCR

The dissected tissue was extracted using the Trizol method and reverse transcribed as described in Chapter 2. The primer design and validation method was also performed as previously described, as was the relative qPCR procedure.

The primers used are described in Table 6.1.

Target	Sequence Forward	Sequence Reverse
Pan-pacap	5'-CTCCAGTGCTGTTCATGCTT-3'	5'-GAGGGTCTCCAGAAAATCCA-3'
Pan-bdnf	5'-AGAGCAGGCTCTGGAATGAT-3'	5'-TTGCTGTGCCATATTTGGAT-3'
gprc5c	5'-GAGGTCTCACAGGTGACCAA-3'	5'-AGCTGTCCATTGTAGCCACT-3'

Table 6.1 **List of primer pairs.** The table lists the primer pairs used in qPCR experiments in this chapter. A description of the primer designing technique used is included in Chapter 2.

6.3 Results

6.3.1 Biometric traits of the BXD lines

A total of 50 BXD mice from 16 different lines were put on HED at 6 weeks of age for 8 weeks. The animals body weight were recorded once a week, starting at week 0, and during the course of the 8 weeks the animals displayed notable strain differences in actual body weight and relative body weight gain, indicated by the high correlation between body weight gain and BXD line number ($p=0.0003$)(Figure 6.2.a). This analysis does not include body weight data collected at week 8 as a couple of animals showed a reduction in body weight following the OGTT at week 7 of the experiment.

Following the 8 weeks on HED the animals were culled and several tissues were collected, including white adipose tissue (WAT). Notable strain differences were seen in adiposity as well, again indicated by the high correlation between the trait and BXD line number ($p<0.0001$) (Figure 6.2.b).

At week 7 of the experiment, an OGTT was performed on all the mice. Glucose tolerance was also shown to be highly correlated with BXD line number ($p=0.0002$) (Figure 6.2.c). These collected biometric traits show that there was heterogeneity between the lines, which indicated that the data warranted further analysis.

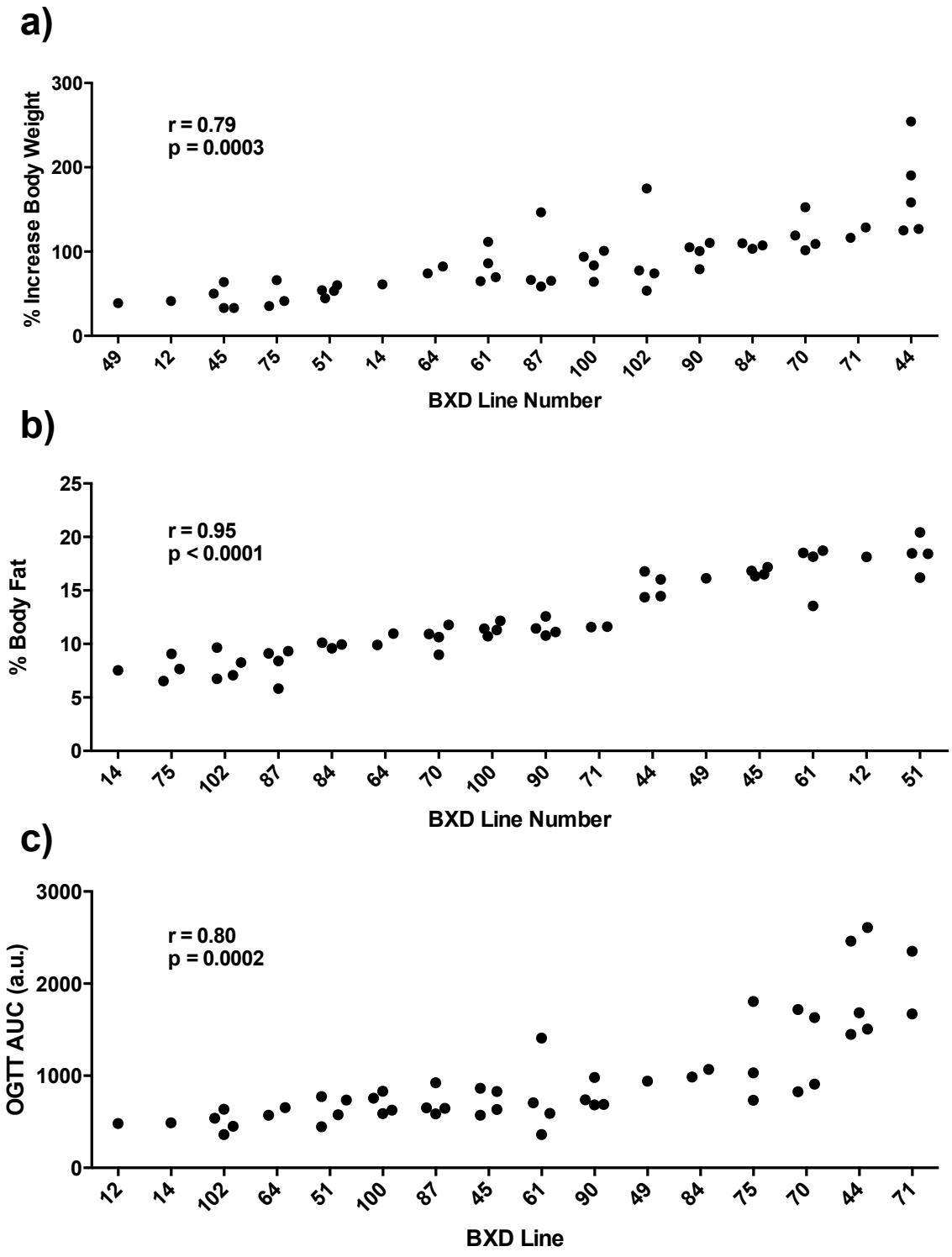

Figure 6.2 **Phenotypes of different BXD lines.** Individual values for each mouse are plotted against line number on the x-axis in increasing mean trait values. On the y-axis, the trait values for body weight (a), adiposity (b) and glucose tolerance (c) are plotted. The increase in body weight was measured from week 0 to week 7 of the experiment; the mice were 6 weeks of age at the start of the experiment and 13 weeks at the end. Fat pad weight was adjusted for body weight. Glucose tolerance was expressed as area under the curve (AUC) with the minimum plasma glucose level as baseline. Pearson's r and p values are expressed on graphs. (12 n=1, 14 n=1, 44 n=5, 45 n=4, 49 n=1, 51 n=4, 61 n=4, 64 n=2, 70 n=4, 71 n=2, 75 n=3, 84 n=2, 87 n=4, 90 n=4, 100 n=4, 102 n=4)

6.3.2 QTL analysis of the biometric traits for the BXD mice

QTL analysis was performed using the biometric data collected and 12 loci were identified that had likelihood ratio statistic scores (LRS), indicating their possible role in the phenotypic trait variation. LRS, which is a chi-square statistic, is a measurement of the association between differences in traits and differences in particular genetic markers above 13 (an arbitrary threshold). As an example, a QTL on chromosome 11 was identified that contains variation that explains differences between the body adiposity of animals on HED. Interestingly, this QTL includes annotated genes that are involved in fat metabolism (Figure 6.3), including acylcoenzyme A oxidase (*acox1*) and fatty acid desaturase 6 (*fads6*).

There were also many genes that are expressed in the brain identified at the 12 QTL loci, including a gene coding for galanin receptor 2 (*galr2*) Further, the QTL analysis of fat mass and fasting glucose levels identified three orphan G-protein coupled receptors (GPCRs), i.e. *gpr142*, *gpr146* and *gprc5c*. The BXD database suggests that these GPCR genes are expressed in both the hypothalamus and liver.

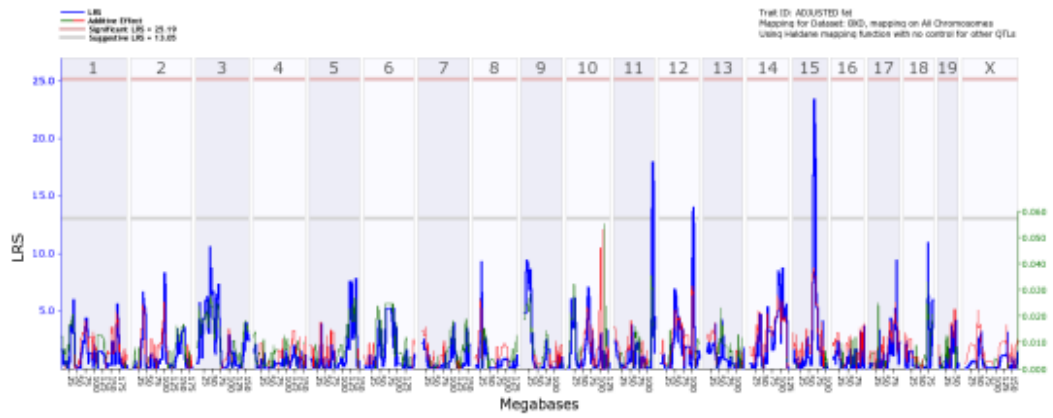

Figure 6.3 **Genome wide QTL-map for body adiposity.** The QTL analysis identified three possible QTLs on chromosome 11, 12 and 13. On the y-axis, LRS scores are shown in blue and additive effect in green. Body adiposity was calculated by adjusting fat pad weight for body weight. The blue line plots the strength of the association and chromosomal location. The genome wide significant threshold of 25.0 LRS is shown in red, and the suggestive of 13.0 LRS is shown in grey, both horizontal lines. LRS scores above 13.0 warrant further investigation. The red line plots the effect of the D allele on trait values, and the green line plots the B allele. The x-axis shows the location by chromosome on the upper level, and by megabases on the lower. (n=50, 16 lines)

6.3.3 Correlational analyses

Correlational analyses were performed using the phenotypes recorded in this study and gene expression data in different tissues, collected in other labs and retrieved from the BXD database. In our preliminary correlational analysis (Figure 6.4), the three fat pad weights were strongly positively correlated (represented by red lines, $0.7 < r < 1$), as was fasting glucose with glucose

tolerance (or OGTT AUC), and weight gain with weight at week 7. As introduced in chapter 3, *pacap* and *bdnf* are two neuropeptide genes that have previously been shown to be up regulated in DIO-R mice and these genes were therefore included in the analysis, as well as *gprc5c* as it was a new candidate gene identified in our initial QTL analysis. The hypothalamic expression of *pacap, bdnf* and *gprc5c* data included in the network were from RNA sequencing studies that measured the expression levels in BXD mice on normal diet, these studies were performed by other labs and the data was obtained from the database freely available on the GeneNetwork website. Here, we show that *pacap* expression is negatively correlated with fat mass (represented by green lines, $-0.7 < r < -0.5$). Furthermore, *bdnf* expression showed a weak positive correlation to *pacap* expression (yellow lines, $0.5 < r < 0.7$). The expression of our new candidate, *gprc5c* in chow fed mice was inversely correlated with weight gain and positively correlated with body weight at week 0.

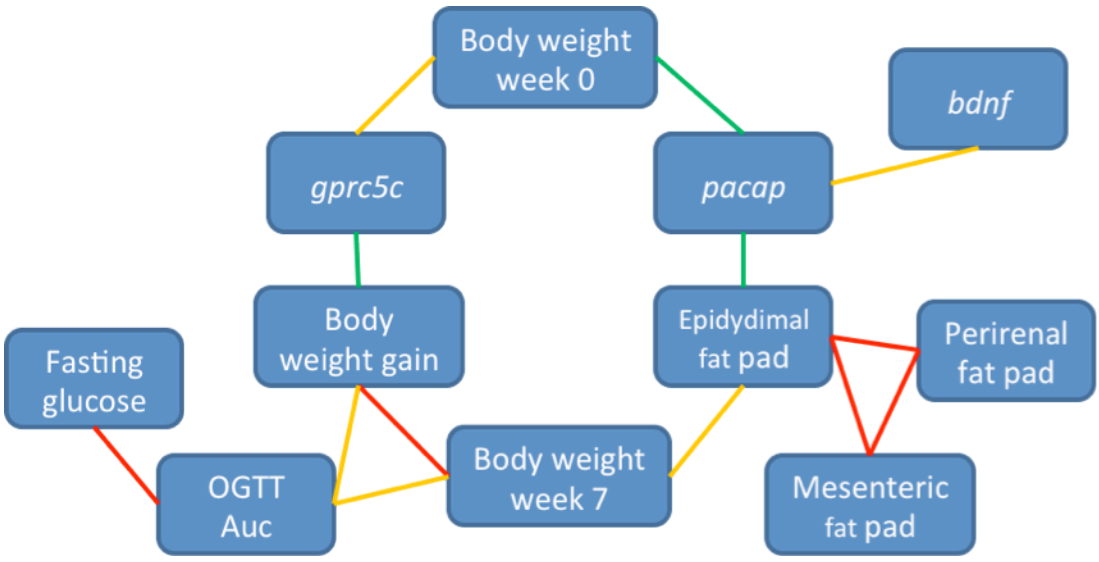

Figure 6.4 **Joint mapping network.** A diagram illustrating the covariance between traits measured in our preliminary study with hypothalamic expression of *pacap, bdnf* and *gprc5c* measured in other labs. Red lines indicate strong positive correlation ($0.7 < r < 1$), yellow weak positive correlation ($0.5 < r < 0.7$), and green weak negative correlation ($-0.7 < r < -0.5$). (n=50, 16 lines)

6.3.4 BXD *pacap* and *bdnf* hypothalamic expression

Due to the unrecoverable loss of collected tissue from the BXD experiment, only 30 hypothalamic samples were reverse transcribed and analyzed using qPCR. Both *pacap* and *bdnf* mRNA expression was analysed. However, as there was no specific control group in this experiment to relate the expression levels to, the reported values represent the ΔC_t values of each mRNA

without being normalized against the control group and can thus only be interpreted as higher or lower in relation to each other. The expression values are arbitrary.

Although a large proportion of the samples are missing, the BXD lines appear to exhibit heterogeneity in the mRNA expression of *pacap* and *bdnf,* with correlation analysis showing very low p values for both *pacap* (p=0.0002) and *bdnf* (p=0.0038) (Figure 6.5.a and b), indicating that these traits can be used for future QTL analysis and joint mapping. Linear regression analysis reveals that the mRNA expression of *pacap* and *bdnf* are positively correlated (Figure 6.5.c) where the individual mice with high mRNA expression of one gene also has high expression levels for the other.

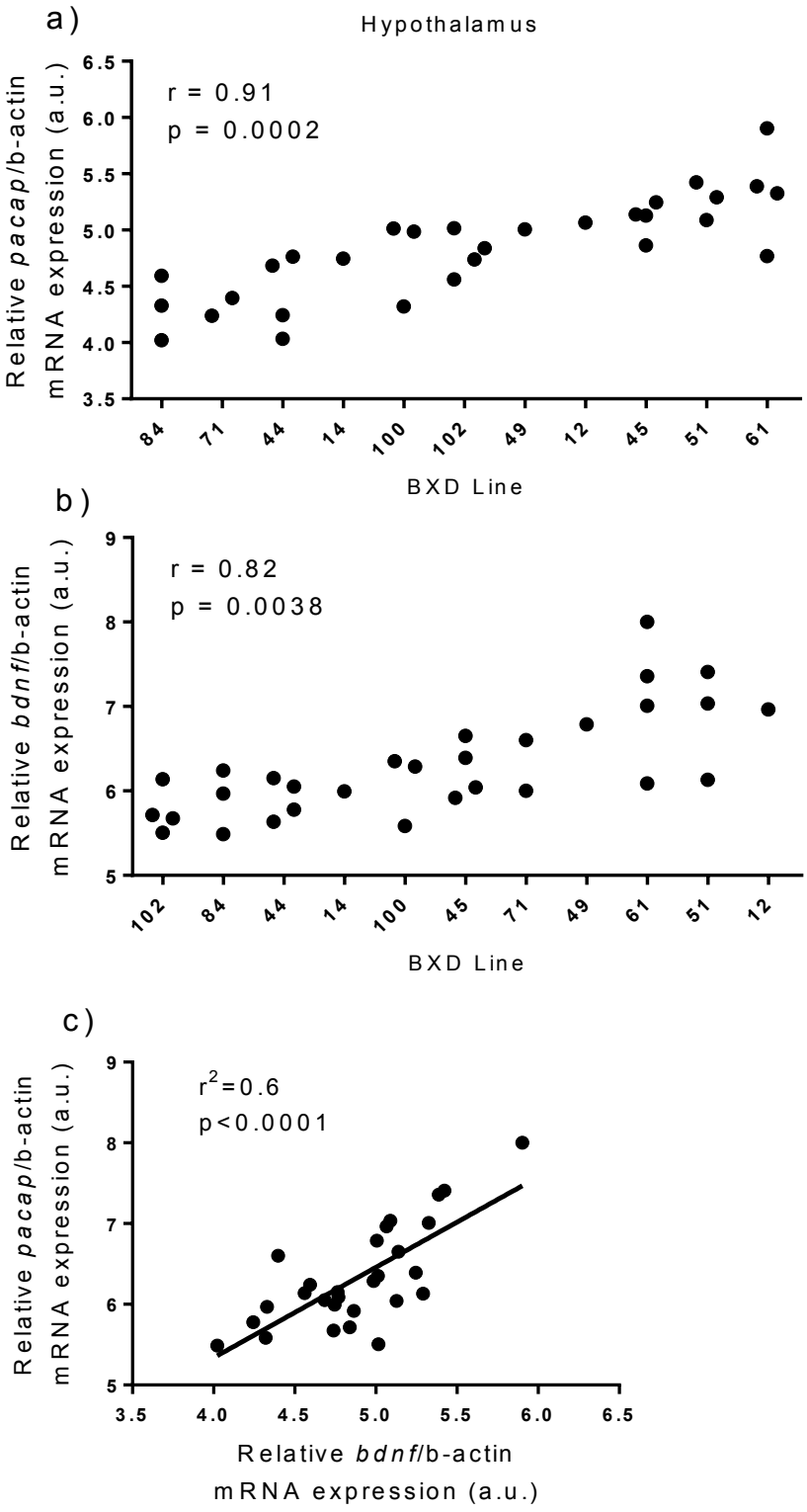

Figure 6.5 **mRNA expression of hypothalamic genes in BXD lines.** Graphs showing the hypothalamic mRNA expression of 30 BXD animals after 8 weeks on HED, with graph a) showing *pacap* and graph b) showing *bdnf* (Pearson's r and p values are expressed on both graphs). Individual values for each mouse are plotted against line number on the x-axis in increasing mean trait values. On the y-axis, the mRNA level of each gene is shown as the ΔC_t value, normalized

against the β-actin C_t for the same sample. The linear regression analysis of these two traits are shown in c), r^2=0.6, p<0.0001. (12 n=1, 14 n=1, 44 n=5, 45 n=4, 49 n=1, 51 n=4, 61 n=4, 71 n=2, 84 n=2, 100 n=4, 102 n=4)

6.3.5 C57 mice on HED and the expression of *gprc5c*

To investigate the global expression of *gprc5c*, several tissues were collected from a single C57 mouse in order to confirm the presence of the mRNA. These tissues included hypothalamus, brainstem, BAT, WAT, adrenal gland, heart, kidney, liver, and skeletal muscle. The tissues were analysed using qPCR, and here again there was no control group to relate the expression levels to. Hence, the ΔC_t values of the different tissues were normalized against the hypothalamic ΔC_t value, which was forced to the arbitrary unit of 1. This means that the other tissues' expression levels can be read as either higher or lower than the level in the hypothalamus. In this case, the *gprc5c* mRNA levels in all the other tissues were higher than that in the hypothalamus, with the levels in kidney, liver, and skeletal muscle being considerably higher (between 30-40 times higher) (Figure 6.6.a).

A group of 20 C57 male mice were put on either HED (10 mice) or continued on the control diet (10 mice) for 8 weeks, starting from the age of 6 weeks, to investigate the regulation of *gprc5c* in the hypothalamus and other tissues. Their body weight was recorded once a week up until week 7 and the body weight curves form the two groups are shown in Figure 6.6.c. The two treatment groups started to significantly diverge in body weight after 5 weeks on HED, with an apparent heterogeneity in the HED group at week 6 and 7. At culling, blood plasma was collected and the plasma glucose level was obtained shown in Figure 6.6.b. The fed plasma glucose level was significantly higher in the HED group.

Several tissues were collected from the mice at week 8 of the experiment, including hypothalamus, BAT, inguinal WAT, epididymal WAT, heart, kidney, liver, and skeletal muscle. RNA was then extracted form these tissues and the mRNA levels of *gprc5c* was then analysed using qPCR (Figure 6.6.d). In the HED group, the *gprc5c* mRNA levels were significantly down regulated in the hypothalamus, BAT and heart tissues and significantly up regulated in the liver. There was no change seen in the other tissues.

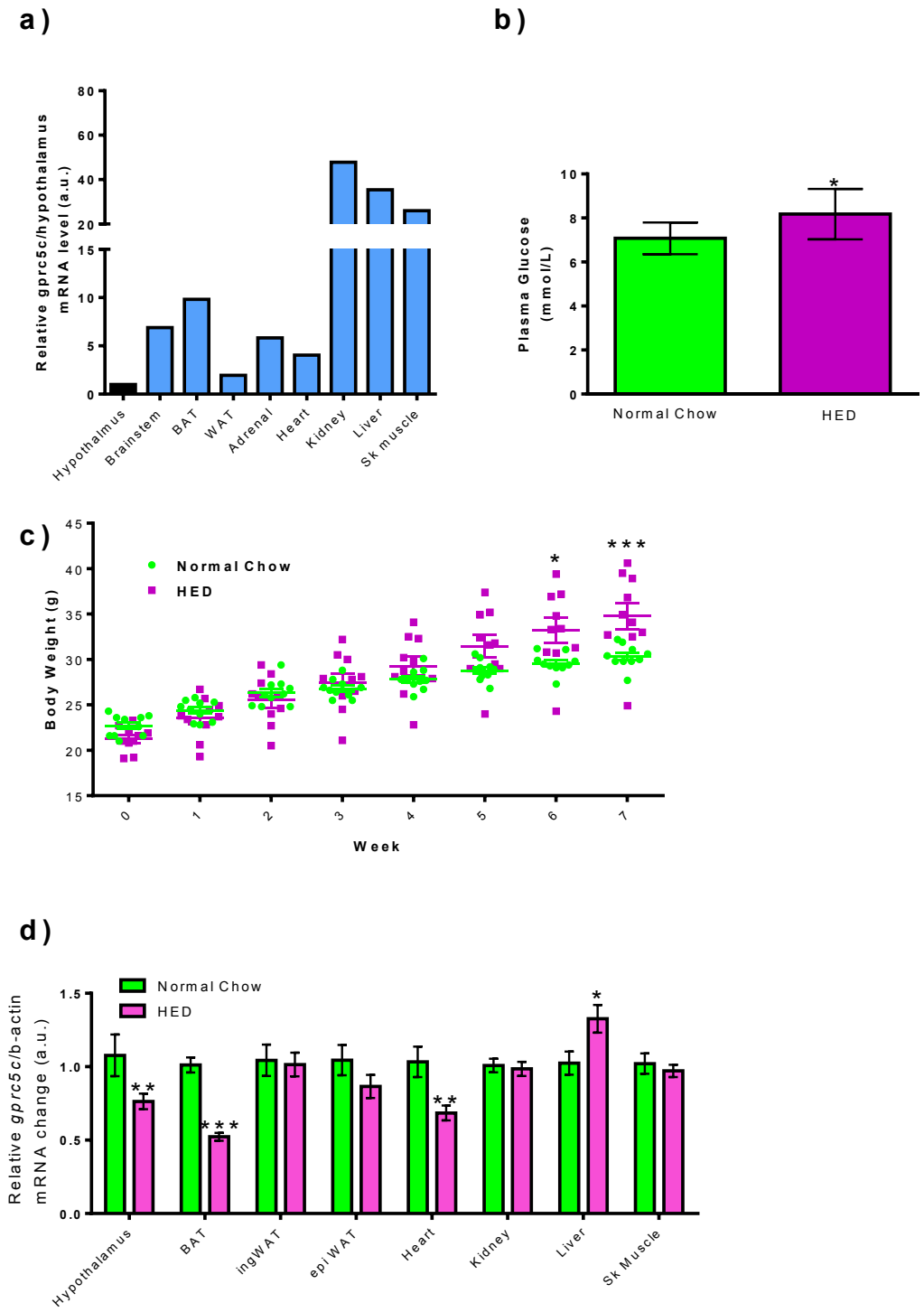

Figure 6.6 **The expression and regulation of *gprc5c.*** The expression of *gprc5c* mRNA detected using qPCR in the hypothalamus, brainstem, BAT, WAT, adrenal gland, heart, kidney, liver, and skeletal muscle (a) (n=1). All the expression levels were related to the hypothalamus, which was forced to 1. A group of n=10 C57 male mice were kept on HED for 8 weeks, with a control group of n=10 kept on normal chow. At week 8, their plasma glucose level was measured and shown in (b). Their body weight curve is shown in c). Tissues were collected at week 8 including hypothalamus, BAT, inguinal WAT, epididymal WAT, heart, kidney, liver, and skeletal muscle. The regulation of *gprc5c*

mRNA was analysed using qPCR (d). Data are expressed as mean ± SEM. *P<0.05, **P<0.01, *** P<0.001; two-way ANOVA followed by Bonferroni's *post hoc* test (c), Student's unpaired *t*-test (b, d).

6.3.6 Expression of *gprc5c* in the BXD hypothalamus, liver and BAT

Following the confirmation of *gprc5c* expression in the hypothalamus and the liver, and its apparent regulation in the response to HED in these tissues, but also BAT, the BXD samples were analysed for the expression of the *gprc5c* mRNA. As previously mentioned, there was no specific control group in this experiment to relate the expression levels to, and the reported values represent the ΔC_t values of each mRNA. In the hypothalamus (only 30 samples available), there appears to be heterogeneity between the lines with the correlation analysis confirming this ($p=0.0056$) (Figure 6.7.a). In the liver and BAT the heterogeneous pattern is more obvious, with expression levels showing a good range from lowest to highest (liver $p<0.0001$; BAT $p<0.0001$) (Figure 6.7.b and c).

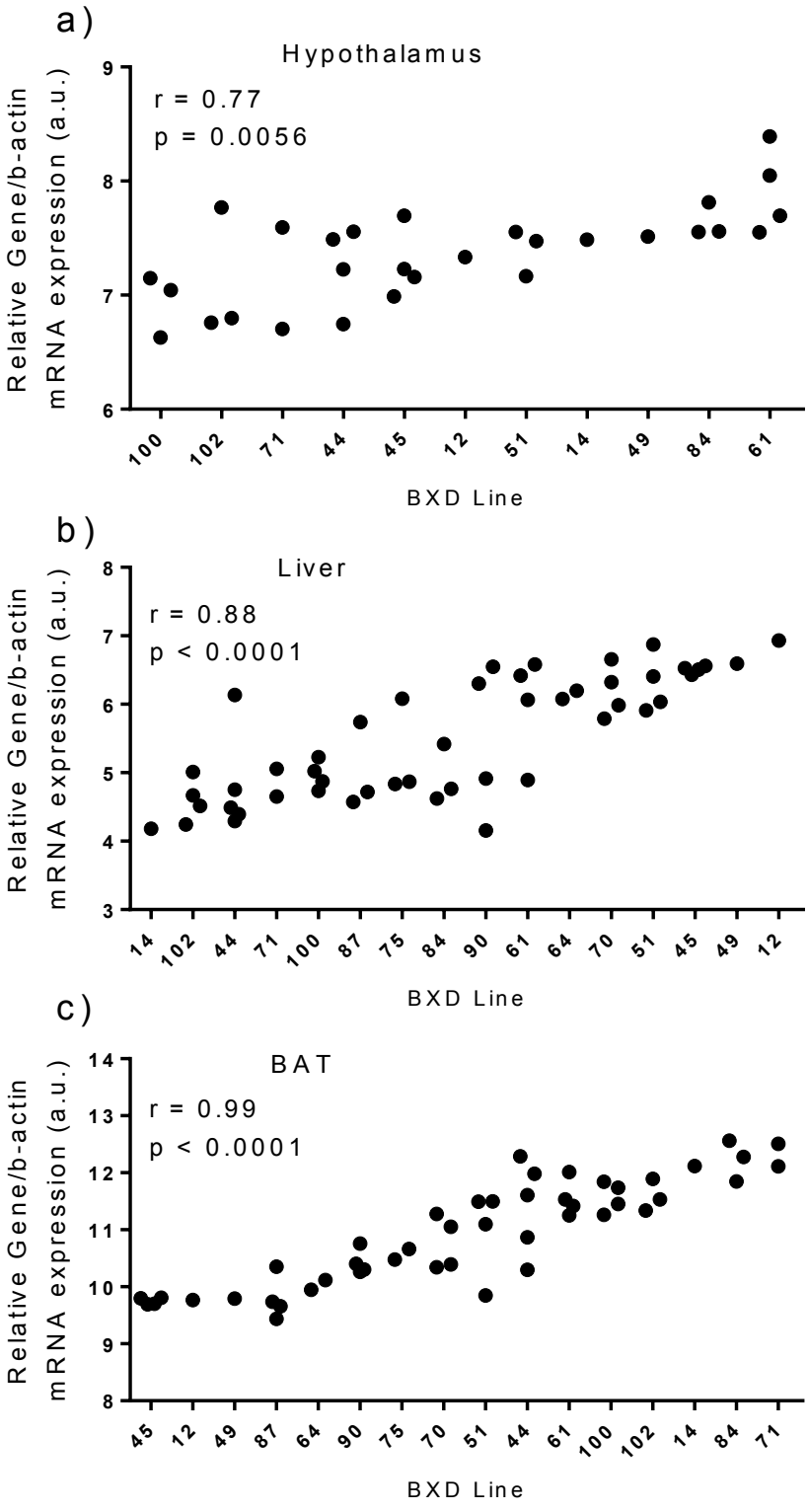

Figure 6.7 mRNA expression of *gprc5c* in hypothalamus and liver in BXD lines. Graph showing the hypothalamic mRNA expression of *gprc5c* of 30 BXD animals after 8 weeks on HED (a), and graph showing the mRNA expression of *gprc5c* of 50 BXD animals after 8 weeks on HED in liver (b) and in BAT (c). Individual values for each mouse are plotted against line number on the x-axis in increasing mean trait values. On the y-axis, the mRNA level of each gene is shown as the ΔC_t value, normalized against the β-actin C_t for the same sample. Pearson's r and p values are expressed

on all three graphs. (12 n=1, 14 n=1, 44 n=5, 45 n=4, 49 n=1, 51 n=4, 61 n=4, 64 n=2, 70 n=4, 71 n=2, 75 n=3, 84 n=2, 87 n=4, 90 n=4, 100 n=4, 102 n=4)

6.3.7 Final correlational analyses and mapping

Correlational analyses were performed using the phenotypes recorded in the beginning of this study and gene expression data measured later in the different tissues that were collected. In our final joint mapping correlational analysis (Figure 6.8), the addition of *pacap* and *bdnf* expression in the VMH, the expression of *gprc5c* in the VMH, liver and BAT and plasma triglycerides to the previous map showed in Figure 6.4 reveal a more interconnected network between traits. For simplicity, the three fat pad weights (epididymal, perirenal and mesenteric) were added together and are here referred to as adiposity.

In addition to the correlations seen previously between the biometric traits, the hypothalamic *pacap* expression was shown to be positively correlated with liver *gprc5c* expression, adiposity, hypothalamic *bdnf* expression and body weight at week 0 (red lines representing strong positive correlation ($0.7 < r < 1$) and yellow weak ($0.5 < r < 0.7$)), and was shown to be negatively correlated with BAT *gprc5c* expression, body weight at week 7, glucose tolerance (or OGTT AUC), body weight gain and plasma triglycerides (blue lines representing strong negative correlation ($-1 < r < -0.7$) and green weak ($-0.7 < r < -0.5$)).

The hypothalamic *bdnf* expression was positively correlated with liver *gprc5c* expression, adiposity, hypothalamic *pacap* expression and body weight at week 0, and to be negatively correlated with BAT *gprc5c* expression, body weight gain and plasma triglycerides.

The liver *gprc5c* expression was positively correlated to adiposity, hypothalamic *pacap* expression and hypothalamic *bdnf* expression, and seen to be negatively correlated with body weight gain and BAT *gprc5c* expression. The BAT *gprc5c* expression was positively correlated with body weight gain and body weight at week 7, and to be negatively correlated to liver *gprc5c* expression, hypothalamic *pacap* expression and hypothalamic *bdnf* expression.

Plasma levels of triglycerides was positively correlated to body weight gain, and negatively correlated to hypothalamic *pacap, bdnf* and *gprc5c* expression.

The hypothalamic *gprc5c* expression had a strong negative correlation with plasma triglycerides and showed no other correlation with other traits. Triglycerides were measured separate from this thesis by Ms Amy Worth, but was included here because of its correlation with hypothalamic *gprc5c.*

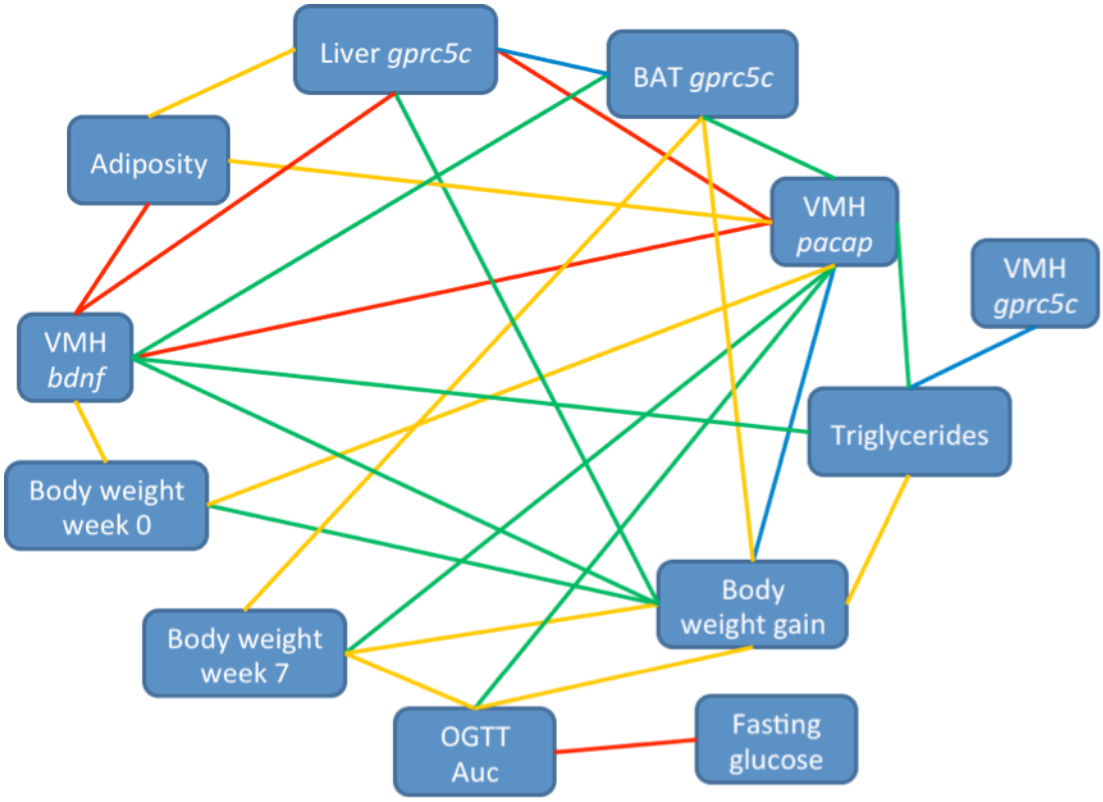

Figure 6.8 **Final joint mapping network.** A diagram illustrating the covariance between the collective traits measured in our preliminary study from BXD mice following an 8-week course of HED. Red lines indicate strong positive correlation ($0.7 < r < 1$), yellow weak positive correlation ($0.5 < r < 0.7$), green weak negative correlation ($-0.7 < r < -0.5$) and blue strong negative correlation ($-1 < r < -0.7$). (n=50, 16 lines)

6.4 Discussion

The main challenge in today's biomedical research is to decipher the genetic interactions that affect human health and lifespan. Understanding of the underlying pathology of complex disease, such as obesity, is confounded by the genetic heterogeneity underlying the disease and the disrupted complex gene-by-environment interactions leading up to its development. New effective strategies need to be developed in order to improve diagnosis, treatment and prevention of chronic multifactorial metabolic disease. While many studies focussing on single genes have shed light on distinct pathways, they lack insight into the genetic complexity that is the reality behind variation in metabolic traits. Complex systems were first studied utilising F2 intercrosses, which has the benefit of rapid generation, but requires a very large sample (n>500) to have decent mapping resolution, and suffers from the lack of reproducibility as every organism is unique. These limitations have been overcome by the development of murine genetic reference populations such as the BXD where, apart from its reproducibility, the main advantage is the generation of a vast database of genotypes under different conditions that is accessible

electronically. Here, in a pilot experiment utilizing this systems-genetics approach, we attempted to start untangling the genetic basis of obesity and the BXD recombinant inbred mouse model was used to investigate the effect of HED on gene mRNA expression, intermediate phenotypes such as adiposity and glucose tolerance, and the development of metabolic syndrome.

Following an 8-week course of HED, several biometric traits were collected including percentage body weight gain over 7 weeks, final percentage body fat and glucose tolerance at week 7 from our BXD model. As seen previously in Chapter 3, 8 weeks on HED results in varying degrees of weight gain in outbred (CD1) mice, and this was repeated here where the animals displayed notable line differences; variance across lines indicates a genetic component. The same pattern was seen in % body fat. The animals that gained the least % body weight during the course of the experiment interestingly recorded the highest in % body fat at the end of the 8 weeks on HED. However, as we have no data for initial body fat percentage, the significance of this observation is questionable. Glucose tolerance, as reported by OGTT AUC, also showed variation between lines. When looking closer at specific lines, for example 51 and 102 in Figure 6.2, it can be noted that even though both the strains are relatively glucose tolerant the two strains differ widely in fat mass. These collected biometric traits show that there was heterogeneity between the lines and this variation, similar to that found in the human population, is what lends the data to QTL and correlational analyses.

Using the data for the biometric traits collected, the QTL analysis identified 14 candidate loci with suggestive roles in the phenotypic variation observed and hence in the regulation of energy balance. As has been noted in human GWAS studies related to metabolic diseases, many of our loci code for brain-expressed genes; for example, the gene for galanin receptor 2 (or *galr2*). Data previously published by this lab indicate that central GALR2 plays a role in appetite and energy balance (Lawrence et al 2002, Lawrence et al 2003). The QTL analysis of adiposity and fasting glucose further identified three orphan GPCRs, i.e. *gpr142*, *gpr146* and *gprc5c*; that is, no ligands have yet been identified for *gpr142*, *gpr146* or *gprc5c.* These genes for these GPCRs, including *galr2*, each contain SNPs identified by the BXD database that could underlie some of the variance seen in association with the QTLs. Interestingly, knock down of the *gpr142* receptor is known to significantly reduce fat content in *C. elegans* and zebrafish (Jones et al 2008, Schlegel & Stainier 2006), and the receptor is expressed in the both the brain and the liver (Susens et al 2006). The physiological functions of these receptors are also unknown. However, the BXD database suggests

that *gpr142*, *gpr146* and *gprc5c*, along with *galr2*, are expressed in the mouse hypothalamus and liver, indicating a possible role in metabolic regulation and energy balance.

The power of the BXD model is that we can look at how the phenotypes recorded in this experiment covary with each other. These analyses reveal whether correlated traits have a common genetic basis, so called joint mapping, and this is crucial in identifying potential 'master' genes. The additional strength of the BXD system is that we can include data collected in other labs that are available in the BXD online database. Here, we also included data from RNA sequencing performed in another lab looking at mRNA expression in the hypothalamus of BXD mice on normal diet. By comparing, their gene expression from the database, with our measured traits, we found that the mRNA expression of *pacap, bdnf* and *gprc5c* correlated within our network. The *pacap* and *bdnf* correlation fits in with previous findings outlined in Chapter 3, where the two genes are similarly regulated in response to HED. Here, the BXD lines with higher starting body weight in our experiment have low levels of hypothalamic *pacap* in mice on normal diet. The same relationship was seen in the BXD lines that we reported to score high in adiposity at the end of the experiment, i.e. there is a strong negative correlation between pacap expression and weight gain. The hypothalamic *bdnf* showed a positive correlation with *pacap* (both on normal diet and on HED), suggesting that that one of them might regulate the other or that they share a regulator. To investigate further, we looked at hypothalamic expression of *pacap* and *bdnf* in our BXD mice, and following the course of HED there was an apparent heterogeneity in the mRNA expression levels even though there was a reduction in n-numbers due to loss of tissue. Although regression analysis confirmed that the expression levels for *pacap* and *bdnf* are positively correlated in the BXD mice, because of the loss of tissue, we were unable to carry out QTL analysis using these mRNA levels as quantitative traits.

Going back to the joint mapping, the mRNA levels of *gprc5c* in the hypothalamus of mice on normal diet was inversely correlated with weight gain and positively correlated with initial body weight in our experiment, indicating a potential role in energy metabolism and, possibly, in counteracting body weight gain as we have suggested previously for pacap and bdnf. Little is known about this orphan receptor; it belongs to the glutamate subfamily of GPCRs (or family C) that also includes metabotropic glutamate receptors, a calcium sensing receptor, γ-aminobutyric acid type B receptors, the sweet and umami taste receptors, GPRC6A receptor and several other orphan receptors (Lagerstrom & Schioth 2008). Unlike the other receptors in the family C that are characterised by large extracellular amino-terminal domain acting as the ligand binding site, the

GPRC5 receptors have comparably shorter N-terminus (Lagerstrom & Schioth 2008). There are four known members of this group: GPRC5A, GPRC5B, GPRC5C and GPRC5D and there are no known ligands for any of the receptors (Bjarnadottir et al 2005). The GPRC5A receptor is highly expressed in the lung (Sporn 2007, Tao et al 2004, Xu et al 2005); GPRC5B mainly in the brain and placenta (Brauner-Osborne & Krogsgaard-Larsen 2000, Imanishi et al 2007, Robbins et al 2002, Robbins et al 2000); GPRC5C is more widely expressed and has been reported in kidney, liver and brain (Robbins et al 2000); GPRC5D is present in the skin specifically (Brauner-Osborne et al 2001, Inoue et al 2004). The physiological role these receptors play in the tissues where they are expressed is not yet known, though *in vitro* studies have shown that the GPRC5 groups' expression is up regulated by retinoic acid (which is a metabolite of vitamin A), a fact leading to their earlier classification as retinoic acid-inducible genes (or RAIGs) (Imanishi et al 2007, Robbins et al 2000, Ye et al 2009). This is noteworthy, as retinoic acid is known to play crucial roles in cell differentiation and neurogenesis, indicating a similar role for the GRPC5 receptors (Maden 2007). Further, the distribution pattern of GPRC5B and GPRC5C suggests possible roles in important neuronal functions, such as transmitter release, neurite extension, axon guidance, neuronal development and synaptic plasticity for these receptors (Sano et al 2011). This hypothesis led Sano et al (2011) to generate GPRC5B and GPRC5C *Lacz* knockin mice and characterise their behaviours. While the GPRC5B$^{-/-}$ mouse showed some behavioural abnormalities, the GPRC5C$^{-/-}$ mouse exhibited none in the tests the group administered. They did link the receptor deletion to affects in the regulation of the hematopoietic system, and to a rise in general indicators of hepatic damage. The group also looked at *Lacz* staining of the brains from both mice, and the two receptor proteins appeared to be present in distinct areas mostly, with some overlap in the cerebellum and the hippocampus. In the sagittal sections they examined only GPRC5B was present in the hypothalamus. While these results are slightly discouraging, the group did not test the GPRC5C$^{-/-}$ mouse for any metabolic phenotype, which would be of more interest to us.

With this in mind, we proceeded to do our own expression experiment looking at the distribution of *gprc5c* in several tissues of the C57 mouse, and we confirmed the presence of mRNA in hypothalamus, brainstem, brown adipose tissue, white adipose tissue, adrenal gland and heart with relatively higher levels in kidney, liver and skeletal muscle. We also conducted an experiment where a group of C57 male mice were maintained on a HED for 8 weeks (as well as a control group on normal diet). Following the experiment several tissues were collected including plasma, which indicated a higher fed-state plasma glucose level in the mice on HED. The qPCR analysis of the tissues revealed that *gprc5c* mRNA expression was significantly down regulated in the

hypothalamus, brown adipose tissue and heart and significantly up regulated in the liver in the group on HED compared with that on control diet. As gprc5c expression appear to be regulated by HED, these results support a hypothesis that *gprc5c* is involved in metabolism and may have a potential role, similar to that proposed for *pacap* and *bdnf,* in protection against diet-induced obesity. We went back to our BXD tissue and looked for mRNA expression of *gprc5c* in the hypothalamus, brown adipose tissue and liver. In all three tissues a heterogeneity in expression levels was apparent, although less so in the hypothalamus due to the loss of n-numbers mentioned above.

This heterogeneity led us to investigate how these new mRNA traits fit into our initial correlational mapping network. The new network is rather more complex, with the new traits having many correlations with the initial biometric traits collected from our BXD. This again supports our previous hypothesis of the integral role hypothalamic *pacap* and *bdnf* play in energy metabolism, and also confirms *gprc5c* as a candidate receptor involved in energy balance maintenance in the hypothalamus, brown adipose tissue and liver. However, it is unclear whether these candidate genes, which are associated with metabolic trait variation, are directly (and individually) causal to the phenotype (i.e. cis-genes), whether they are regulated by other genes (i.e. trans-genes) in the genome (so called 'master' genes), or whether they interact with external dietary environment. This will need further study to be established and could be achieved by maintaining BXD mice on different diets.

After challenging our BXD mice with HED we saw variance in all the traits we collected. This was aided as the parental strains behind the BXD mice, C57BL/6 and DBA/2J, differ in their susceptibility to HED induced obesity (Svenson et al 2007) and regional fat storage patterns (Funkat et al 2004). In one study of males from 29 BXD lines that were kept on HED for 16 weeks, the DBA/2J mice gained more weight than the C57BL/6 mice (Dogan et al 2013). The DBA/2J also had more than two-fold higher relative contents of total fat, saturated fat, unsaturated fat, collagen and lipid to protein ratio in the adipose tissue, with similar results found in the liver. Additionally, the Funkat et al (2004) study showed that the DBA/2J mouse exhibited decreased spontaneous and voluntary activity as well as a reduction in resting energy expenditure compared to the C57BL/6 mouse after a period of 6 weeks on normal diet, while also gaining more weight. But only the spontaneous activity patterns of the C57BL/6 mice were affected by a course of HED. What is clear from these studies is that the two mouse strains behind the BXD have different

basal physical activity patterns and respond differently to HED, leaving the BXD system a good model for investigating metabolic disease and underlying pathology.

The main disadvantage with our pilot study is its size. When using the BXD system to study complex disease that are largely dependent on environmental factors, the study size needs to be adapted in order to detect traits of low heritability. Andreux et al (2012) performed a power analysis that indicated that when using 20 BXD lines with four animals per line, loci will be detected that are responsible for 50% or more of the variation of a moderately heritable trait. To achieve identification of the less heritable traits loci, studies with >40 lines are required, and so will detect loci responsible for as low as 30% of the variance. In our pilot study, we only used 16 BXD lines and we did not have four mice in each of these lines. This may have limited the number of loci we have discovered, but also probably led to the relatively broad QTL containing many genes. Another limitation to our study is that we only used male mice. As highlighted in the Andreux et al (2012) study, where they performed an intraperitoneal glucose tolerance test on both male and female mice fed on a normal diet, the AUC for the males was significantly higher than for the females (although still positively correlated) and the males AUC was linked to body weight and body composition, which was not seen in the females. The authors go on to say that the variation they saw in glucose tolerance is determined by genetics and partly dependent on sex, which is supported by the fact that they identified both common and distinct loci in both sexes when mapping QTLs for glucose levels. They also state that nearly half of the metabolic phenotypes they studied differed between the sexes. So, to attain a thorough picture of the complex network underlying metabolic disease, studies including both sexes will be required. However, that said our belief is still that the power of using the BXD lines is that we can change the environment in a controlled manner, e.g. by using different diets and, thus, interrogate real gene x environment interactions, which is impossible in large-scale human studies.

We did identify several loci in our BXD study even though we had a small sample size and this lead to the identification of several genes of potential interest, especially the orphan G protein-coupled receptors, such as GPRC5C. The real test for the significance of these findings is whether the results can be replicated in a study with a bigger panel of BXD lines, and if so might also be found to contribute to obesity-related diseases in humans. All in all, this pilot study has illustrated the usefulness of the BXD system as a powerful resource for hypothesis generation and validation in metabolic disease, and has left us with candidate genes to take our research further.

6.5 Summary

We utilised a systems genetics approach to investigate the genetic networks underlying obesity and, by challenging BXD mice with HED in a pilot experiment, we generated biometric traits describing metabolic phenotypes. These traits were used in QTL analysis to identify loci encoding for several genes of interest, including an orphan receptor of specific interest (GPRC5C). Joint mapping, where our traits were seen to correlate with each other and with traits recorded in other labs, supporting the role of PACAP and BDNF in body-weight management. GPRC5C was further investigated and its mRNA was found to be widely distributed in peripheral tissues, but also present in the hypothalamus. The receptor mRNA was regulated by HED in normal C57 mice in the hypothalamus, liver and brown adipose tissue, indicating a possible role for GPRC5C similar to PACAP and BDNF. In our BXD mice, expression of *pacap* and *bdnf* in the hypothalamus and *gprc5c* in the hypothalamus, liver and brown adipose tissue fit into the previous joint mapping of our biometric traits, further supporting the hypothesis. This study has highlighted the usefulness of the BXD system to identify candidate genes, and how we can go about testing these candidates to validate the results. We suggest that the BXD model, as the largest and best-characterised recombinant inbred murine system, will become an important part in the future study of complex disease such as obesity.

Chapter 7. Summary of conclusions and future work

The hypothalamus is an established regulatory hub with regards to energy homeostasis. While the Arc has been extensively researched and substantial emphasis has been put on its role in energy balance, the VMN is still poorly understood. In the Arc, the discovery of the NPY/AgRP and POMC neuronal pathways have lead to significant advances in the field, but the lack of neuronal markers for the VMN has contributed to slow progress in understanding of the role the nucleus plays in energy balance. However, the anorexic acting PACAP and BDNF have been proposed as potential candidates, amongst others, and mRNA of both neuropeptides is seen to be up regulated in diet-induced obesity (DIO)-resistant mice, indicating that they could be responsible for signalling in the VMN, especially in terms of countering the effects of an obesogenic diet. In this thesis, we looked closer at how metabolic manipulation regulates *pacap* and *bdnf* transcripts in the VMN. We also evaluated the effect of leptin and glucose on VMN PACAP neurons. The effect of PACAP on feeding and c-Fos brain activation was also investigated, as well as the downstream targets of PACAP signalling. Finally, we utilised a systems-genetics approach to identify new neuronal marker candidates for the VMN and other tissues, which may be implicated in energy homeostasis.

7.1 *Pacap* and *bdnf* transcripts are differentially regulated in the VMN in response to metabolic manipulation

Changes in the hypothalamic expression of genes involved in energy homeostasis have been seen previously following stimuli such as fasting or leptin administration (Schwartz et al 2000). The VMN has an established role in glucose (Oomura 1983, Silver & Erecinska 1998) and leptin sensing (Elmquist et al 1997, Irani et al 2008), however, relatively few studies have examined the effect on regulation of gene-expression in response to different nutritional states in the VMN. Fasting has previously been shown to down regulate *pacap* and *bdnf* mRNA (Hawke et al 2009, Mounien et al 2008, Xu et al 2003), and we took these investigations further by including a high-fat diet (HED) stimulus as well as a 48-hour fast. We hypothesised that PACAP and BDNF might be involved in protection against the development of diet-induced obesity, as their mRNAs were up regulated in DIO-resistant, but not DIO-prone mice following HED diet, seen previously in the lab (Hawke

2009a). Our findings did not fully support this hypothesis, but we determined that metabolic manipulation differentially regulates *pacap* and *bdnf* transcripts in the VMN of outbred mice. The findings did also further support the role of PACAP and BDNF as important signalling molecules in the VMN and the energy homeostasis circuitry. The presence of several *bdnf* transcripts in the VMN, and their differential regulation, indicates that the transcripts play distinct roles in the response to metabolic manipulation. For example, the literature suggests that roles in synaptic plasticity and expression maintenance are determined by transcript size and location.

It is not yet clear what regulates *pacap* and *bdnf* in the VMN, but hormonal inputs (e.g. from leptin) or neuronal inputs (possibly originating in the Arc) are likely to play a role. However, the VMN has all the sensing capabilities to suggest it is not receiving the control from outside, but instead it is likely to be a hub for integration, perhaps in parallel with the Arc. Another possibility is the presence of a 'master gene', which drives the expression of some genes, while inhibiting the expression of others. The transcription factors SF-1 or FOXO1 are promising possibilities, as both are present in the VMN and are necessary to maintain energy homeostasis (Kim et al 2012, Kim et al 2011). Finally, *pacap* and *bdnf* could be subject to epigenetic modulation, with SIRT1 being one potential candidate for the regulation of histone acetylation and, therefore, rates of transcription (Li 2013).

7.2 PACAP neurons in the VMN are glucose inhibited

As described previously, one strong potential candidate for an important VMN phenotype, are neurones containing PACAP. Here we aimed to establish whether PACAP neurons in the VMN are involved in metabolic sensing of circulating leptin and glucose. Previous research has shown that when the leptin receptor is specifically knocked out in VMN-specific SF-1 cells, obesity is induced (Dhillon et al 2006), and as we have shown previously in the lab, PACAP strongly co-localises with SF-1 (Hawke et al 2009). We utilised a transgenic mouse model where leptin receptor deletion is driven by *pacap* expression to study whether leptin is having a physiological role through PACAP neurons. From our findings this is not made clear, which leaves open the question of what are the roles of PACAP neurons in the VMN in terms of metabolism? Further, attempts have been made here to characterise that a subtype of VMN neurons that contain PACAP, using the Adcyap1-eGFP and PACAP-i-cre X Z/EG transgenic mouse lines. These were used to study the responsiveness of PACAP neurons to fluctuations in glucose availability. We were not able to induce c-Fos in PACAP cell in the VMN following hypoglycaemia using systemic 2DG. However, currently we do not know

whether this is because the neurons do not show a c-Fos response or because the genetic background of the reporter mouse strain is not particularly susceptible to the 2DG stimulus (Lewis et al 2006). However, progress has been made in both experimental procedures and findings that will work towards characterisation of the VMN in relation to energy homeostasis. Important steps forward have been made by electrophysiological and Ca^{2+}-imaging techniques, highlighting the value of our two transgenic reporter strains.

7.3 The anorectic effects of PACAP and downstream targets

PACAP has a well-established anorexic action when administered centrally (Hawke et al 2009, Mizuno et al 1998b, Morley et al 1992, Mounien et al 2008), though the receptors and downstream effectors, or how it relates to normal physiology is currently unknown. Here we attempted to dissect the target pathways through which the effect of PACAP is propagated. PACAP binds to three receptors with equal affinity: the $VPAC_1$ and $VPAC_2$ receptors, which are shared with the related peptide VIP, and the PAC_1 receptor (Vaudry et al 2009). While central VIP elicited a very small reduction in food intake, findings here confirmed that a small dose of PACAP has a robust effect on feeding. When experiments were repeated in $VPAC_1$ and $VPAC_2$ receptor knockout animals, PACAP was found to elicit the same effect as in wild-type controls, which implicates the PAC_1 receptor in the anorexic effect of PACAP. These results compliment earlier findings, where the PAC_1 receptor was found to mediate the thermogenic effect of PACAP and that the PAC_1 receptor is likely mediating some of leptin's metabolic actions (Hawke et al 2009). Of note, the $VPAC_2$ receptor has been found to mediate PACAP's endogenous glucose-increasing properties (Yi et al 2010).

A functional mapping study showed neuronal activation in the paraventricular nucleus (PVN) and the central amygdala, two areas that express corticotrophin-releasing hormone (CRH) (Makino et al 1994) and the PAC_1 receptor (Hashimoto et al 1996, Joo et al 2004, Nomura et al 1996). As central PACAP injection alters expression levels of CRH mRNA in the PVN (Grinevich et al 1997, Mounien et al 2008), these findings point towards a connection between the PACAP and CRH systems.

Although central injection of exogenous PACAP acts as a powerful anorexigen, this may not be a normal physiological function. Indeed, we have shown that high doses of exogenous PACAP cause non-appetitive behaviours (Hawke et al 2009), which could indicate nausea or aversion. This might be supported by our current finding that PACAP-induced hypophagia is at least partially

dependent in CRH receptor signalling, which could indicate non-selective activation of the HPA axis. In these experiments, antagonists of CRH, melanocortin and oxytocin receptors were co-injected centrally with PACAP. Both of the two CRH receptor antagonists tested, astressin and α-helical CRH, were able to significantly attenuate the degree of hypophagia in response to central PACAP injection. In contrast, while the inverse agonist of melanocortin 4 receptor, AgRP, completely abolished the feeding response of PAPAC, there was no effect of the true antagonist, SHU9119. Hence, the *in vivo* evidence for a role of POMC cells/melanocortin signalling downstream of PACAP remains ambiguous. One explanation is that AgRP is simply inhibiting the neurones on which PACAP itself is acting. The effect of leptin on VMN neurons, which co-express PACAP, and on Arc neurons that express POMC are non-convergent (Dhillon et al 2006), and given that impairment of PACAP signalling disrupts carbohydrate and lipid metabolism, glucose handling and brown adipose tissue thermogenesis (Adams et al 2008, Gray et al 2001, Gray et al 2002, Hashimoto et al 2000), a leptin-sensitive role in these metabolic functions may be more important physiologically than appetite regulation.

7.4 Identification of a new target, GPRc5c, and confirmation of old in hypothalamic signaling in obesity

We utilised a systems genetics approach to investigate the genetic networks underlying obesity. By challenging BXD mice with HED in a pilot experiment, we generated biometric traits describing metabolic phenotypes. These traits were used in QTL analysis to identify loci, which overlapped several annotated genes of potential interest, including an orphan G-protein-coupled receptor (GPRC5C). Joint mapping also revealed that our traits correlated with each other and with traits recorded in other labs, for example, supporting the role of PACAP and BDNF in body-weight management. GPRC5C was further investigated and its mRNA was found to be widely distributed in peripheral tissues, but also present in the hypothalamus. The receptor mRNA was regulated by HED in normal C57 mice in the hypothalamus, liver and brown adipose tissue, indicating a possible role for GPRC5C in metabolism. In fact, similar to PACAP and BDNF, in our BXD mice, expression of *gprc5c* in the hypothalamus was inversely correlated to body weight gain. The expression of *gprc5c* in the hypothalamus, liver and brown adipose tissue also fitted into joint correlation mapping of all our biometric traits, further supporting the hypothesis.

7.5 Future work

The identification of the regulator of *pacap* and *bdnf* transcript expression in the VMN could potentially lead to breakthrough discoveries in the field of obesity research, especially if it is dysfunctional in individual animals that are prone to diet-induced obesity, while still effective in those that are resistant. The use of the BXD model might be crucial here, as well as investigations into the epigenetic regulation of *pacap* and *bdnf.*

Further work confirming the hypothesis that PACAP VMN neurons are glucose inhibited is warranted, and is required to fully clarify the role of PACAP in the CRR to hypoglycaemia. It would also be interesting to use these techniques in order to study PACAP neuron response to leptin, ghrelin and PYY as well as other nutritional signals, for example lipids, and to see if these effects are mediated by a common cellular effector, such as AMPK.

The final chapter of this thesis has highlighted the usefulness of the BXD system to identify candidate genes, and how we can go about testing these candidates to validate the results. We suggest that the BXD model, as the largest and best-characterised recombinant inbred murine system, will become an important part in the future study of complex disease such as obesity.

7.6 Final remarks

This thesis project has demonstrated a robust way of identifying new candidate genes involved in energy homeostasis in several tissues, using a systems-genetics approach. The role of these genes can then be validated using techniques described in the preceding chapters which used pacap as an examplar: evaluation of target regulation in response to a change in metabolic status; examination of the neurons expressing the candidate genes and their sensitivity to circulating nutritional signals; if known ligands are available, investigate whether an injection elicits a response; and finally manipulate the gene expression in specific neuronal populations. In addition, the effect of up- or downregulation of gene cell expression could be investigated.

References

Abbott CR, Small CJ, Kennedy AR, Neary NM, Sajedi A, et al. 2005. Blockade of the neuropeptide Y Y2 receptor with the specific antagonist BIIE0246 attenuates the effect of endogenous and exogenous peptide YY(3-36) on food intake. *Brain Res* 1043: 139-44

Adams BA, Gray SL, Isaac ER, Bianco AC, Vidal-Puig AJ, Sherwood NM. 2008. Feeding and metabolism in mice lacking pituitary adenylate cyclase-activating polypeptide. *Endocrinology* 149: 1571-80

Adrian TE, Ferri GL, Bacarese-Hamilton AJ, Fuessl HS, Polak JM, Bloom SR. 1985. Human distribution and release of a putative new gut hormone, peptide YY. *Gastroenterology* 89: 1070-77

Agarwal A, Halvorson LM, Legradi G. 2005. Pituitary adenylate cyclase-activating polypeptide (PACAP) mimics neuroendocrine and behavioral manifestations of stress: Evidence for PKA-mediated expression of the corticotropin-releasing hormone (CRH) gene. *Brain research* 138: 45-57

Aid T, Kazantseva A, Piirsoo M, Palm K, Timmusk T. 2007. Mouse and rat BDNF gene structure and expression revisited. *J Neurosci Res* 85: 525-35

Aliaga EE, Mendoza I, Tapia-Arancibia L. 2009. Distinct subcellular localization of BDNF transcripts in cultured hypothalamic neurons and modification by neuronal activation. *J Neural Transm* 116: 23-32

An JJ, Gharami K, Liao GY, Woo NH, Lau AG, et al. 2008. Distinct role of long 3' UTR BDNF mRNA in spine morphology and synaptic plasticity in hippocampal neurons. *Cell* 134: 175-87

Anand BK, Brobeck JR. 1951. Hypothalamic control of food intake in rats and cats. *Yale J Biol Med* 24: 123-40

Anand BK, Chhina GS, Sharma KN, Dua S, Singh B. 1964. ACTIVITY OF SINGLE NEURONS IN THE HYPOTHALAMIC FEEDING CENTERS: EFFECT OF GLUCOSE. *Am.J.Physiol* 207: 1146

Andersson U, Filipsson K, Abbott CR, Woods A, Smith K, et al. 2004. AMP-activated protein kinase plays a role in the control of food intake. *J.Biol.Chem.* 279: 12005

Andreux PA, Williams EG, Koutnikova H, Houtkooper RH, Champy MF, et al. 2012. Systems genetics of metabolism: the use of the BXD murine reference panel for multiscalar integration of traits. *Cell* 150: 1287-99

Asakawa A, Inui A, Kaga T, Yuzuriha H, Nagata T, et al. 2001. Ghrelin is an appetite-stimulatory signal from stomach with structural resemblance to motilin. *Gastroenterology* 120: 337

Atasoy D, Betley JN, Su HH, Sternson SM. 2012. Deconstruction of a neural circuit for hunger. *Nature* 488: 172-7

Auwerx J, Avner P, Baldock R, Ballabio A, Balling R, et al. 2004. The European dimension for the mouse genome mutagenesis program. *Nature genetics* 36: 925-7

Bagdade JD, Bierman EL, Porte D, Jr. 1967. The significance of basal insulin levels in the evaluation of the insulin response to glucose in diabetic and nondiabetic subjects. *J Clin Invest* 46: 1549-57

Bagnasco M, Kalra PS, Kalra SP. 2002. Ghrelin and leptin pulse discharge in fed and fasted rats. *Endocrinology* 143: 726

Balthasar N, Coppari R, McMinn J, Liu SM, Lee CE, et al. 2004. Leptin receptor signaling in POMC neurons is required for normal body weight homeostasis. *Neuron* 42: 983-91

Banks WA. 2006. Blood-brain barrier and energy balance. *Obesity (Silver Spring)* 14 Suppl 5: 234S-37S

Batterham RL, Cowley MA, Small CJ, Herzog H, Cohen MA, et al. 2002. Gut hormone PYY(3-36) physiologically inhibits food intake. *Nature* 418: 650

Bechtold DA, Brown TM, Luckman SM, Piggins HD. 2008. Metabolic rhythm abnormalities in mice lacking VIP-VPAC2 signaling. *Am J Physiol Regul Integr Comp Physiol* 294: R344-51

Bechtold DA, Luckman SM. 2006. Prolactin-releasing Peptide mediates cholecystokinin-induced satiety in mice. *Endocrinology* 147: 4723-9

Beckers S, Peeters A, Zegers D, Mertens I, Van Gaal L, Van Hul W. 2008. Association of the BDNF Val66Met variation with obesity in women. *Molecular genetics and metabolism* 95: 110-2

Berthoud HR, Mogenson GJ. 1977. Ingestive behavior after intracerebral and intracerebroventricular infusions of glucose and 2-deoxy-D-glucose. *Am J Physiol* 233: R127-33

Berthoud HR, Morrison C. 2008. The brain, appetite, and obesity. *Annu Rev Psychol* 59: 55-92

Bi S, Robinson BM, Moran TH. 2003. Acute food deprivation and chronic food restriction differentially affect hypothalamic NPY mRNA expression. *Am.J.Physiol Regul.Integr.Comp Physiol* 285: R1030

Billington CJ, Briggs JE, Grace M, Levine AS. 1991. Effects of intracerebroventricular injection of neuropeptide Y on energy metabolism. *Am J Physiol* 260: R321-7

Binder DK, Scharfman HE. 2004. Brain-derived neurotrophic factor. *Growth Factors* 22: 123-31

Bjarnadottir TK, Fredriksson R, Schioth HB. 2005. The gene repertoire and the common evolutionary history of glutamate, pheromone (V2R), taste(1) and other related G protein-coupled receptors. *Gene* 362: 70-84

Borg MA, Borg WP, Tamborlane WV, Brines ML, Shulman GI, Sherwin RS. 1999. Chronic hypoglycemia and diabetes impair counterregulation induced by localized 2-deoxy-glucose perfusion of the ventromedial hypothalamus in rats. *Diabetes* 48: 584-7

Borg MA, Sherwin RS, Borg WP, Tamborlane WV, Shulman GI. 1997. Local ventromedial hypothalamus glucose perfusion blocks counterregulation during systemic hypoglycemia in awake rats. *J.Clin.Invest* 99: 361

Borg WP, During MJ, Sherwin RS, Borg MA, Brines ML, Shulman GI. 1994. Ventromedial hypothalamic lesions in rats suppress counterregulatory responses to hypoglycemia. *J.Clin.Invest* 93: 1677

Borg WP, Sherwin RS, During MJ, Borg MA, Shulman GI. 1995. Local ventromedial hypothalamus glucopenia triggers counterregulatory hormone release. *Diabetes* 44: 180-4

Bouyer K, Loudes C, Robinson IC, Epelbaum J, Faivre-Bauman A. 2007. Multiple co-localizations in arcuate GHRH-eGFP neurons in the mouse hypothalamus. *J Chem Neuroanat* 33: 1-8

Brauner-Osborne H, Jensen AA, Sheppard PO, Brodin B, Krogsgaard-Larsen P, O'Hara P. 2001. Cloning and characterization of a human orphan family C G-protein coupled receptor GPRC5D. *Biochimica et biophysica acta* 1518: 237-48

Brauner-Osborne H, Krogsgaard-Larsen P. 2000. Sequence and expression pattern of a novel human orphan G-protein-coupled receptor, GPRC5B, a family C receptor with a short amino-terminal domain. *Genomics* 65: 121-8

Broberger C. 2005. Brain regulation of food intake and appetite: molecules and networks. *J Intern Med* 258: 301-27

Broberger C, De Lecea L, Sutcliffe JG, Hokfelt T. 1998. Hypocretin/orexin- and melanin-concentrating hormone-expressing cells form distinct populations in the rodent lateral hypothalamus: relationship to the neuropeptide Y and agouti gene-related protein systems. *J.Comp Neurol.* 402: 460

Bruning JC, Gautam D, Burks DJ, Gillette J, Schubert M, et al. 2000. Role of brain insulin receptor in control of body weight and reproduction. *Science* 289: 2122-5

Burdakov D, Gerasimenko O, Verkhratsky A. 2005a. Physiological changes in glucose differentially modulate the excitability of hypothalamic melanin-concentrating hormone and orexin neurons in situ. *J Neurosci* 25: 2429-33

Burdakov D, Luckman SM, Verkhratsky A. 2005b. Glucose-sensing neurons of the hypothalamus. *Philos Trans R Soc Lond B Biol Sci* 360: 2227-35

Butler AA, Cone RD. 2002. The melanocortin receptors: lessons from knockout models. *Neuropeptides* 36: 77-84

Bystrykh L, Weersing E, Dontje B, Sutton S, Pletcher MT, et al. 2005. Uncovering regulatory pathways that affect hematopoietic stem cell function using 'genetical genomics'. *Nat Genet* 37: 225-32

Cakir I, Perello M, Lansari O, Messier NJ, Vaslet CA, Nillni EA. 2009. Hypothalamic Sirt1 regulates food intake in a rodent model system. *PloS one* 4: e8322

Campfield LA, Brandon P, Smith FJ. 1985. On-line continuous measurement of blood glucose and meal pattern in free-feeding rats: the role of glucose in meal initiation. *Brain Res.Bull.* 14: 605

Carling D, Hardie DG. 1989. The substrate and sequence specificity of the AMP-activated protein kinase. Phosphorylation of glycogen synthase and phosphorylase kinase. *Biochim Biophys Acta* 1012: 81-6

Cha SH, Wolfgang M, Tokutake Y, Chohnan S, Lane MD. 2008. Differential effects of central fructose and glucose on hypothalamic malonyl-CoA and food intake. *Proc Natl Acad Sci U S A* 105: 16871-5

Chai BX, Neubig RR, Millhauser GL, Thompson DA, Jackson PJ, et al. 2003. Inverse agonist activity of agouti and agouti-related protein. *Peptides* 24: 603-9

Chakravarthy MV, Zhu Y, Lopez M, Yin L, Wozniak DF, et al. 2007. Brain fatty acid synthase activates PPARalpha to maintain energy homeostasis. *J Clin Invest* 117: 2539-52

Chambers JC, Elliott P, Zabaneh D, Zhang W, Li Y, et al. 2008. Common genetic variation near MC4R is associated with waist circumference and insulin resistance. *Nat Genet* 40: 716-8

Chen H, Charlat O, Tartaglia LA, Woolf EA, Weng X, et al. 1996. Evidence that the diabetes gene encodes the leptin receptor: identification of a mutation in the leptin receptor gene in db/db mice. *Cell* 84: 491-5

Chen HY, Trumbauer ME, Chen AS, Weingarth DT, Adams JR, et al. 2004. Orexigenic action of peripheral ghrelin is mediated by neuropeptide Y and agouti-related protein. *Endocrinology* 145: 2607

Chen ZY, Jing D, Bath KG, Ieraci A, Khan T, et al. 2006. Genetic variant BDNF (Val66Met) polymorphism alters anxiety-related behavior. *Science (New York, N.Y* 314: 140-3

Chesler EJ, Lu L, Shou S, Qu Y, Gu J, et al. 2005. Complex trait analysis of gene expression uncovers polygenic and pleiotropic networks that modulate nervous system function. *Nat Genet* 37: 233-42

Chesler EJ, Wang J, Lu L, Qu Y, Manly KF, Williams RW. 2003. Genetic correlates of gene expression in recombinant inbred strains: a relational model system to explore neurobehavioral phenotypes. *Neuroinformatics* 1: 343-57

Cheung CC, Clifton DK, Steiner RA. 1997. Proopiomelanocortin neurons are direct targets for leptin in the hypothalamus. *Endocrinology* 138: 4489

Cohen P, Zhao C, Cai X, Montez JM, Rohani SC, et al. 2001. Selective deletion of leptin receptor in neurons leads to obesity. *J Clin Invest* 108: 1113-21

Cone RD, Cowley MA, Butler AA, Fan W, Marks DL, Low MJ. 2001. The arcuate nucleus as a conduit for diverse signals relevant to energy homeostasis. *Int.J.Obes.Relat Metab Disord.* 25 Suppl 5: S63

Cota D, Proulx K, Smith KA, Kozma SC, Thomas G, et al. 2006. Hypothalamic mTOR signaling regulates food intake. *Science* 312: 927-30

Cotero VE, Routh VH. 2009. Insulin blunts the response of glucose-excited neurons in the ventrolateral-ventromedial hypothalamic nucleus to decreased glucose. *Am J Physiol Endocrinol Metab* 296: E1101-9

Cruciani-Guglielmacci C, Hervalet A, Douared L, Sanders NM, Levin BE, et al. 2004. Beta oxidation in the brain is required for the effects of non-esterified fatty acids on glucose-induced insulin secretion in rats. *Diabetologia* 47: 2032-8

Cryer PE. 2004. Diverse causes of hypoglycemia-associated autonomic failure in diabetes. *N Engl J Med* 350: 2272-9

Cryer PE. 2005. Mechanisms of hypoglycemia-associated autonomic failure and its component syndromes in diabetes. *Diabetes* 54: 3592-601

Cummings DE, Purnell JQ, Frayo RS, Schmidova K, Wisse BE, Weigle DS. 2001. A preprandial rise in plasma ghrelin levels suggests a role in meal initiation in humans. *Diabetes* 50: 1714

Cummings KJ, Gray SL, Simmons CJ, Kozak CA, Sherwood NM. 2002. Mouse pituitary adenylate cyclase-activating polypeptide (PACAP): gene, expression and novel splicing. *Mol Cell Endocrinol* 192: 133-45

Cutler DJ, Haraura M, Reed HE, Shen S, Sheward WJ, et al. 2003. The mouse VPAC2 receptor confers suprachiasmatic nuclei cellular rhythmicity and responsiveness to vasoactive intestinal polypeptide in vitro. *Eur J Neurosci* 17: 197-204

Das M, Vihlen CS, Legradi G. 2007. Hypothalamic and brainstem sources of pituitary adenylate cyclase-activating polypeptide nerve fibers innervating the hypothalamic paraventricular nucleus in the rat. *J Comp Neurol* 500: 761-76

Davidowa H, Plagemann A. 2000. Different responses of ventromedial hypothalamic neurons to leptin in normal and early postnatally overfed rats. *Neurosci Lett* 293: 21-4

Davis JD, Wirtshafter D, Asin KE, Brief D. 1981. Sustained intracerebroventricular infusion of brain fuels reduces body weight and food intake in rats. *Science* 212: 81-3

Davis MR, Shamoon H. 1991. Counterregulatory adaptation to recurrent hypoglycemia in normal humans. *J Clin Endocrinol Metab* 73: 995-1001

Dhillon H, Zigman JM, Ye C, Lee CE, McGovern RA, et al. 2006. Leptin directly activates SF1 neurons in the VMH, and this action by leptin is required for normal body-weight homeostasis. *Neuron* 49: 191-203

Dhillon WS, Bloom SR. 2004. Gastrointestinal hormones and regulation of food intake. *Horm.Metab Res.* 36: 846

Dietrich MO, Antunes C, Geliang G, Liu ZW, Borok E, et al. 2010. Agrp neurons mediate Sirt1's action on the melanocortin system and energy balance: roles for Sirt1 in neuronal firing and synaptic plasticity. *J Neurosci* 30: 11815-25

Dina C, Meyre D, Gallina S, Durand E, Korner A, et al. 2007. Variation in FTO contributes to childhood obesity and severe adult obesity. *Nat Genet* 39: 724-6

Dogan A, Lasch P, Neuschl C, Millrose MK, Alberts R, et al. 2013. ATR-FTIR spectroscopy reveals genomic loci regulating the tissue response in high fat diet fed BXD recombinant inbred mouse strains. *BMC Genomics* 14: 386

Dube MG, Kalra PS, Crowley WR, Kalra SP. 1995. Evidence of a physiological role for neuropeptide Y in ventromedial hypothalamic lesion-induced hyperphagia. *Brain Res* 690: 275-8

Dube MG, Sahu A, Kalra PS, Kalra SP. 1992. Neuropeptide Y release is elevated from the microdissected paraventricular nucleus of food-deprived rats: an in vitro study. *Endocrinology* 131: 684

Durr K, Norsted E, Gomuc B, Suarez E, Hannibal J, Meister B. 2007. Presence of pituitary adenylate cyclase-activating polypeptide (PACAP) defines a subpopulation of hypothalamic POMC neurons. *Brain Res* 1186: 203-11

Egawa M, Yoshimatsu H, Bray GA. 1991. Neuropeptide Y suppresses sympathetic activity to interscapular brown adipose tissue in rats. *Am J Physiol* 260: R328-34

Elias CF, Aschkenasi C, Lee C, Kelly J, Ahima RS, et al. 1999. Leptin differentially regulates NPY and POMC neurons projecting to the lateral hypothalamic area. *Neuron* 23: 775

Elias CF, Saper CB, Maratos-Flier E, Tritos NA, Lee C, et al. 1998. Chemically defined projections linking the mediobasal hypothalamus and the lateral hypothalamic area. *J.Comp Neurol.* 402: 442

Elmquist JK, Scammell TE, Saper CB. 1997. Mechanisms of CNS response to systemic immune challenge: the febrile response. *Trends Neurosci.* 20: 565

Enriori PJ, Evans AE, Sinnayah P, Jobst EE, Tonelli-Lemos L, et al. 2007. Diet-induced obesity causes severe but reversible leptin resistance in arcuate melanocortin neurons. *Cell Metab* 5: 181-94

Ernfors P, Lee KF, Jaenisch R. 1994. Mice lacking brain-derived neurotrophic factor develop with sensory deficits. *Nature* 368: 147-50

Farooqi IS, Jebb SA, Langmack G, Lawrence E, Cheetham CH, et al. 1999. Effects of recombinant leptin therapy in a child with congenital leptin deficiency. *N Engl J Med* 341: 879-84

Farooqi IS, Keogh JM, Kamath S, Jones S, Gibson WT, et al. 2001. Partial leptin deficiency and human adiposity. *Nature* 414: 34-5

Farooqi IS, Keogh JM, Yeo GS, Lank EJ, Cheetham T, O'Rahilly S. 2003. Clinical spectrum of obesity and mutations in the melanocortin 4 receptor gene. *N.Engl.J.Med.* 348: 1085

Fioramonti X, Contie S, Song Z, Routh VH, Lorsignol A, Penicaud L. 2007. Characterization of glucosensing neuron subpopulations in the arcuate nucleus: integration in neuropeptide Y and pro-opio melanocortin networks? *Diabetes* 56: 1219-27

Fraley GS, Ritter S. 2003. Immunolesion of norepinephrine and epinephrine afferents to medial hypothalamus alters basal and 2-deoxy-D-glucose-induced neuropeptide Y and agouti gene-related protein messenger ribonucleic acid expression in the arcuate nucleus. *Endocrinology* 144: 75-83

Franklin KBJ, Paxinos G. 2008. *The mouse brain in stereotaxic coordinates*. Elsevier Inc.

Frayling TM, Timpson NJ, Weedon MN, Zeggini E, Freathy RM, et al. 2007. A common variant in the FTO gene is associated with body mass index and predisposes to childhood and adult obesity. *Science* 316: 889-94

Frederich RC, Hamann A, Anderson S, Lollmann B, Lowell BB, Flier JS. 1995. Leptin levels reflect body lipid content in mice: evidence for diet-induced resistance to leptin action. *Nat Med* 1: 1311-4

Frizzell RT, Jones EM, Davis SN, Biggers DW, Myers SR, et al. 1993. Counterregulation during hypoglycemia is directed by widespread brain regions. *Diabetes* 42: 1253-61

Funkat A, Massa CM, Jovanovska V, Proietto J, Andrikopoulos S. 2004. Metabolic adaptations of three inbred strains of mice (C57BL/6, DBA/2, and 129T2) in response to a high-fat diet. *J Nutr* 134: 3264-9

Gaglani SM, Lu L, Williams RW, Rosen GD. 2009. The genetic control of neocortex volume and covariation with neocortical gene expression in mice. *BMC Neurosci* 10: 44

Ghourab S, Beale KE, Semjonous NM, Simpson KA, Martin NM, et al. 2011. Intracerebroventricular administration of vasoactive intestinal peptide inhibits food intake. *Regul Pept* 172: 8-15

Gini B, Hager R. 2012. Recombinant inbred systems can advance research in behavioral ecology. *Frontiers in genetics* 3: 198

Gold RM. 1973. Hypothalamic obesity: the myth of the ventromedial nucleus. *Science* 182: 488-90

Gomez-Pinilla F, Ying Z. 2010. Differential effects of exercise and dietary docosahexaenoic acid on molecular systems associated with control of allostasis in the hypothalamus and hippocampus. *Neuroscience* 168: 130-7

Gourlet P, Vandermeers A, Vandermeers-Piret MC, Rathe J, De Neef P, Robberecht P. 1995. Fragments of pituitary adenylate cyclase activating polypeptide discriminate between type I and II recombinant receptors. *Eur J Pharmacol* 287: 7-11

Grandison L, Guidotti A. 1977. Stimulation of food intake by muscimol and beta endorphin. *Neuropharmacology* 16: 533-6

Gray SL, Cummings KJ, Jirik FR, Sherwood NM. 2001. Targeted disruption of the pituitary adenylate cyclase-activating polypeptide gene results in early postnatal death associated with dysfunction of lipid and carbohydrate metabolism. *Mol Endocrinol* 15: 1739-47

Gray SL, Yamaguchi N, Vencova P, Sherwood NM. 2002. Temperature-sensitive phenotype in mice lacking pituitary adenylate cyclase-activating polypeptide. *Endocrinology* 143: 3946-54

Grinevich V, Fournier A, Pelletier G. 1997. Effects of pituitary adenylate cyclase-activating polypeptide (PACAP) on corticotropin-releasing hormone (CRH) gene expression in the rat hypothalamic paraventricular nucleus. *Brain Res* 773: 190-6

Guerra-Crespo M, Ubieta R, Joseph-Bravo P, Charli JL, Perez-Martinez L. 2001. BDNF increases the early expression of TRH mRNA in fetal TrkB+ hypothalamic neurons in primary culture. *The European journal of neuroscience* 14: 483-94

Halaas JL, Gajiwala KS, Maffei M, Cohen SL, Chait BT, et al. 1995. Weight-reducing effects of the plasma protein encoded by the obese gene. *Science* 269: 543-6

Han JC, Liu QR, Jones M, Levinn RL, Menzie CM, et al. 2008. Brain-derived neurotrophic factor and obesity in the WAGR syndrome. *The New England journal of medicine* 359: 918-27

Hannibal J. 2002. Pituitary adenylate cyclase-activating peptide in the rat central nervous system: an immunohistochemical and in situ hybridization study. *J Comp Neurol* 453: 389-417

Hannibal J, Mikkelsen JD, Clausen H, Holst JJ, Wulff BS, Fahrenkrug J. 1995. Gene expression of pituitary adenylate cyclase activating polypeptide (PACAP) in the rat hypothalamus. *Regul Pept* 55: 133-48

Hashimoto H, Nogi H, Mori K, Ohishi H, Shigemoto R, et al. 1996. Distribution of the mRNA for a pituitary adenylate cyclase-activating polypeptide receptor in the rat brain: an in situ hybridization study. *J Comp Neurol* 371: 567-77

Hashimoto H, Shintani N, Nishino A, Okabe M, Ikawa M, et al. 2000. Mice with markedly reduced PACAP (PAC(1)) receptor expression by targeted deletion of the signal peptide. *J Neurochem* 75: 1810-7

Hashimoto H, Shintani N, Tanaka K, Mori W, Hirose M, et al. 2001. Altered psychomotor behaviors in mice lacking pituitary adenylate cyclase-activating polypeptide (PACAP). *Proc Natl Acad Sci U S A* 98: 13355-60

Hawke Z. 2009a. *Ventromedial hypothalamic neurones involved in energy homeostasis*. University of Manchester

Hawke Z. 2009b. *Ventromedial Hypothalamic Neurons Involved in Energy Homeostasis*. University of Manchester, Manchester. 211 pp.

Hawke Z, Ivanov TR, Bechtold DA, Dhillon H, Lowell BB, Luckman SM. 2009. PACAP neurons in the hypothalamic ventromedial nucleus are targets of central leptin signaling. *J Neurosci* 29: 14828-35

Hayes MR, Bradley L, Grill HJ. 2009. Endogenous hindbrain glucagon-like peptide-1 receptor activation contributes to the control of food intake by mediating gastric satiation signaling. *Endocrinology* 150: 2654-9

Heisler LK, Cowley MA, Kishi T, Tecott LH, Fan W, et al. 2003. Central serotonin and melanocortin pathways regulating energy homeostasis. *Ann N Y Acad Sci* 994: 169-74

Herzog H. 2003. Neuropeptide Y and energy homeostasis: insights from Y receptor knockout models. *Eur.J.Pharmacol.* 480: 21

Ho JM, Blevins JE. 2013. Coming full circle: contributions of central and peripheral oxytocin actions to energy balance. *Endocrinology* 154: 589-96

Huang EJ, Reichardt LF. 2001. Neurotrophins: roles in neuronal development and function. *Annu Rev Neurosci* 24: 677-736

Hummel KP, Dickie MM, Coleman DL. 1966. Diabetes, a new mutation in the mouse. *Science* 153: 1127-8

Ibrahim N, Bosch MA, Smart JL, Qiu J, Rubinstein M, et al. 2003. Hypothalamic proopiomelanocortin neurons are glucose responsive and express K(ATP) channels. *Endocrinology* 144: 1331

Imanishi S, Sugimoto M, Morita M, Kume S, Manabe N. 2007. Changes in expression and localization of GPRC5B and RARalpha in the placenta and yolk sac during middle to late gestation in mice. *The Journal of reproduction and development* 53: 1131-6

Inoue S, Nambu T, Shimomura T. 2004. The RAIG family member, GPRC5D, is associated with hard-keratinized structures. *The Journal of investigative dermatology* 122: 565-73

Inui A. 1999. Neuropeptide Y feeding receptors: are multiple subtypes involved? *Trends Pharmacol.Sci.* 20: 43

Irani BG, Le Foll C, Dunn-Meynell A, Levin BE. 2008. Effects of leptin on rat ventromedial hypothalamic neurons. *Endocrinology* 149: 5146-54

Jia M, Xue N, Cao Z, Liu H. 2009. [Effects of dietary different ratios of n-3 to n-6 polyunsaturated fatty acids influence lipid metabolism and appetite of rats]. *Wei Sheng Yan Jiu* 38: 175-8

Jolicoeur FB, Bouali SM, Fournier A, St-Pierre S. 1995. Mapping of hypothalamic sites involved in the effects of NPY on body temperature and food intake. *Brain Res Bull* 36: 125-9

Jones KS, Alimov AP, Rilo HL, Jandacek RJ, Woollett LA, Penberthy WT. 2008. A high throughput live transparent animal bioassay to identify non-toxic small molecules or genes that regulate vertebrate fat metabolism for obesity drug development. *Nutr Metab (Lond)* 5: 23

Joo KM, Chung YH, Kim MK, Nam RH, Lee BL, et al. 2004. Distribution of vasoactive intestinal peptide and pituitary adenylate cyclase-activating polypeptide receptors (VPAC1, VPAC2, and PAC1 receptor) in the rat brain. *J Comp Neurol* 476: 388-413

Kahn BB, Alquier T, Carling D, Hardie DG. 2005. AMP-activated protein kinase: ancient energy gauge provides clues to modern understanding of metabolism. *Cell Metab* 1: 15-25

Kahn CR. 1994. Banting Lecture. Insulin action, diabetogenes, and the cause of type II diabetes. *Diabetes* 43: 1066-84

Kalra PS, Kalra SP. 2000. Use of antisense oligodeoxynucleotides to study the physiological functions of neuropeptide Y. *Methods* 22: 249-54

Kalra SP, Dube MG, Pu S, Xu B, Horvath TL, Kalra PS. 1999. Interacting appetite-regulating pathways in the hypothalamic regulation of body weight. *Endocr Rev* 20: 68-100

Kalra SP, Dube MG, Sahu A, Phelps CP, Kalra PS. 1991. Neuropeptide Y secretion increases in the paraventricular nucleus in association with increased appetite for food. *Proc.Natl.Acad.Sci.U.S.A* 88: 10931

Kang H, Schuman EM. 1996. A requirement for local protein synthesis in neurotrophin-induced hippocampal synaptic plasticity. *Science (New York, N.Y* 273: 1402-6

Kang L, Sanders NM, Dunn-Meynell AA, Gaspers LD, Routh VH, et al. 2008. Prior hypoglycemia enhances glucose responsiveness in some ventromedial hypothalamic glucosensing neurons. *Am J Physiol Regul Integr Comp Physiol* 294: R784-92

Kent WJ, Sugnet CW, Furey TS, Roskin KM, Pringle TH, et al. 2002. The human genome browser at UCSC. *Genome research* 12: 996-1006

Kernie SG, Liebl DJ, Parada LF. 2000. BDNF regulates eating behavior and locomotor activity in mice. *Embo J* 19: 1290-300

Kim KW, Donato J, Jr., Berglund ED, Choi YH, Kohno D, et al. 2012. FOXO1 in the ventromedial hypothalamus regulates energy balance. *The Journal of clinical investigation* 122: 2578-89

Kim KW, Zhao L, Donato J, Jr., Kohno D, Xu Y, et al. 2011. Steroidogenic factor 1 directs programs regulating diet-induced thermogenesis and leptin action in the ventral medial hypothalamic nucleus. *Proceedings of the National Academy of Sciences of the United States of America* 108: 10673-8

Kim MS, Park JY, Namkoong C, Jang PG, Ryu JW, et al. 2004. Anti-obesity effects of alpha-lipoic acid mediated by suppression of hypothalamic AMP-activated protein kinase. *Nat Med* 10: 727-33

Kindler S, Wang H, Richter D, Tiedge H. 2005. RNA transport and local control of translation. *Annual review of cell and developmental biology* 21: 223-45

Kojima M, Hosoda H, Date Y, Nakazato M, Matsuo H, Kangawa K. 1999. Ghrelin is a growth-hormone-releasing acylated peptide from stomach. *Nature* 402: 656

Kola B, Hubina E, Tucci SA, Kirkham TC, Garcia EA, et al. 2005. Cannabinoids and ghrelin have both central and peripheral metabolic and cardiac effects via AMP-activated protein kinase. *J Biol Chem* 280: 25196-201

Komori T, Morikawa Y, Nanjo K, Senba E. 2006. Induction of brain-derived neurotrophic factor by leptin in the ventromedial hypothalamus. *Neuroscience* 139: 1107-15

Koves K, Arimura A, Gorcs TG, Somogyvari-Vigh A. 1991. Comparative distribution of immunoreactive pituitary adenylate cyclase activating polypeptide and vasoactive intestinal polypeptide in rat forebrain. *Neuroendocrinology* 54: 159-69

Koza RA, Nikonova L, Hogan J, Rim JS, Mendoza T, et al. 2006. Changes in gene expression foreshadow diet-induced obesity in genetically identical mice. *PLoS Genet* 2: e81

Kurata K, Fujimoto K, Sakata T, Etou H, Fukagawa K. 1986. D-glucose suppression of eating after intra-third ventricle infusion in rat. *Physiol Behav* 37: 615-20

Kurrasch DM, Cheung CC, Lee FY, Tran PV, Hata K, Ingraham HA. 2007. The neonatal ventromedial hypothalamus transcriptome reveals novel markers with spatially distinct patterning. *J Neurosci* 27: 13624-34

Lage R, Dieguez C, Vidal-Puig A, Lopez M. 2008. AMPK: a metabolic gauge regulating whole-body energy homeostasis. *Trends Mol Med* 14: 539-49

Lagerstrom MC, Schioth HB. 2008. Structural diversity of G protein-coupled receptors and significance for drug discovery. *Nature reviews* 7: 339-57

Lam TK, Gutierrez-Juarez R, Pocai A, Rossetti L. 2005. Regulation of blood glucose by hypothalamic pyruvate metabolism. *Science* 309: 943-7

Laughlin RE, Grant TL, Williams RW, Jentsch JD. 2011. Genetic dissection of behavioral flexibility: reversal learning in mice. *Biol Psychiatry* 69: 1109-16

Lawrence CB, Snape AC, Baudoin FM, Luckman SM. 2002. Acute central ghrelin and GH secretagogues induce feeding and activate brain appetite centers. *Endocrinology* 143: 155-62

Lawrence CB, Williams T, Luckman SM. 2003. Intracerebroventricular galanin-like peptide induces different brain activation compared with galanin. *Endocrinology* 144: 3977-84

Legradi G, Hannibal J, Lechan RM. 1997. Association between pituitary adenylate cyclase-activating polypeptide and thyrotropin-releasing hormone in the rat hypothalamus. *J Chem Neuroanat* 13: 265-79

Legradi G, Hannibal J, Lechan RM. 1998. Pituitary adenylate cyclase-activating polypeptide-nerve terminals densely innervate corticotropin-releasing hormone-neurons in the hypothalamic paraventricular nucleus of the rat. *Neurosci Lett* 246: 145-8

Levin BE. 2006. Metabolic sensing neurons and the control of energy homeostasis. *Physiology & behavior* 89: 486-9

Lewis SR, Ahmed S, Khaimova E, Israel Y, Singh A, et al. 2006. Genetic variance contributes to ingestive processes: a survey of 2-deoxy-D-glucose-induced feeding in eleven inbred mouse strains. *Physiol Behav* 87: 595-601

Li X. 2013. SIRT1 and energy metabolism. *Acta biochimica et biophysica Sinica* 45: 51-60

Liao GY, An JJ, Gharami K, Waterhouse EG, Vanevski F, et al. 2012. Dendritically targeted Bdnf mRNA is essential for energy balance and response to leptin. *Nature medicine* 18: 564-71

Loftus TM, Jaworsky DE, Frehywot GL, Townsend CA, Ronnett GV, et al. 2000. Reduced food intake and body weight in mice treated with fatty acid synthase inhibitors. *Science* 288: 2379

Loos RJ, Lindgren CM, Li S, Wheeler E, Zhao JH, et al. 2008. Common variants near MC4R are associated with fat mass, weight and risk of obesity. *Nat Genet* 40: 768-75

Lopez M, Lage R, Saha AK, Perez-Tilve D, Vazquez MJ, et al. 2008. Hypothalamic fatty acid metabolism mediates the orexigenic action of ghrelin. *Cell Metab* 7: 389-99

Lopez M, Lelliott CJ, Tovar S, Kimber W, Gallego R, et al. 2006. Tamoxifen-induced anorexia is associated with fatty acid synthase inhibition in the ventromedial nucleus of the hypothalamus and accumulation of malonyl-CoA. *Diabetes* 55: 1327-36

Loudes C, Petit F, Kordon C, Faivre-Bauman A. 1999. Distinct populations of hypothalamic dopaminergic neurons exhibit differential responses to brain-derived neurotrophic factor (BDNF) and neurotrophin-3 (NT3). *The European journal of neuroscience* 11: 617-24

Louis-Sylvestre J, Le Magnen J. 1980. Fall in blood glucose level precedes meal onset in free-feeding rats. *Neurosci Biobehav Rev* 4 Suppl 1: 13-5

Lubin FD, Roth TL, Sweatt JD. 2008. Epigenetic regulation of BDNF gene transcription in the consolidation of fear memory. *J Neurosci* 28: 10576-86

Luckman SM, Dyball RE, Leng G. 1994. Induction of c-fos expression in hypothalamic magnocellular neurons requires synaptic activation and not simply increased spike activity. *J Neurosci* 14: 4825-30

Luckman SM, Lawrence CB. 2003. Anorectic brainstem peptides: more pieces to the puzzle. *Trends in endocrinology and metabolism: TEM* 14: 60-5

Luquet S, Perez FA, Hnasko TS, Palmiter RD. 2005. NPY/AgRP neurons are essential for feeding in adult mice but can be ablated in neonates. *Science* 310: 683-5

Luquet S, Phillips CT, Palmiter RD. 2007. NPY/AgRP neurons are not essential for feeding responses to glucoprivation. *Peptides* 28: 214-25

Maden M. 2007. Retinoic acid in the development, regeneration and maintenance of the nervous system. *Nat Rev Neurosci* 8: 755-65

Maekawa F, Fujiwara K, Tsukahara S, Yada T. 2006. Pituitary adenylate cyclase-activating polypeptide neurons of the ventromedial hypothalamus project to the midbrain central gray. *Neuroreport* 17: 221-4

Maffei M, Stoffel M, Barone M, Moon B, Dammerman M, et al. 1996. Absence of mutations in the human OB gene in obese/diabetic subjects. *Diabetes* 45: 679-82

Majdic G, Young M, Gomez-Sanchez E, Anderson P, Szczepaniak LS, et al. 2002. Knockout mice lacking steroidogenic factor 1 are a novel genetic model of hypothalamic obesity. *Endocrinology* 143: 607-14

Makimura H, Mizuno TM, Mastaitis JW, Agami R, Mobbs CV. 2002. Reducing hypothalamic AGRP by RNA interference increases metabolic rate and decreases body weight without influencing food intake. *BMC Neurosci* 3: 18

Makino S, Gold PW, Schulkin J. 1994. Corticosterone effects on corticotropin-releasing hormone mRNA in the central nucleus of the amygdala and the parvocellular region of the paraventricular nucleus of the hypothalamus. *Brain Res* 640: 105-12

Marty N, Dallaporta M, Thorens B. 2007. Brain glucose sensing, counterregulation, and energy homeostasis. *Physiology (Bethesda)* 22: 241-51

Matsuda K, Maruyama K, Nakamachi T, Miura T, Uchiyama M, Shioda S. 2005. Inhibitory effects of pituitary adenylate cyclase-activating polypeptide (PACAP) and vasoactive intestinal peptide (VIP) on food intake in the goldfish, Carassius auratus. *Peptides* 26: 1611-6

Matzinger D, Degen L, Drewe J, Meuli J, Duebendorfer R, et al. 2000. The role of long chain fatty acids in regulating food intake and cholecystokinin release in humans. *Gut* 46: 688-93

Mavanji V, Billington CJ, Kotz CM, Teske JA. 2012. Sleep and obesity: a focus on animal models. *Neurosci Biobehav Rev* 36: 1015-29

McAllister EJ, Dhurandhar NV, Keith SW, Aronne LJ, Barger J, et al. 2009. Ten putative contributors to the obesity epidemic. *Crit Rev Food Sci Nutr* 49: 868-913

McClellan KM, Parker KL, Tobet S. 2006. Development of the ventromedial nucleus of the hypothalamus. *Front Neuroendocrinol* 27: 193-209

McMinn JE, Sindelar DK, Havel PJ, Schwartz MW. 2000. Leptin deficiency induced by fasting impairs the satiety response to cholecystokinin. *Endocrinology* 141: 4442-8

Meister B. 2007. Neurotransmitters in key neurons of the hypothalamus that regulate feeding behavior and body weight. *Physiology & behavior* 92: 263-71

Mendieta-Zeron H, Lopez M, Dieguez C. 2008. Gastrointestinal peptides controlling body weight homeostasis. *General and comparative endocrinology* 155: 481-95

Mercer JG, Hoggard N, Williams LM, Lawrence CB, Hannah LT, et al. 1996. Coexpression of leptin receptor and preproneuropeptide Y mRNA in arcuate nucleus of mouse hypothalamus. *J.Neuroendocrinol.* 8: 733

Miller JC, Gnaedinger JM, Rapoport SI. 1987. Utilization of plasma fatty acid in rat brain: distribution of [14C]palmitate between oxidative and synthetic pathways. *J Neurochem* 49: 1507-14

Minokoshi Y, Alquier T, Furukawa N, Kim YB, Lee A, et al. 2004. AMP-kinase regulates food intake by responding to hormonal and nutrient signals in the hypothalamus. *Nature* 428: 569

Minokoshi Y, Kim YB, Peroni OD, Fryer LG, Muller C, et al. 2002. Leptin stimulates fatty-acid oxidation by activating AMP-activated protein kinase. *Nature* 415: 339-43

Miselis RR, Epstein AN. 1975. Feeding induced by intracerebroventricular 2-deoxy-D-glucose in the rat. *Am J Physiol* 229: 1438-47

Mitrakou A, Ryan C, Veneman T, Mokan M, Jenssen T, et al. 1991. Hierarchy of glycemic thresholds for counterregulatory hormone secretion, symptoms, and cerebral dysfunction. *Am J Physiol* 260: E67-74

Miyairi I, Tatireddigari VR, Mahdi OS, Rose LA, Belland RJ, et al. 2007. The p47 GTPases Iigp2 and Irgb10 regulate innate immunity and inflammation to murine Chlamydia psittaci infection. *J Immunol* 179: 1814-24

Miyata A, Arimura A, Dahl RR, Minamino N, Uehara A, et al. 1989. Isolation of a novel 38 residue-hypothalamic polypeptide which stimulates adenylate cyclase in pituitary cells. *Biochem Biophys Res Commun* 164: 567-74

Mizuno TM, Kleopoulos SP, Bergen HT, Roberts JL, Priest CA, Mobbs CV. 1998a. Hypothalamic pro-opiomelanocortin mRNA is reduced by fasting and [corrected] in ob/ob and db/db mice, but is stimulated by leptin. *Diabetes* 47: 294-7

Mizuno Y, Kondo K, Terashima Y, Arima H, Murase T, Oiso Y. 1998b. Anorectic effect of pituitary adenylate cyclase activating polypeptide (PACAP) in rats: lack of evidence for involvement of hypothalamic neuropeptide gene expression. *J Neuroendocrinol* 10: 611-6

Monnikes H, Lauer G, Bauer C, Tebbe J, Zittel TT, Arnold R. 1997. Pathways of Fos expression in locus ceruleus, dorsal vagal complex, and PVN in response to intestinal lipid. *Am J Physiol* 273: R2059-71

Montague CT, Farooqi IS, Whitehead JP, Soos MA, Rau H, et al. 1997. Congenital leptin deficiency is associated with severe early-onset obesity in humans. *Nature* 387: 903

Morgan K, Obici S, Rossetti L. 2004. Hypothalamic responses to long-chain fatty acids are nutritionally regulated. *J Biol Chem* 279: 31139-48

Morley JE, Horowitz M, Morley PM, Flood JF. 1992. Pituitary adenylate cyclase activating polypeptide (PACAP) reduces food intake in mice. *Peptides* 13: 1133-5

Morton GJ, Cummings DE, Baskin DG, Barsh GS, Schwartz MW. 2006. Central nervous system control of food intake and body weight. *Nature* 443: 289-95

Mounien L, Bizet P, Boutelet I, Gourcerol G, Fournier A, et al. 2006. Pituitary adenylate cyclase-activating polypeptide directly modulates the activity of proopiomelanocortin neurons in the rat arcuate nucleus. *Neuroscience* 143: 155-63

Mounien L, Do Rego JC, Bizet P, Boutelet I, Gourcerol G, et al. 2008. Pituitary adenylate cyclase-activating polypeptide inhibits food intake in mice through activation of the hypothalamic melanocortin system. *Neuropsychopharmacology* 34: 424-35

Mountjoy KG, Mortrud MT, Low MJ, Simerly RB, Cone RD. 1994. Localization of the melanocortin-4 receptor (MC4-R) in neuroendocrine and autonomic control circuits in the brain. *Mol Endocrinol* 8: 1298-308

Mountjoy PD, Bailey SJ, Rutter GA. 2007. Inhibition by glucose or leptin of hypothalamic neurons expressing neuropeptide Y requires changes in AMP-activated protein kinase activity. *Diabetologia* 50: 168-77

Muroya S, Yada T, Shioda S, Takigawa M. 1999. Glucose-sensitive neurons in the rat arcuate nucleus contain neuropeptide Y. *Neurosci.Lett.* 264: 113

Murphy KG, Dhillo WS, Bloom SR. 2006. Gut peptides in the regulation of food intake and energy homeostasis. *Endocrine reviews* 27: 719-27

Nakagawa T, Ogawa Y, Ebihara K, Yamanaka M, Tsuchida A, et al. 2003. Anti-obesity and anti-diabetic effects of brain-derived neurotrophic factor in rodent models of leptin resistance. *Int J Obes Relat Metab Disord* 27: 557-65

Nakazato M, Murakami N, Date Y, Kojima M, Matsuo H, et al. 2001. A role for ghrelin in the central regulation of feeding. *Nature* 409: 194

Nomura M, Ueta Y, Serino R, Kabashima N, Shibuya I, Yamashita H. 1996. PACAP type I receptor gene expression in the paraventricular and supraoptic nuclei of rats. *Neuroreport* 8: 67-70

Norgren R. 1978. Projections from the nucleus of the solitary tract in the rat. *Neuroscience* 3: 207-18

Novak A, Guo C, Yang W, Nagy A, Lobe CG. 2000. Z/EG, a double reporter mouse line that expresses enhanced green fluorescent protein upon Cre-mediated excision. *Genesis* 28: 147-55

Obici S, Feng Z, Arduini A, Conti R, Rossetti L. 2003. Inhibition of hypothalamic carnitine palmitoyltransferase-1 decreases food intake and glucose production. *Nat.Med.* 9: 756

Obici S, Feng Z, Morgan K, Stein D, Karkanias G, Rossetti L. 2002. Central administration of oleic acid inhibits glucose production and food intake. *Diabetes* 51: 271-5

Ollmann MM, Wilson BD, Yang YK, Kerns JA, Chen Y, et al. 1997. Antagonism of central melanocortin receptors in vitro and in vivo by agouti-related protein. *Science* 278: 135-8

Olszewski PK, Klockars A, Schioth HB, Levine AS. 2010. Oxytocin as feeding inhibitor: maintaining homeostasis in consummatory behavior. *Pharmacology, biochemistry, and behavior* 97: 47-54

Oomura Y. 1983. Glucose as a regulator of neuronal activity. *Adv Metab Disord* 10: 31-65

Oomura Y, Ono T, Ooyama H, Wayner MJ. 1969. Glucose and osmosensitive neurones of the rat hypothalamus. *Nature* 222: 282

Oomura Y, Yoshimatsu H. 1984. Neural network of glucose monitoring system. *J Auton Nerv Syst* 10: 359-72

Page KA, Arora J, Qiu M, Relwani R, Constable RT, Sherwin RS. 2009. Small decrements in systemic glucose provoke increases in hypothalamic blood flow prior to the release of counterregulatory hormones. *Diabetes* 58: 448-52

Panksepp J, Rossi J, 3rd. 1981. D-glucose infusions into the basal ventromedial hypothalamus and feeding. *Behav Brain Res* 3: 381-92

Parker JA, Bloom SR. 2012. Hypothalamic neuropeptides and the regulation of appetite. *Neuropharmacology* 63: 18-30

Pattabiraman PP, Tropea D, Chiaruttini C, Tongiorgi E, Cattaneo A, Domenici L. 2005. Neuronal activity regulates the developmental expression and subcellular localization of cortical BDNF mRNA isoforms in vivo. *Molecular and cellular neurosciences* 28: 556-70

Peirce JL, Lu L, Gu J, Silver LM, Williams RW. 2004. A new set of BXD recombinant inbred lines from advanced intercross populations in mice. *BMC genetics* 5: 7

Pelleymounter MA, Cullen MJ, Baker MB, Hecht R, Winters D, et al. 1995a. Effects of the obese gene product on body weight regulation in ob/ob mice. *Science* 269: 540-3

Pelleymounter MA, Cullen MJ, Baker MB, Hecht R, Winters D, et al. 1995b. Effects of the obese gene product on body weight regulation in ob/ob mice. *Science* 269: 540

Pfluger PT, Kirchner H, Gunnel S, Schrott B, Perez-Tilve D, et al. 2008. Simultaneous deletion of ghrelin and its receptor increases motor activity and energy expenditure. *Am J Physiol Gastrointest Liver Physiol* 294: G610-8

Philip VM, Duvvuru S, Gomero B, Ansah TA, Blaha CD, et al. 2010. High-throughput behavioral phenotyping in the expanded panel of BXD recombinant inbred strains. *Genes Brain Behav* 9: 129-59

Piggins HD, Stamp JA, Burns J, Rusak B, Semba K. 1996. Distribution of pituitary adenylate cyclase activating polypeptide (PACAP) immunoreactivity in the hypothalamus and extended amygdala of the rat. *J Comp Neurol* 376: 278-94

Plum L, Belgardt BF, Bruning JC. 2006. Central insulin action in energy and glucose homeostasis. *J Clin Invest* 116: 1761-6

Polonsky KS, Given BD, Hirsch L, Shapiro ET, Tillil H, et al. 1988a. Quantitative study of insulin secretion and clearance in normal and obese subjects. *J Clin Invest* 81: 435-41

Polonsky KS, Given BD, Van Cauter E. 1988b. Twenty-four-hour profiles and pulsatile patterns of insulin secretion in normal and obese subjects. *J Clin Invest* 81: 442-8

Porte D, Jr., Woods SC. 1981. Regulation of food intake and body weight in insulin. *Diabetologia* 20 Suppl: 274-80

Powell AM, Sherwin RS, Shulman GI. 1993. Impaired hormonal responses to hypoglycemia in spontaneously diabetic and recurrently hypoglycemic rats. Reversibility and stimulus specificity of the deficits. *J Clin Invest* 92: 2667-74

Qi K, Hall M, Deckelbaum RJ. 2002. Long-chain polyunsaturated fatty acid accretion in brain. *Curr Opin Clin Nutr Metab Care* 5: 133-8

Rage F, Riteau B, Alonso G, Tapia-Arancibia L. 1999. Brain-derived neurotrophic factor and neurotrophin-3 enhance somatostatin gene expression through a likely direct effect on hypothalamic somatostatin neurons. *Endocrinology* 140: 909-16

Ramadori G, Fujikawa T, Fukuda M, Anderson J, Morgan DA, et al. 2010. SIRT1 deacetylase in POMC neurons is required for homeostatic defenses against diet-induced obesity. *Cell metabolism* 12: 78-87

Ramadori G, Gautron L, Fujikawa T, Vianna CR, Elmquist JK, Coppari R. 2009. Central administration of resveratrol improves diet-induced diabetes. *Endocrinology* 150: 5326-33

Rapoport SI. 1996. In vivo labeling of brain phospholipids by long-chain fatty acids: relation to turnover and function. *Lipids* 31 Suppl: S97-101

Rapoport SI. 2001. In vivo fatty acid incorporation into brain phosholipids in relation to plasma availability, signal transduction and membrane remodeling. *J Mol Neurosci* 16: 243-61; discussion 79-84

Rentsch J, Levens N, Chiesi M. 1995. Recombinant ob-gene product reduces food intake in fasted mice. *Biochem Biophys Res Commun* 214: 131-6

Resch JM, Boisvert JP, Hourigan AE, Mueller CR, Yi SS, Choi S. 2011. Stimulation of the hypothalamic ventromedial nuclei by pituitary adenylate cyclase-activating polypeptide induces hypophagia and thermogenesis. *American journal of physiology* 301: R1625-34

Rios M, Fan G, Fekete C, Kelly J, Bates B, et al. 2001. Conditional deletion of brain-derived neurotrophic factor in the postnatal brain leads to obesity and hyperactivity. *Mol Endocrinol* 15: 1748-57

Ritter S, Bugarith K, Dinh TT. 2001. Immunotoxic destruction of distinct catecholamine subgroups produces selective impairment of glucoregulatory responses and neuronal activation. *J Comp Neurol* 432: 197-216

Robbins MJ, Charles KJ, Harrison DC, Pangalos MN. 2002. Localisation of the GPRC5B receptor in the rat brain and spinal cord. *Brain research* 106: 136-44

Robbins MJ, Michalovich D, Hill J, Calver AR, Medhurst AD, et al. 2000. Molecular cloning and characterization of two novel retinoic acid-inducible orphan G-protein-coupled receptors (GPRC5B and GPRC5C). *Genomics* 67: 8-18

Rodriguez A, Gomez-Ambrosi J, Catalan V, Gil MJ, Becerril S, et al. 2009. Acylated and desacyl ghrelin stimulate lipid accumulation in human visceral adipocytes. *International journal of obesity* 33: 541-52

Rooney K, Ozanne SE. 2011. Maternal over-nutrition and offspring obesity predisposition: targets for preventative interventions. *International journal of obesity* 35: 883-90

Ropelle ER, Fernandes MF, Flores MB, Ueno M, Rocco S, et al. 2008a. Central exercise action increases the AMPK and mTOR response to leptin. *PLoS One* 3: e3856

Ropelle ER, Pauli JR, Fernandes MF, Rocco SA, Marin RM, et al. 2008b. A central role for neuronal AMP-activated protein kinase (AMPK) and mammalian target of rapamycin (mTOR) in high-protein diet-induced weight loss. *Diabetes* 57: 594-605

Roselli-Rehfuss L, Mountjoy KG, Robbins LS, Mortrud MT, Low MJ, et al. 1993. Identification of a receptor for gamma melanotropin and other proopiomelanocortin peptides in the hypothalamus and limbic system. *Proc.Natl.Acad.Sci.U.S.A* 90: 8856

Rother E, Konner AC, Bruning JC. 2008. Neurocircuits integrating hormone and nutrient signaling in control of glucose metabolism. *Am J Physiol Endocrinol Metab* 294: E810-6

Sakaguchi T, Bray GA. 1987. The effect of intrahypothalamic injections of glucose on sympathetic efferent firing rate. *Brain Res Bull* 18: 591-5

Sakaguchi T, Bray GA. 1988. Sympathetic activity following paraventricular injections of glucose and insulin. *Brain Res Bull* 21: 25-9

Sanchez-Lasheras C, Konner AC, Bruning JC. 2010. Integrative neurobiology of energy homeostasis-neurocircuits, signals and mediators. *Front Neuroendocrinol* 31: 4-15

Sano T, Kim YJ, Oshima E, Shimizu C, Kiyonari H, et al. 2011. Comparative characterization of GPRC5B and GPRC5CLacZ knockin mice; behavioral abnormalities in GPRC5B-deficient mice. *Biochem Biophys Res Commun* 412: 460-5

Satoh A, Brace CS, Ben-Josef G, West T, Wozniak DF, et al. 2010. SIRT1 promotes the central adaptive response to diet restriction through activation of the dorsomedial and lateral nuclei of the hypothalamus. *J Neurosci* 30: 10220-32

Satoh N, Ogawa Y, Katsuura G, Numata Y, Tsuji T, et al. 1999. Sympathetic activation of leptin via the ventromedial hypothalamus: leptin-induced increase in catecholamine secretion. *Diabetes* 48: 1787

Schlegel A, Stainier DY. 2006. Microsomal triglyceride transfer protein is required for yolk lipid utilization and absorption of dietary lipids in zebrafish larvae. *Biochemistry* 45: 15179-87

Schwartz GJ, Salorio CF, Skoglund C, Moran TH. 1999a. Gut vagal afferent lesions increase meal size but do not block gastric preload-induced feeding suppression. *Am J Physiol* 276: R1623-9

Schwartz MW, Baskin DG, Kaiyala KJ, Woods SC. 1999b. Model for the regulation of energy balance and adiposity by the central nervous system. *Am J Clin Nutr* 69: 584-96

Schwartz MW, Seeley RJ, Campfield LA, Burn P, Baskin DG. 1996. Identification of targets of leptin action in rat hypothalamus. *J Clin Invest* 98: 1101-6

Schwartz MW, Woods SC, Porte D, Jr., Seeley RJ, Baskin DG. 2000. Central nervous system control of food intake. *Nature* 404: 661

Scott V, Kimura N, Stark JA, Luckman SM. 2005. Intravenous peptide YY3-36 and Y2 receptor antagonism in the rat: effects on feeding behaviour. *J Neuroendocrinol* 17: 452-7

Segal JP, Stallings NR, Lee CE, Zhao L, Socci N, et al. 2005. Use of laser-capture microdissection for the identification of marker genes for the ventromedial hypothalamic nucleus. *J Neurosci* 25: 4181-8

Segal NL, Allison DB. 2002. Twins and virtual twins: bases of relative body weight revisited. *Int J Obes Relat Metab Disord* 26: 437-41

Sherwood NM, Krueckl SL, McRory JE. 2000. The origin and function of the pituitary adenylate cyclase-activating polypeptide (PACAP)/glucagon superfamily. *Endocr Rev* 21: 619-70

Shutter JR, Graham M, Kinsey AC, Scully S, Luthy R, Stark KL. 1997. Hypothalamic expression of ART, a novel gene related to agouti, is up-regulated in obese and diabetic mutant mice. *Genes Dev.* 11: 593

Silver IA, Erecinska M. 1994. Extracellular glucose concentration in mammalian brain: continuous monitoring of changes during increased neuronal activity and upon limitation in oxygen supply in normo-, hypo-, and hyperglycemic animals. *J Neurosci* 14: 5068-76

Silver IA, Erecinska M. 1998. Glucose-induced intracellular ion changes in sugar-sensitive hypothalamic neurons. *J.Neurophysiol.* 79: 1733

Skledar M, Nikolac M, Dodig-Curkovic K, Curkovic M, Borovecki F, Pivac N. 2011. Association between brain-derived neurotrophic factor Val66Met and obesity in children and adolescents. *Progress in neuro-psychopharmacology & biological psychiatry* 36: 136-40

Small CJ, Kim MS, Stanley SA, Mitchell JR, Murphy K, et al. 2001. Effects of chronic central nervous system administration of agouti-related protein in pair-fed animals. *Diabetes* 50: 248-54

Song CK, Jackson RM, Harris RB, Richard D, Bartness TJ. 2005. Melanocortin-4 receptor mRNA is expressed in sympathetic nervous system outflow neurons to white adipose tissue. *Am J Physiol Regul Integr Comp Physiol* 289: R1467-76

Song CK, Vaughan CH, Keen-Rhinehart E, Harris RB, Richard D, Bartness TJ. 2008. Melanocortin-4 receptor mRNA expressed in sympathetic outflow neurons to brown adipose tissue: neuroanatomical and functional evidence. *Am J Physiol Regul Integr Comp Physiol* 295: R417-28

Song Z, Levin BE, McArdle JJ, Bakhos N, Routh VH. 2001. Convergence of pre- and postsynaptic influences on glucosensing neurons in the ventromedial hypothalamic nucleus. *Diabetes* 50: 2673

Song Z, Routh VH. 2006. Recurrent hypoglycemia reduces the glucose sensitivity of glucose-inhibited neurons in the ventromedial hypothalamus nucleus. *Am J Physiol Regul Integr Comp Physiol* 291: R1283-7

Sorensen A, Travers MT, Vernon RG, Price NT, Barber MC. 2002. Localization of messenger RNAs encoding enzymes associated with malonyl-CoA metabolism in mouse brain. *Brain Res Gene Expr Patterns* 1: 167-73

Speakman JR. 2004. Obesity: the integrated roles of environment and genetics. *J Nutr* 134: 2090S-105S

Speakman JR, Levitsky DA, Allison DB, Bray MS, de Castro JM, et al. 2011. Set points, settling points and some alternative models: theoretical options to understand how genes and environments combine to regulate body adiposity. *Dis Model Mech* 4: 733-45

Speliotes EK, Willer CJ, Berndt SI, Monda KL, Thorleifsson G, et al. 2010a. Association analyses of 249,796 individuals reveal 18 new loci associated with body mass index. *Nat Genet* 42: 937-48

Speliotes EK, Willer CJ, Berndt SI, Monda KL, Thorleifsson G, et al. 2010b. Association analyses of 249,796 individuals reveal 18 new loci associated with body mass index. *Nature genetics* 42: 937-48

Spiegelman BM, Flier JS. 2001. Obesity and the regulation of energy balance. *Cell* 104: 531-43

Sporn MB. 2007. A new tumor suppressor gene, selective for lung cancer. *Journal of the National Cancer Institute* 99: 1654-5

Susens U, Hermans-Borgmeyer I, Urny J, Schaller HC. 2006. Characterisation and differential expression of two very closely related G-protein-coupled receptors, GPR139 and GPR142, in mouse tissue and during mouse development. *Neuropharmacology* 50: 512-20

Svenson KL, Von Smith R, Magnani PA, Suetin HR, Paigen B, et al. 2007. Multiple trait measurements in 43 inbred mouse strains capture the phenotypic diversity characteristic of human populations. *J Appl Physiol* 102: 2369-78

Swart I, Jahng JW, Overton JM, Houpt TA. 2002. Hypothalamic NPY, AGRP, and POMC mRNA responses to leptin and refeeding in mice. *Am J Physiol Regul Integr Comp Physiol* 283: R1020-6

Symonds ME, Budge H, Perkins AC, Lomax MA. 2011. Adipose tissue development--impact of the early life environment. *Prog Biophys Mol Biol* 106: 300-6

Symonds ME, Sebert SP, Hyatt MA, Budge H. 2009. Nutritional programming of the metabolic syndrome. *Nat Rev Endocrinol* 5: 604-10

Taborsky GJ, Jr., Ahren B, Havel PJ. 1998. Autonomic mediation of glucagon secretion during hypoglycemia: implications for impaired alpha-cell responses in type 1 diabetes. *Diabetes* 47: 995-1005

Tachibana T, Saito S, Tomonaga S, Takagi T, Saito ES, et al. 2003. Intracerebroventricular injection of vasoactive intestinal peptide and pituitary adenylate cyclase-activating polypeptide inhibits feeding in chicks. *Neurosci Lett* 339: 203-6

Takahashi A, Ishimaru H, Ikarashi Y, Kishi E, Maruyama Y. 1997. Effects of ventromedial hypothalamus stimulation on glycogenolysis in rat liver using in vivo microdialysis. *Metabolism: clinical and experimental* 46: 897-901

Takeda S, Elefteriou F, Levasseur R, Liu X, Zhao L, et al. 2002. Leptin regulates bone formation via the sympathetic nervous system. *Cell* 111: 305-17

Tao Q, Cheng Y, Clifford J, Lotan R. 2004. Characterization of the murine orphan G-protein-coupled receptor gene Rai3 and its regulation by retinoic acid. *Genomics* 83: 270-80

Tejwani GA, Richard CW, 3rd. 1986. Effect of electrolytic and chemical ventromedial hypothalamic lesions on food intake, body weight, analgesia and the CNS opioid peptides in rats and mice. *NIDA Res Monogr* 75: 497-500

Thiele TE, Van Dijk G, Campfield LA, Smith FJ, Burn P, et al. 1997. Central infusion of GLP-1, but not leptin, produces conditioned taste aversions in rats. *Am J Physiol* 272: R726-30

Thorleifsson G, Walters GB, Gudbjartsson DF, Steinthorsdottir V, Sulem P, et al. 2009. Genome-wide association yields new sequence variants at seven loci that associate with measures of obesity. *Nat Genet* 41: 18-24

Timmusk T, Palm K, Metsis M, Reintam T, Paalme V, et al. 1993. Multiple promoters direct tissue-specific expression of the rat BDNF gene. *Neuron* 10: 475-89

Tong Q, Ye C, McCrimmon RJ, Dhillon H, Choi B, et al. 2007. Synaptic glutamate release by ventromedial hypothalamic neurons is part of the neurocircuitry that prevents hypoglycemia. *Cell Metab* 5: 383-93

Tran PV, Akana SF, Malkovska I, Dallman MF, Parada LF, Ingraham HA. 2006. Diminished hypothalamic bdnf expression and impaired VMH function are associated with reduced SF-1 gene dosage. *J Comp Neurol* 498: 637-48

Tsankova NM, Berton O, Renthal W, Kumar A, Neve RL, Nestler EJ. 2006. Sustained hippocampal chromatin regulation in a mouse model of depression and antidepressant action. *Nat Neurosci* 9: 519-25

Tschop M, Smiley DL, Heiman ML. 2000. Ghrelin induces adiposity in rodents. *Nature* 407: 908

Unger TJ, Calderon GA, Bradley LC, Sena-Esteves M, Rios M. 2007. Selective deletion of Bdnf in the ventromedial and dorsomedial hypothalamus of adult mice results in hyperphagic behavior and obesity. *J Neurosci* 27: 14265-74

Vaudry D, Falluel-Morel A, Bourgault S, Basille M, Burel D, et al. 2009. Pituitary adenylate cyclase-activating polypeptide and its receptors: 20 years after the discovery. *Pharmacol Rev* 61: 283-357

Velloso LA, Schwartz MW. 2011. Altered hypothalamic function in diet-induced obesity. *International journal of obesity* 35: 1455-65

Wang C, Bomberg E, Levine A, Billington C, Kotz CM. 2007. Brain-derived neurotrophic factor in the ventromedial nucleus of the hypothalamus reduces energy intake. *Am J Physiol Regul Integr Comp Physiol* 293: R1037-45

Wang J, Williams RW, Manly KF. 2003. WebQTL: web-based complex trait analysis. *Neuroinformatics* 1: 299-308

Wang R, Cruciani-Guglielmacci C, Migrenne S, Magnan C, Cotero VE, Routh VH. 2006. Effects of oleic acid on distinct populations of neurons in the hypothalamic arcuate nucleus are dependent on extracellular glucose levels. *J Neurophysiol* 95: 1491-8

Warden CH, Fisler JS. 2008. Gene-nutrient and gene-physical activity summary--genetics viewpoint. *Obesity (Silver Spring)* 16 Suppl 3: S55-9

Wibrand K, Messaoudi E, Havik B, Steenslid V, Lovlie R, et al. 2006. Identification of genes co-upregulated with Arc during BDNF-induced long-term potentiation in adult rat dentate gyrus in vivo. *The European journal of neuroscience* 23: 1501-11

Willer CJ, Speliotes EK, Loos RJ, Li S, Lindgren CM, et al. 2009. Six new loci associated with body mass index highlight a neuronal influence on body weight regulation. *Nat Genet* 41: 25-34

Willesen MG, Kristensen P, Romer J. 1999. Co-localization of growth hormone secretagogue receptor and NPY mRNA in the arcuate nucleus of the rat. *Neuroendocrinology* 70: 306

Williams RW, Gu J, Qi S, Lu L. 2001. The genetic structure of recombinant inbred mice: high-resolution consensus maps for complex trait analysis. *Genome biology* 2: RESEARCH0046

Wilson BD, Ollmann MM, Barsh GS. 1999. The role of agouti-related protein in regulating body weight. *Mol Med Today* 5: 250-6

Wolffe AP, Guschin D. 2000. Review: chromatin structural features and targets that regulate transcription. *J Struct Biol* 129: 102-22

Wolfgang MJ, Cha SH, Sidhaye A, Chohnan S, Cline G, et al. 2007. Regulation of hypothalamic malonyl-CoA by central glucose and leptin. *Proc Natl Acad Sci U S A* 104: 19285-90

Wolfgang MJ, Lane MD. 2006. Control of energy homeostasis: role of enzymes and intermediates of fatty acid metabolism in the central nervous system. *Annu Rev Nutr* 26: 23-44

Woods A, Cheung PC, Smith FC, Davison MD, Scott J, et al. 1996. Characterization of AMP-activated protein kinase beta and gamma subunits. Assembly of the heterotrimeric complex in vitro. *J Biol Chem* 271: 10282-90

Woods SC, D'Alessio DA. 2008. Central control of body weight and appetite. *The Journal of clinical endocrinology and metabolism* 93: S37-50

Woods SC, Lotter EC, McKay LD, Porte D, Jr. 1979. Chronic intracerebroventricular infusion of insulin reduces food intake and body weight of baboons. *Nature* 282: 503-5

Woods SC, Stein LJ, McKay LD, Porte D, Jr. 1984. Suppression of food intake by intravenous nutrients and insulin in the baboon. *Am J Physiol* 247: R393-401

Wortley KE, del Rincon JP, Murray JD, Garcia K, Iida K, et al. 2005. Absence of ghrelin protects against early-onset obesity. *J Clin Invest* 115: 3573-8

Wozniak SE, Gee LL, Wachtel MS, Frezza EE. 2009. Adipose tissue: the new endocrine organ? A review article. *Digestive diseases and sciences* 54: 1847-56

Wren AM, Seal LJ, Cohen MA, Brynes AE, Frost GS, et al. 2001a. Ghrelin enhances appetite and increases food intake in humans. *J.Clin.Endocrinol.Metab* 86: 5992

Wren AM, Small CJ, Abbott CR, Dhillo WS, Seal LJ, et al. 2001b. Ghrelin causes hyperphagia and obesity in rats. *Diabetes* 50: 2540

Xu B, Goulding EH, Zang K, Cepoi D, Cone RD, et al. 2003. Brain-derived neurotrophic factor regulates energy balance downstream of melanocortin-4 receptor. *Nat Neurosci* 6: 736-42

Xu J, Tian J, Shapiro SD. 2005. Normal lung development in RAIG1-deficient mice despite unique lung epithelium-specific expression. *American journal of respiratory cell and molecular biology* 32: 381-7

Xue B, Kahn BB. 2006. AMPK integrates nutrient and hormonal signals to regulate food intake and energy balance through effects in the hypothalamus and peripheral tissues. *J Physiol* 574: 73-83

Yasuda M, Fukuchi M, Tabuchi A, Kawahara M, Tsuneki H, et al. 2007. Robust stimulation of TrkB induces delayed increases in BDNF and Arc mRNA expressions in cultured rat cortical neurons via distinct mechanisms. *Journal of neurochemistry* 103: 626-36

Ye X, Tao Q, Wang Y, Cheng Y, Lotan R. 2009. Mechanisms underlying the induction of the putative human tumor suppressor GPRC5A by retinoic acid. *Cancer biology & therapy* 8: 951-62

Yeo GS, Connie Hung CC, Rochford J, Keogh J, Gray J, et al. 2004. A de novo mutation affecting human TrkB associated with severe obesity and developmental delay. *Nature neuroscience* 7: 1187-9

Yi CX, Sun N, Ackermans MT, Alkemade A, Foppen E, et al. 2010. Pituitary adenylate cyclase-activating polypeptide stimulates glucose production via the hepatic sympathetic innervation in rats. *Diabetes* 59: 1591-600

Zarjevski N, Cusin I, Vettor R, Rohner-Jeanrenaud F, Jeanrenaud B. 1993. Chronic intracerebroventricular neuropeptide-Y administration to normal rats mimics hormonal and metabolic changes of obesity. *Endocrinology* 133: 1753-8

Zhang Y, Proenca R, Maffei M, Barone M, Leopold L, Friedman JM. 1994. Positional cloning of the mouse obese gene and its human homologue. *Nature* 372: 425-32

Zhao L, Bakke M, Hanley NA, Majdic G, Stallings NR, et al. 2004. Tissue-specific knockouts of steroidogenic factor 1. *Mol Cell Endocrinol* 215: 89-94

Zheng F, Wang H. 2009. NMDA-mediated and self-induced bdnf exon IV transcriptions are differentially regulated in cultured cortical neurons. *Neurochemistry international* 54: 385-92

Zheng F, Zhou X, Luo Y, Xiao H, Wayman G, Wang H. 2011. Regulation of brain-derived neurotrophic factor exon IV transcription through calcium responsive elements in cortical neurons. *PloS one* 6: e28441

Zigman JM, Jones JE, Lee CE, Saper CB, Elmquist JK. 2006. Expression of ghrelin receptor mRNA in the rat and the mouse brain. *J Comp Neurol* 494: 528-48

Zigman JM, Nakano Y, Coppari R, Balthasar N, Marcus JN, et al. 2005. Mice lacking ghrelin receptors resist the development of diet-induced obesity. *J Clin Invest* 115: 3564-72